CHARIM

Caribbean Handbook on Risk Information Management

National scale landslide susceptibility assessment for Saint Vincent

June 2016

C.J. Van Westen

Faculty of Geo-information Science and Earth Observation (ITC), University of Twente.

E-mail: c.j.vanwesten@utwente.nl

WORLD BANK GROUP

ACP-EU Natural Disaster Risk Reduction Program

An initiative of the African, Caribbean and Pacific Group, funded by the European Union and managed by GFDRR

Table of Contents

Author:
Dr. Cees J. van Westen
Associate Professor
University Twente, Faculty of Geo-Information Science and Earth Observation (ITC)
PO Box 217, 7500 AA Enschede, the Netherlands
T: +31534874263
E: c.j.vanwesten@utwente.nl
I: http://www.itc.nl/about_itc/resumes/westen.aspx

This report should be cited as:
Van Westen, C.J. (2016) National Scale Landslide Susceptibility Assessment for SVG. CHARIM Caribbean Handbook on Risk Information Management, World Bank GFDRR, ACP-EU Natural Disaster Risk Reduction Program. www.charim.net

http://www.charim.net/sites/default/files/handbook/maps/SAINT_VICENT/SVGLandslideReport.pdf

Summary

The aim of this study was to generate a national-scale landslide susceptibility map for the island of Saint Vincent, and not for the other islands (Grenadines) that are part of Saint Vincent and the Grenadines (SVG). As the available data turned out to be insufficient to generate reliable results, we decided to generate several new data layers and significantly improved some of the existing data. We generated a new database of hydro-meteorological disaster events for Saint Vincent, for the period 1718 to 2014, making use of many different sources. This is the most complete inventory up to our knowledge. It is quite clear from this database that the disaster reporting became more frequent in recent years, although limited information on landslides is available for Saint Vincent, even more when going back in time, whereas the data on tropical storms and hurricanes seems to be much more constant over time. The underreporting of landslides is a big problem in trying to evaluation landslide frequency/magnitude relations, which are required to convert susceptibility maps into hazard maps. We also compiled all available landslide data from different sources. Unfortunately there was only one inventory available, generated in 1988 by DeGraff which contained 554 landslides polygons, which cannot be linked to a particular triggering event. We generated a completely new landslide inventory using multi-temporal visual image interpretation using high resolution satellite images from 2014 and historical images from Google Earth, and generated an extensive landslide database for Saint Vincent. The resulting landslide database contains 1647 landslides. We also used digital image interpretation for generating a Geomorphological map for Saint Vincent.

We analyzed the triggering conditions for landslides as far as was possible given the available data, and generated rainfall magnitude-frequency relations. However, there were not enough data (both in terms of landslide dates and date-related inventories) to be able to calculate magnitude-frequency relations for landslides, in terms of the number or density of landslide for different frequencies. We applied a method for landslide susceptibility assessment that is the best possible, given the availability of data. A bi-variate statistical analysis provided indications on the importance of the possible contributing factors, but the actual combination of the factor maps was done using a subjective expert-based iterative weighing approach using Spatial Multi-Criteria Evaluation. The method for landslide susceptibility assessment was further expanded by including the historical landslides in the susceptibility map and by manual editing of the final map. The map was visually checked, and the modelled zones of high, moderate and low susceptibility were adapted when necessary, so that they reflect the best situation according to the mapping geomorphologist. This was a rather time consuming activity, but it allowed to analyse the different parts of the map separately. The manual editing of the susceptibility map was also done to simplify the susceptibility units. The method is transparent, as the stakeholders (e.g. the engineers and planners) and other consultants can consult the criteria trees and evaluate the standardization and weights, and make adjustments. In the final landslide susceptibility map 42.3% of the area has a low susceptibility, 31.5 moderate and 26.2 high susceptibility, in which also all historical landslides are included. The total area of the historical landslides (including debris flow runout zones) is 232 hectares, which is 0.67% of the total area of the country. The expected landslide density varies from 0.1 % for low susceptibility zones, to 1.5% in the high class, and in terms of numbers between 4.25 and 16 landslides/km^2. However, for individual events these values are expected to be lower, as less landslides are expected to be triggered by a single triggering event. The exception however might be the river channels that are close to higher area, and which may be affected by a combination of flash floods and debris flows Generally it was not possible to determine the frequency of the landslide densities due to a lack of sufficient event-based inventories.

Future work should also focus on landslide susceptibility along the road network by subdividing the primary road network into homogeneous segments which could be characterized by information from various GIS layers. But primarily by data from field studies along the road network.

A basic landslide exposure analysis was carried out for buildings. We analyzed all buildings in Saint Vincent using a GIS overlay with the edited building footprints. The results show that in the entire country 400 buildings (0.8 % of the total) are located in high landslide susceptibility zones, 2508 (4.8 %) in moderate susceptibility zones and the vast majority of 48950 buildings (94.4%) in low landslide susceptibility zones. When we evaluate these values per Parish, St David parish has the largest percentage of buildings located in high susceptibility zones (187 buildings), followed by St Patrick (91 buildings). One should be careful when using the national-scale landslide susceptibility map for evaluating the landslide hazard of individual buildings and critical infrastructure. The scale of this map is not appropriate to utilize it for local or detailed scale analysis. Other, more detailed landslide hazard methods should be used for these scales, which also require more detailed information on soil characteristics, such as soil depth, hydrological and geotechnical properties.

Acknowledgements

We would like to thank the following persons who carried out MSc research in Saint Vincent in the framework of this project:

- Jovani Yifru Bogale (Ethiopia) who worked on landslides susceptibility assessment along roads in Dominica and Saint Lucia,
- Diana Lozana Zafra (Colombia) who worked on national scale landslide susceptibility assessment in Dominica and Saint Vincent,
- Chishala Mulenga (Zambia) who studied the influence of weathering on geotechnical properties of road-cut slope mass and embankment fill in Saint Lucia and Saint Vincent
- Xsa Anacio Cabria (Philippines) who studied the weathering and its contribution to rock falls in the pyroclastic rock masses along coastal road cuts in Dominica and Saint Vincent

Marcella Soriano supported in some of the rainfall analysis, and Victor Jetten did the rainfall frequency analysis. Koert Sijmons generated the cartographic products in the form of a landslide inventory map and landslide susceptibility map. Wim Feringa and developed the web-based platform where all results can be found: www.charim.net and Ramesh Da Silva (AIT) developed the GeoNode where you can download the GIS data from: http://charim-geonode.net/
We thank Dinand Alkema for his patience and work as project coordinator. We thank Colm Jordan, Stephen Grebby, Tom Dijkstra, Claire Dashwood and Francesca Cigna (British Geological Survey, Natural Environment Research Council) for their work on land use mapping for Saint Vincent and their attempt to map landslides from recent satellite images.

We would like to thank the following persons and organisations for their great support while being in Saint Vincent for fieldwork and during several of the workshops in Saint Vincent and the Netherlands:

- **Ministry of Transport, Works, Urban Development & Local Government.**
  - Brent Bailey (Chief Engineer), Alistair Campbell (Deputy Chief Engineer), Cecil Harris, Andy Baptiste, Franklyn Haynes
- **Ministry of Housing, Informal Human Settlements, Lands & Surveys and Physical Planning**
  - Anthony Bowman (Chief Technical Officer), Kendahli Crichton, Shelford Stowe, Dwane Allen, Desmond Shallow, Dornet Hull
- **The National Emergency Management Organization (NEMO)**
  - Howie Prince (Director)
- **Ministry of Agriculture, Forestry, Fisheries and Rural Transformation**
  - **Forestry Department**
    - Cornelius Lyttle
  - **Ministry of Agriculture**.
    - Gertheryn Bascombe,
- **Water Resources.**
  - Danroy Ballertyne, Zascha Robertson.

We would like to thank Cynthia Linero and Melanie Kappes for their comments on the draft of the report.

1. Introduction

1.1. About CHARIM

In 2014 the World Bank initiated the Caribbean Risk Information Program with a grant from the ACP-EU Natural Disaster Risk Reduction Program. A consortium led by the Faculty ITC of the University of Twente is responsible for conducting capacity-building workshops, generating training materials, and creating hazard maps to expand the capabilities within participating infrastruct60ure and spatial planning ministries to use hazard and risk information for decision-making.
The main objective of this project is to build capacity of government clients in the Caribbean region, and specifically in the countries of Belize, Dominica, St. Lucia, St. Vincent and the Grenadines and Grenada, to generate landslide and flood hazards and risks information and apply this in disaster risk reduction use cases focusing on planning and infrastructure (i.e. health, education, transport and government buildings) through the development of a handbook and, hazard maps, use cases, and data management strategy. The results of the CHARIM project are shared through a web-based platform: www.charim.net

One of the sub-objectives of the project was to "***develop a theoretical framework for landslide and flood hazards and risks assessments, based on the review of existing quantitative and qualitative assessment methods and their appropriate use".*** Another sub-objective was to ***"develop nine national hazard mapping studies in the five target countries. One in Belize related to floods and two on each island for landslides and flood".***

This report addresses specifically the methods and results used for the national-scale landslide susceptibility assessment for the country of Dominica.
It will do so by first introducing the method of analysis, and the reasons for selecting this method. In the next chapter the available data for landslide susceptibility assessment will be presented, focusing on the existing landslide inventories and factor maps.
The third chapter presents the methods and results used for generating the compiled landslide inventory. The fourth chapter presents the method used for statistical analysis and the presentation of the results. The fifth chapter presents the method of Spatial Multi-Criteria Evaluation and the results for the country of Dominica. The Sixth chapter will present the validation and generation of the final susceptibility map. The report will end by discussing the critical points in relation to the available data and suggestions for additional data collection.

1.2. Definitions and requirements

The terminology used in this report follows that of the Guidelines for landslide susceptibility, hazard and risk assessment and zoning, produced by the comprehensive landslide research project “SAFELAND, Living with landslide risk in Europe: Assessment, effects of global change, and risk management strategies”, funded by the European Commission. The guidelines were also worked out as a publication by Corominas et al. (2014), based on a large number of literature sources, among which Fell et al (2008), TC32, UN-ISDR (2004):
For this reports the following three definitions are of importance:

***Landslide inventory**: The collection of landslide features in a certain area for a certain period, preferably in digital form with spatial information related to the location (as points or polygons) combined with attribute information. These attributes should ideally contain information on the type of landslide, date of occurrence or relative age, size and/or volume, current activity, and causes. Landslide inventories are either continuous in time, or provide so-called event-based landslide inventories, which are inventories of landslides that happened as a result of a particular triggering event (rainfall, earthquake).*

***Landslide susceptibility map**: A landslide susceptibility map contains a subdivision of the terrain in zones that have a different spatial likelihood that landslides may occur. The likelihood may be indicated either qualitatively (as high, moderate low, and not susceptible) or quantitatively (e.g. as the density in number per square kilometres, or area affected per square kilometre). Landslide susceptibility maps should indicate the zones where landslides have occurred in the past and where they may occur in future and possibly also the run-out zones.*

***Landslide hazard map**: The subdivision of the terrain in zones that are characterized by the expected intensity of landslides within a given period of time, or the probability of landslide occurrence. Landslide hazard maps should indicate both the zones where landslides may occur as well as the run-out zones. Landslide hazard maps differ from landslide susceptibility maps as they would indicate for specific zones, what can be expected, with which frequency and with which intensity. A complete quantitative landslide hazard assessment includes:*

- *Spatial probability: the probability that a given area is hit by a landslide.*
- *Temporal probability: the probability that a given triggering event will cause landslides*
- *Volume/intensity probability: probability that the slide has a given volume/intensity*
- *Run-out probability: probability that the slide will reach a certain distance downslope*

Depending on the scale of the hazard assessment, and the available input data, hazard may be expressed in different ways. At large scales it could be expressed as failure probability, using a factor of safety approach, and given certain triggering events with a given return period. At medium to small scales it may be expressed as the expected landslide density within particular units for a given return period.

Based on these definitions and the situation in the country of SVG, it is currently only possible to generate landslide susceptibility maps at the national scale, and it is not possible to generate a national landslide hazard map, as we are not able to represent spatial, temporal, size and run-out probability for landslides for the entire island at a scale of around 50.000, giving the limitations in the available data. These limitations are mostly related to lack of sufficient information between the relation of the frequency and magnitude of triggering events (extreme rainfall) and the landslide caused by them. At a national scale we were only able to generate a qualitative map that shows the subdivision of the terrain in zones that have a different likelihood that landslides of a type may occur, without actual information on the frequency of landslides for different return periods, the size probability and the run-out probability. At best we were able to generate national scale qualitative landslide hazard maps that have semi-quantitative descriptions of the legend classes, indicating the expected landslide densities for different return periods.

1.3. Previous work on landslide susceptibility assessment

In the country of SVG only limited previous attempts to generate landslide susceptibility maps have been carried out. In 1988, (DeGraff, 1988) a national landslide hazard assessment was done through the analysis of three factors: geology, geomorphology and topography. The geomorphology was represented by a 1:25,000 landslide inventory map obtained through the interpretation of aerial photographs from 1981 at a scale of 1:20,000 that covered the whole island from north to south, except a strip on the east-central part of the island and fieldwork on the major roads. A geology map was combined with a slope class map, and this composite map was compared with the map of past landslides. Landslide density was calculated for each geology-slope class. No rainfall information was used, as well as any land cover/use. The final map was a landslide susceptibility map (named as landslide hazard map) obtained from the analysis of the proportion of bedrock-slope combinations subject to past landslide activity (landslide area divided by bedrock – slope area). The resulting map is shown in Figure 1-1.

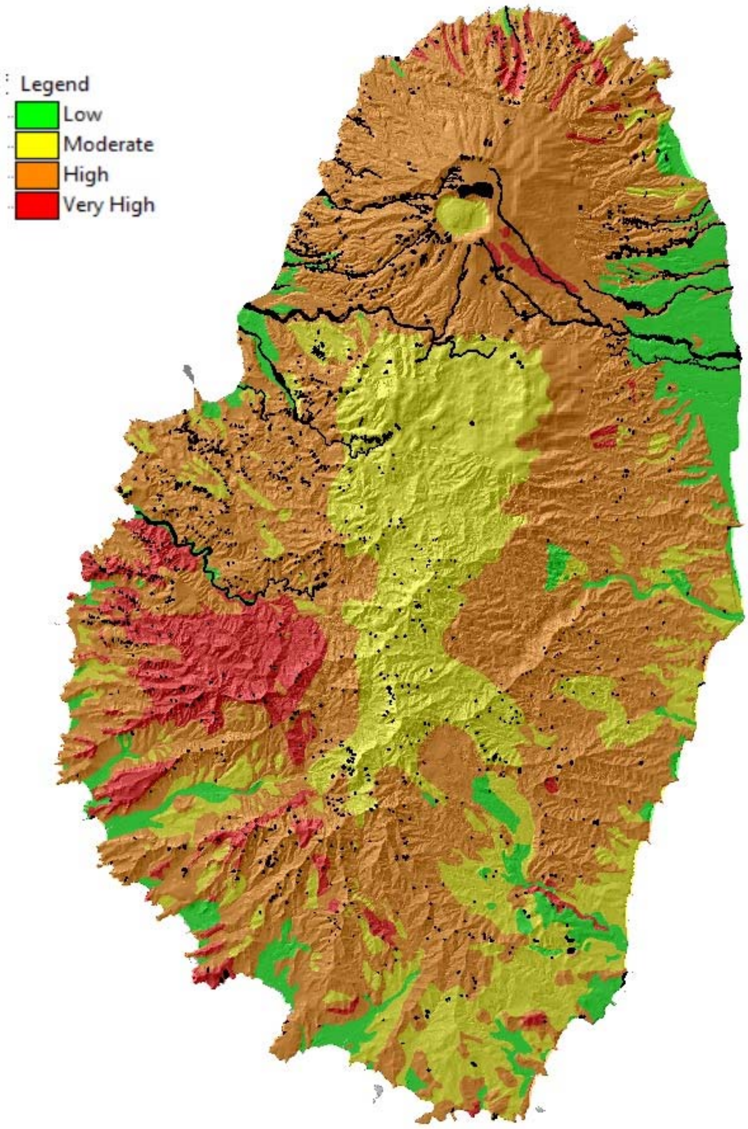

Figure 1-1: Landslide susceptibility map generated in 1988 by DeGraff, with the landslides mapped by both DeGraff in 1988 and Van Westen (2014).

2. Method used for the national-scale landslide susceptibility assessment

2.1. Presentation of the method used

Figure 2-1 presents the method which was used for the national scale landslide susceptibility assessment for the Commonwealth of Dominica. The method focuses on the assessment where landslides are likely to initiate, and not on the possible run-out areas. Run-out susceptibility assessment should be taken into account when doing local and site-investigation studies.
The method consists of a number of steps which are described in detail in the following sections. Here a summary of the steps is give:

Step 1: Generating landslide inventories. The first, and very important step is to generate a comprehensive landslide inventory. Almost no landslide inventories were available for Saint Vincent. Therefore an attempt was made to generate one using several sources of information: interpretation of high resolution satellite images, collection of historical information on the dates of occurrence of past landslide events, collection of available data from the national emergency management organisation and from road maintenance records. The resulting landslide inventory map contains many more landslides than were initially available. Landslides were also classified based on their type, and a differentiation was made between initiation and runout areas.

Step 2: Analysis of triggering events. An analysis of triggering events is carried out in order to be able to correlate landslide inventories of particular triggering events to the frequency of rainfall related to these events. If such a relation could be established we could also characterize the landslide susceptibility classes with indicative landslide densities for different frequencies, and would then be able to convert the susceptibility map into a hazard map. From the available data on landslide occurrences a series of triggering events were identified. Rainfall data was used to estimate return periods of daily rainfall, with the aim to correlate these with triggering events for which landslide information was available.

Step 3: Generation of factor maps that contribute to landslide occurrence. A Digital Elevation Model was generated using available data, which was used for generating derivative maps, such as elevation classes, slope steepness, slope direction and flow accumulation. Exiting geological maps, and soil maps were used. Drainage lines, roads, coastlines and ridges were used to generate distance maps to evaluate the effect of landslide occurrence close to these features. Land cover maps were generated by the British Geological Survey using object oriented image classification based on Pleiades images.

Step 4: Bivariate statistical analysis. The weights of evidence modelling (WOE) was used as an exploratory tool to evaluate the importance of the factor classes. A GIS-based script was used to carry out the WOE modelling for each factor map in combination with the landslide inventory map. Different analysis was done for shallow soil-related landslides and for rock related landslides and rockfall as they were expected to have different importance of causal factors. Based on the calculated weights of evidence a selection was made of the most relevant causal factors. When the results of the statistical analysis provided inconclusive results we went back to the creation of the factor maps. Several new combinations of factor maps were made which were again tested using the weights of evidence method. For instance a factor map lithology can be combined with a map of slope classes, so that the resulting map gives a better relation with landslides, and the combined classes have higher weight values. The process of generating factor maps and evaluating their importance is done in an iterative process, and the factors used may be different for each individual situation.

Step 5 - 7: Spatial Multi-Criteria Evaluation. We decided not to use the results of the weights of evidence directly as the basis for the landslide susceptibility assessment, due to the inaccuracies encountered with the input data, and with the landslide inventories, and due to inconclusive results from the statistical analysis. The importance of the various factor maps should be explainable in terms of their contribution to landslide processes, and therefore we decided to include expert opinion in the process through the SMCE process which consists of several steps.

.

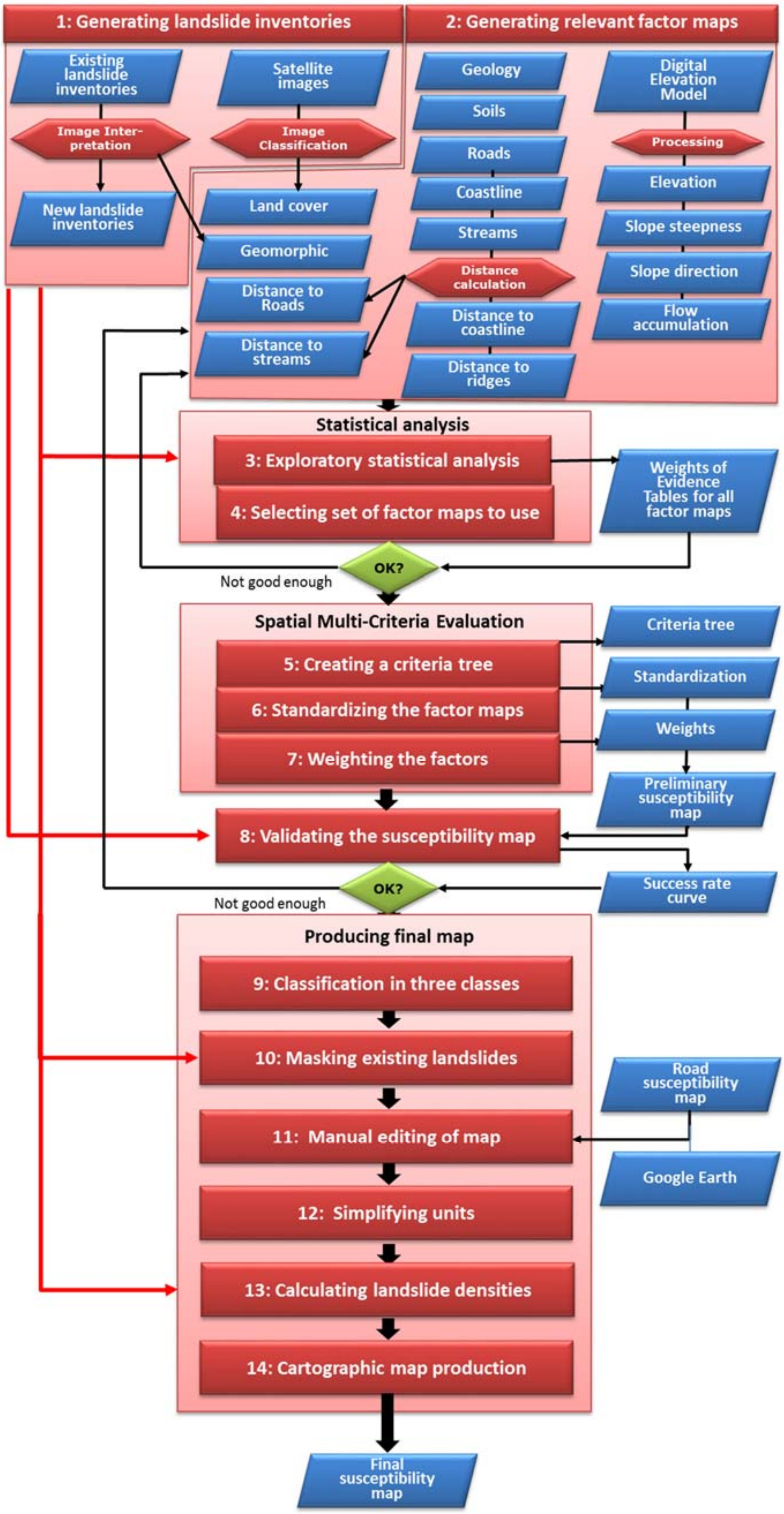

Figure 2-1: Flowchart of the method used for the generation of the national scale landslide susceptibility maps. See text for explanation. See also: http://www.charim.net/methodology/43

First we generated a *criteria tree* in which we grouped the various causal factors in groups. Then we *standardized* the individual causal factors, based on the calculated weights of evidence. However, we used the calculated weights as a guidance and in several occasions we decided to adjust these as they seemed to be more logical based on our observations in the field and our knowledge on landslide occurrences. The standardization resulted in values for each factor map ranging from 0 to 1
After standardization we weighted the individual factor maps and the various groups by comparing them with each other and by assigning a certain rank to them. This resulted in weights which were also represented in a range of 0 to 1. The last stage of the Spatial Multi-Criteria Evaluation was the generation of a composite index map, which integrated the standardization and weighing for all indicators in the criteria tree, resulting a susceptibility map with values ranging from 0 to 1.

Step 8: Validation of the susceptibility map. In order to validate the susceptibility map we combined the composite index map resulting from the Spatial Multi-Criteria Evaluation with the original landslide inventory map. We then calculated the success rate, which indicates the relation between the percentage of the susceptibility map ordered from the highest to the lowest values, and the percentage of landslides occurring in the locations of these values. We applied different methods for analysing the success rate. For instance we only took the initiation areas of all landslides, or separated the landslides in groups with different types and analysed the success rate for them. When we had landslide inventories from different triggering events we also tested the quality of the map for these different inventories. We also carefully analysed the spatial distribution of the susceptibility values visually in the map by overlaying it with a hill shading image of the country and with the landslide inventory in order to evaluate whether the highly susceptible zones were in accordance with our experience in the field, and with the overall geomorphological situation. When we considered that this relation was not good enough or when the success rate was not good enough (e.g. by applying certain rules such as that 70 percent of the landslides should be located within 30 percent of the map) we decided to go back to the selection of relevant factor maps and repeated the statistical analysis and the spatial multi-criteria evaluation for other combinations of factors. So the landslide susceptibility assessment was an iterative procedure, which was done until we were satisfied with the results. We also discussed the results with a group of professionals from the country that visited ITC in the Netherlands during a period of one month in spring of 2015. Based on their suggestions a number of modifications were made.

Step 9: Classification of the landslide susceptibility map. We used the susceptibility value map, and the success rate to subdivide the map in three classes of susceptibility (high, moderate and low). The high susceptibility class has the highest landslide density and the areas should be a small as possible and limited to those zones where landslides have occurred in the past and are most likely to occur in future. The low landslide susceptibility class is used for those areas where landslides are not expected to occur at all, or in very seldom cases. Moderate landslide susceptibility forms the middle class, which should be kept as small as possible, as this is the class which is neither dangerous nor safe, and further studies are needed before planning decisions can be taken.

Step 10: Masking existing landslides. The final map should also contain the areas where landslides have occurred in the past. They should be included in the high susceptible zone, as it is possible that landslides may happen again in these conditions, unless remedial measures have been adopted after the landslide occurrence. Therefore the existing landslide inventories were used and the locations were masked as “high susceptibility”” in the map. Zones immediately surrounding these were indicated a “Moderate susceptibility”.

Step 11: Manual editing. The landslide susceptibility map with the added historical landslides still is in a shape that is too generalized. This is due to the poor quality of the input data, and due to the nature of the analysis method using a combination of statistical analysis and spatial multi-criteria evaluation, which use generalized weights for maps applied to the entire area, whereas there may be exceptions that need to be taken into account locally. Therefore it is important that the final susceptibility map is checked carefully and edited. This is done by exporting the map to an external photo-editing software (CorelPhotoPaint) where it is possible to edit the three classes using the Paint tool. The best is to do this on a dual screen, by comparing the map with a Google Earth image and with a hill shading image overlain with the landslide susceptibility map, plus topographic information, like rivers, roads, buildings etc. This way each part of the area can be visually checked, and the modelled zones of high, moderate and low susceptibility can be adapted, so that they reflect the best situation according to the mapping geomorphologist. If there is a landslide susceptibility map available that is made for the road network, it is also relevant to use this map in editing the final susceptibility map. This is a rather time consuming activity, but it allows to analyse the different parts of the map separately, and therefore obtain results that also are valid for a local scale, and not only for a national scale.

Step 12: Simplifying units. The manual editing of the susceptibility map is also done to simplify the susceptibility units. After running the statistical analysis and spatial multi-criteria analysis, the resulting landslide susceptibility raster map shows many small areas with different degrees of susceptibility. Sometimes the susceptibility differs from pixel to pixel, due to variations in the input maps (e.g. slope classes may differ very locally). In order to be able to use the resulting map as a basis for planning, the area should be subdivided into zones with different likelihood of landslide occurrence. Therefore during the manual editing phases, areas are simplified, and classified into one of the three classes, removing the large local variation. Also after completing the manual editing process, still many locations with isolated pixels remain. These were subsequently removed in GIS using a majority filter. The resulting landslide susceptibility map can also be converted into a polygon map.

Step 13: Calculating densities. One the final landslide susceptibility map has been obtained, it is now possible to calculate the number of landslides in the three susceptibility classes. This is now not done anymore to validate the map, as the historical landslides were included in the map in step 10, but now the aim is to characterize the susceptibility classes in terms of landslide density (both in area and in numbers). If different event-based inventories are available, it is also possible to calculate landslide densities for each of them, and if also frequency information is available it is also possible to give an indication of the spatio-temporal probabilities (the density of landslides per class for different return periods of the triggering event). It is also possible to calculate the number of exposed buildings and other infrastructure if available. Especially the manual editing in step 11 allows a much more realistic estimation of the exposure.

Step 14: Cartographic map production. The final stage of the landslide susceptibility assessment consisted of the cartographic map production. Also a separate map with the landslide inventory itself was produced. The base map was generated using a hill shading map generated from the Digital Elevation Model, together with the drainage network, the road network, the buildings, airports, administrative units, names and other relevant topographic information in order to make the map better readable. These maps are available as PDF's on the CHARIM webpage (http://www.charim.net/stvincent/maps). Also the digital versions of the landslide inventories and the landslide susceptibility maps were made available through the GeoNode (http://charim-geonode.net/maps/244).

2.2. Considerations for selecting this method

The method described above for the national scale landslide susceptibility assessment was selected based on the following considerations:

The mapping scale. The maps are made at a scale of 1:50.000. This allows to represent the entire country into one single map sheet. The map cannot be used for local scale or site investigation scale analysis, however, when the editing of the map is step 11 is done carefully, the map can also be reasonable at the local level. The application of more detailed methods based on physically-based modelling was not possible due to the lack of sufficiently detailed soil information, and Digital Elevation data. For more detailed studies more information should be available on soil depth and on the geotechnical and hydrological soil characteristics so that more detailed types of analysis can be carried out. We decided also to exclude landslide run-out analysis at a national scale as the available data was insufficient for that and the run-out zones are not that significant when looking at a national scale.

The objective of the assessment.
Such national scale maps are intended to be used by the governments to:

- Serve as living and dynamic baseline map for the planning, design, management and implementation of a long-term landslide reduction strategy. This map should be updated regularly as new/improved data becomes available
- Include them as a factor in national scale land use planning, by outlining the zones that are most susceptible to landslides;

- Identify the areas where more detailed investigations are required for the planning of critical infrastructure;
- Form the basis for identification of the strategies to increase the resilience of the national road network by prioritizing the development of contingency plans and required complementary studies during planning and design of new infrastructure;
- Use for the prioritization of creation of contingency plans for exposed communities;
- Contribute to inform required expansions of the hydro-met monitoring system as well as monitoring of landslides;
- Inform watershed management, environmental assessments and studies on environmental degradation; and
- Be used to inform the planning of agricultural or mining activities that could increase slope instability.

The objectives mentioned above are such that the national scale landslide susceptibility should be used as baseline information for national level planning, and for risk communication. The map should also be able to outline areas that should be avoided in future developments, and the high susceptible zones are considered to be a basis for restrictive zoning as a basis for building control, together with other hazard maps. The susceptibility map can also be used together with susceptibility and or hazard maps for other hazardous processes (flash flooding, coastal flooding, tsunamis, volcanic hazards, seismic hazards and wildfire hazard) as a basis for multi-hazard susceptibility assessments. The maps can also be used for analysing the exposure of the existing buildings, people and road infrastructure.

The complexity of the area. The geology of the island is composed of volcanic rocks with strongly varying composition, such as ignimbrites, lava flows, lahar deposits, and volcanic ashes. They are very heterogeneous and have not been mapped in great detail. There is often a vague difference between the term rocks and soils in engineering terms, as many of the volcanic deposits have a relative low degree of cementation and consolidation. Also due to the intense tropical weathering unconsolidated materials may be very thick. These deposits may sustain near vertical road cuts which are stable, however, when weathering is taken into account such road cuts may cause problems in the future.

The available data. After a first inventory of the existing data we discovered that there were major deficiencies with respect to the available data, both in terms of the available landslide inventories and with the available factor maps for carrying out the analysis. The large heterogeneity of volcanic deposits is unfortunately not portrayed in the available maps for the island. The geological maps are rather general and do not focus on the specific volcanic deposits. The soil map is more detailed and show a large differentiation, but they are focusing on pedologic soil characteristics for agriculture purposes.

The resources available. As the assessment was originally planned as a desk study, only limited time was available for image interpretation and fieldwork. Nevertheless, after evaluating the problems with the existing data we decided to spend more time in carrying out a detailed image interpretation for landslide characterization, and also to involve a number of Master of Science students in the basic data collection. Also a collaboration was established with the British Geological Survey that supported in the creating of land cover maps and landslide inventory maps for some of the islands.

3. Evaluating landslide triggering characteristics

One of the key factors for the generation of landslide susceptibility and hazard maps is information on when landslides occurred in the past, and by which triggering events. Intense rainfall events are considered the most important triggering events. Even though there might be earthquakes occurring on the island, their expected intensity is generally not considered to be high enough to cause substantial landslide problems. Also human interventions may trigger landslides, e.g. through deforestation, clear cutting, improper drainage practices, or slope cutting, but still a rainfall trigger would be required to actual cause the landslides.

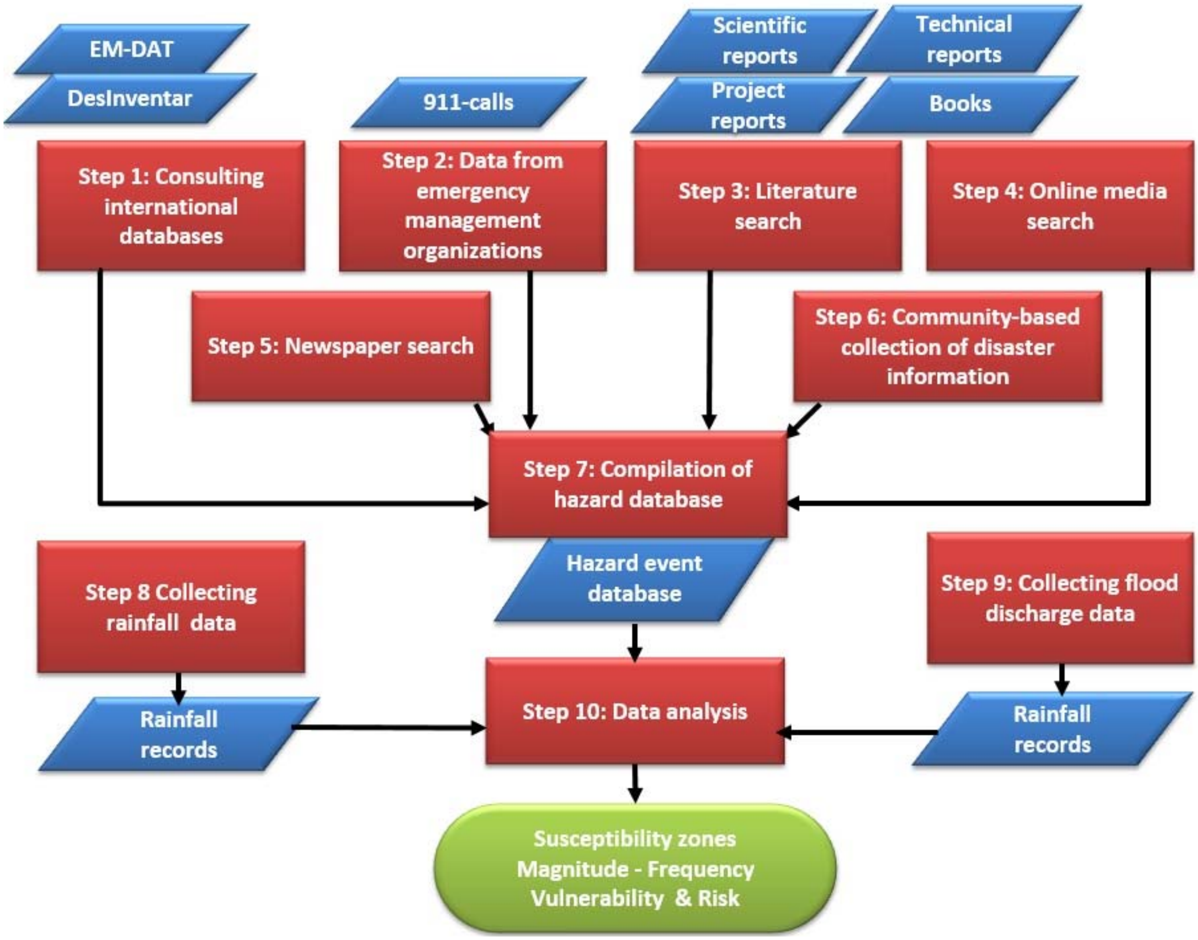

Figure 3-1: Overview of method for collecting information of past events.

3.1. Collection of existing data

In order to collect information on dates of historical disaster events a study was carried out using various sources to reconstruct the major disaster events in the history of the island (See Figure 3-1). Disaster data was downloaded from the CRED-EMDAT database (Guha-Sapir et al., 2015). The information in this database is rather limited (See Table 3-1). No specific landslide information was found related to landslides.

As stated in the SVG country profile for disaster risk reduction (DipEcho, 2014) "At present there is no formal cataloguing of disasters for St Vincent and the Grenadines, however, efforts are underway to populate the DesInventar database making it usable by the end of 2014. Various records have however been compiled which informs this documentation. The records will need to be updated regularly as SVG faces annual impact from hazards".

We also collected information from various other sources on the internet. One of the best sources for older information was O'Keefe and Conway (1977) for the older disaster occurrences. They based their own data on extensive analysis of newspaper searches for the various countries. Cross (1992), Crowards (2000), Chaveriat (2000) and Boruff and Cutter (2007) also did a similar search using various sources of information. We also used damage and Loss estimation for the 2013 event called the "Christmass eve trough" (World Bank, 2014). We also consulted http://www.hurricanecity.com/city/saintvincent.htm. We also consulted online newspaper reports: http://thevincentian.com/ and http://www.iwnsvg.com

3.2. Results

The various sources provided a lot of information in historical events, such as tropical storms, hurricanes, earthquakes and drought. Table 3-1 shows the very meagre results from the EM-DAT records.

Table 3-1: Disaster information from the EMDAT database: http://www.emdat.be/country_profile/index.html

day	month	year	Hazard Type	Deaths	Affected	Economic damage
7	5	1902	Volcanic eruption	1565	?	?
23	9	1955	Storm	122	?	?
8	9	1967	Storm	2	?	4500000
17	10	1971	Volcanic activity	0	2000	?
13	4	1979	Volcanic eruption	2	20000	?
31	7	1980	Storm	0	20500	16300000
0	9	1987	Flood	0	1000	5000000
21	9	1987	Storm	0	208	5300000
29	11	1992	Flood	3	?	?
24	9	2002	Storm	4	?	11000000
8	9	2004	Storm	0	1004	5000000
14	7	2005	Storm	0	530	?
29	10	2010	Storm	0	6100	25000000
11	4	2011	Flood	0	275	?
23	12	2013	Flood	12	17422	108000000
			Totals	1710	69039	180100000

Boruff and Cutter (2007) carried out an extensive literature search for disaster events in Saint Vincent. They augmented the baseline data through local fieldwork and archival and Internet-based research, and obtained information on hazard events that affected Saint Vincent between 1901 and 2000 from books, journal articles, local newspapers, Internet databases, and reports from organizations such as the Caribbean Development Bank and the Organization of American States (OAS). Periodicals and colonial reports housed in the University of Florida's Latin America Collection and at the University of the West Indies' Cave Hill Campus Library yielded additional or overlapping references for more than seventy-two events during the same period. In total, they found information on eighty-one discrete hazard events affecting Saint Vincent between 1901 and 2000.
Table 3-2 below summarizes their results.

Table 3-2: Summary of disaster events for Saint Vincent by Boruff and Cutter (2007)

Hazard	Frequency	Return period
Drought	Occasional	
Earthquake	7	14.14
Flood	4	24.75
Fire	Annual	<1.0
Landslide	Frequent	
Tsunami	1	14.14
Tropical system	7	99
Volcanic eruption	3	33

Figure 3-2 Multi-hazards in Saint Vincent. Top: pyroclastic flow related to eruption of Soufriere volcano in 1902, landslide interrupting road in Belmont, windstorm damage. Below: coastal damage in Georgetown, flooding and debris flow.

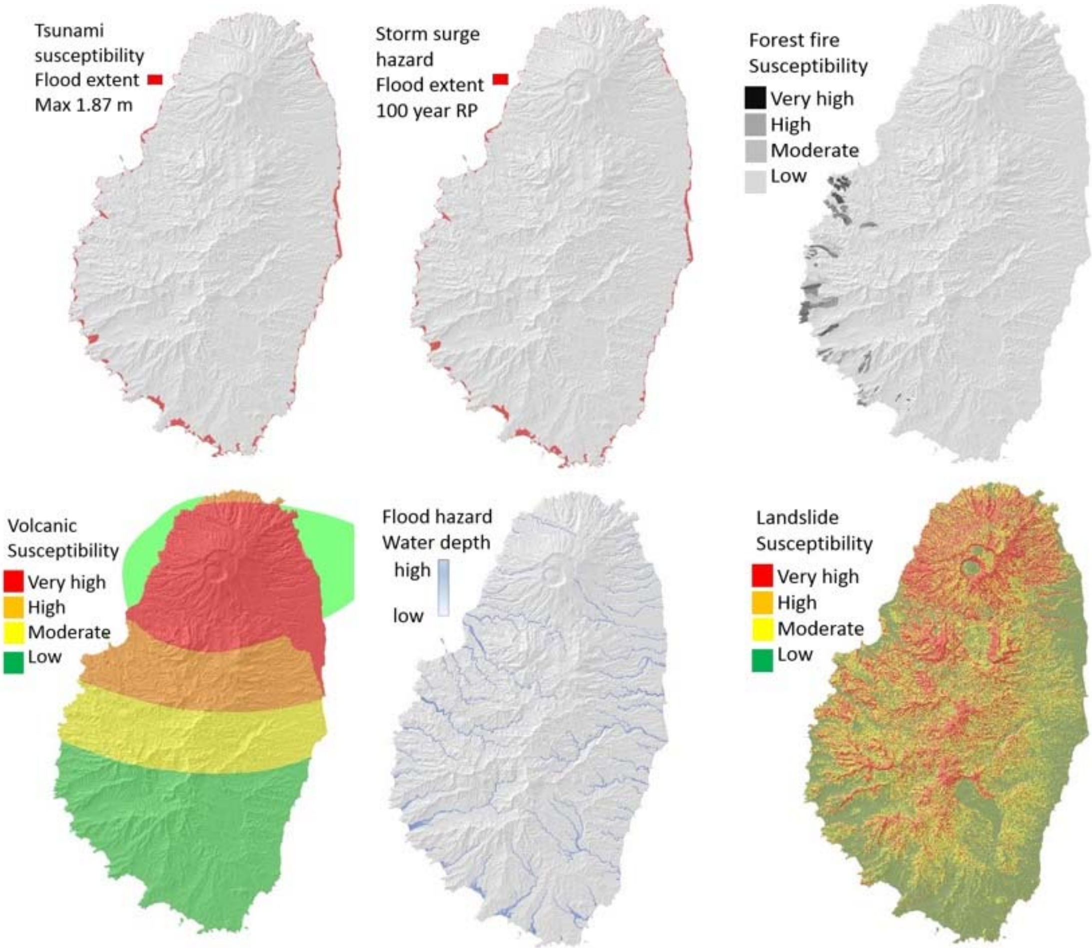

Figure 3-3 Multi-hazards maps in Saint Vincent.

According to the available disaster statistics earthquakes have not caused significant damage on the eastern Caribbean islands which are part of CHARIM. Each year, the Eastern Caribbean experiences about 1200 earthquakes greater than magnitude 2.0. It is also estimated that the region will experience at least one

magnitude 6 earthquakes every 3-5 years. It is also estimated that the earthquake zone where SVG is located could experience earthquakes of level VII in Mercalli intensity scale for a return period of 50 years (OAS USAID/OFDA (2001); DipEcho, 2014).
The same is true of tsunamis. Only limited damage has been recorded on Saint Vincent (NGDC 2003; SRU, 2007). However, some researchers are of the opinion that the underwater volcano Kick 'm Jenny north of Grenada may also produce a tsunami that might be harmful in Saint Vincent (Smith and Shepherd, 1993). There are three historical tsunami events known for Saint Vincent. The 30-year probability of tsunami run-up in excess of 0.5 m in Kingston is considered to be 11.32 % (Parsons and Geist, 2009).

Table 3-3: Historical tsunami events in Saint Vincent

Year	Month	Day	Location	Run-up height in meters	Where?
1755	11	1	Saint Vincent	4.5	
1867	11	18	Saint Vincent	1.68	Beguia island
1886	3	17	Saint Vincent	0.9	Bequia Island

On Saint Vincent, the only active volcano is the Soufriere volcano. In the Volcanic atlas of the Lesser Antilles a detailed description is given of the volcanic situation and the volcanic hazards (Lindsay et al, 2005). The most destructive events in terms of human casualties and losses have been the multiple eruptions of La Soufriere volcano. Volcanic eruptions have affected the country in 1718, 1812, 1902, 1971 and 1979. Three eruptions-in 1902, 1971, and 1979-prompted evacuations of the northern portion of the island. Two of the three events resulted in human fatalities (due to suffocating gases, lahartype debris flows, or volcanic ejecta) and destroyed buildings. During the 1979 eruption a large segment of the travel and communications infrastructure on the island was affected as well (Robertson 1995). A summary of historical activity at the Soufriere volcano (Robertson, 1995; Dipecho 2014) is given in Table 3-4.
Recent statistics from the Forest Department and accounts from historic texts illustrate the frequency of fire events. Bonham Richardson (2004) points out that fire, primarily human-induced fire, has "cleared forests, burned sugar cane, sparked slave rebellions, insurrections, attracted crowds, lighted streets and houses, and symbolized protest in the region for centuries." Not only have sugarcane fires burning out of control or set as acts of defiance created economic hardships for plantation owners and labourers, but wildfires have damaged commercial and residential structures, affected island infrastructure, and, in some cases, resulted in deaths (Richardson 2004).
Saint Vincent has been hit heavily by hurricanes and tropical storms 25 times in 143 years. On average it is brushed or hit by a tropical storm or hurricane once every 6 years. The most significant hurricanes to affect Saint Vincent were Janet in 1955, Lenny in 1999, Ivan in 2004, and Tomas in 2010.
Hurricane Janet in 1955 is responsible for the single largest number of people killed in such events, 122 people. The hurricane also damaged crops and coastal roads. Tropical Storm Danielle on September 8, 1986 triggered landslides which swept away a considerable length of the pipelines conveying water to hydroelectric stations. This affected the generating capacity at South Rivers station in the northeast part of the island and Richmond station in the northwest. Altogether, the landslides reduced electrical generation capacity by 36%. The wood stave pipelines had to be fully repaired prior to restoring generating capacity sometime later.
In May 1981, St. Vincent experienced a major storm during what is normally the dry season. Landslides occurring at three separate locations severed the 8- inch diameter pipeline for the Majorica water supply system. The damaged sections ranged from 5 to 20 feet in length. Nearly 40 percent of the population of St. Vincent was affected by this water system damage. Damage to the system left some inhabitants without water for a few days and others for nearly six months. Repair of the water line took six months due to the inaccessibility of the damaged sections and. cost between $87,000 and $130,000 (Central Water and Sewage Authority, Personal Communication). Records permitting tabulation of costs for clearing landslide debris and repairing damaged roads are not presently available for St. Vincent. Review of damage assessment reports made for Tropical Storm Danielle and the torrential rains which followed in September 1986, and for Hurricane Emily in September 1987 give some indication of the magnitude of this cost to roads. Totalling items noted as clearing of landslide debris or building of retaining walls from a district by district breakdown of road damage due to Tropical Storm Danielle yielded a total of $677,000. For Hurricane Emily, the amount was $191,000. Based on the cost of road clearance and damage from these two recent storms and the experience on neighbouring islands, it is estimated the average annual cost of this impact on St. Vincent is $115100

Table 3-4: Historical volcanic eruptions in Saint Vincent

year	Description
1718	Explosive eruption, preceded by one month of earthquake activity. Ash falls reported on Martinique, St. Kitts, Barbados and Hispaniola. The eruption is estimated to have been the most violent of the historic period (Anderson and Flett, 1903).
1780	Increased fumarolic activity - possibly with lava emission.
1811	Strong earthquakes.
1812	Explosive eruption, preceded by >200 earthquakes during the previous year. Pyroclastic flows, mudflows and ashfalls affected Wallibou to Baleine and Grand Sable to Tourama. Fifty-six people were estimated to have died and a new crater formed. About 80 deaths
1814	Small eruption with rocks thrown 0.5 km from the crater.
1880	Crater lake temperatures increased with a major rise in water level. There was an increase in fumarolic activity with possible emission of lava (dome).
1901	Strong earthquakes.
1902-03	Explosive eruption, preceded by 12 months of earthquake activity. Pyroclastic flows, mudflows and ash falls affected areas to the north-east, east and west of the volcano. At least 1565 died and extensive damage was caused to agriculture in the areas around the volcano.
1945-46	Local earthquake swarm accompanied by an increase in fumarolic activity.
1948-54	Increase in water temperature of the crater lake.
1971-72	An aseismic effusive eruption resulting in discharge of 80 x 10^6 m^3 of lava into the crater lake. The lake level rose 30 m destroying vegetation along the inside crater walls. Communities located north of the Rabacca dry river were evacuated. About 1600 persons killed. Considerable damage to the sugar industry. Economic costs estimated as US $ 200,000,000
1978	Local earthquake swarm.
1979	Explosive eruption accompanied by effusive activity. The eruption was preceded by increased earthquake activity, an increase in crater lake temperature and a slight inflation of the volcano flanks. There were no fatalities but extensive damage to crops and livestock. The total cost of eruption to the economy was estimated to be above 5.2 m USD. There was evacuation of >14,000 people from areas north of Union Village (east) and Belleisle Hill (west). Others (DipEcho) estimate 20,000 people evacuated, and loses of about US $ 100,000,000.

Hurricanes and storms have also severely affected the housing sector in St Vincent and the Grenadines including the impact of Hurricane Allen in 1980, Lenny in 1999, Lilli in 2002 and Ivan in 2004, each of which affected over 700 houses. Hurricane Emily in 2005 affected over 500 houses and hurricane Tomas in 2011 affected about 1,200 houses.

The most costly hazard events in St Vincent and the Grenadines (SVG) resulted from Hurricane Tomas in 2010, which cost about EC$130 million and the 2013 flood in December 2013 which resulted in damage and losses of US$ 108.4 mil or (EC$291.4 million). The cost of the 2013 flood is equivalent to 15% of the country's gross domestic product (GDP), (GOVSVG, 2014) Hurricane Tomas resulted in disaster areas being declared on the North Eastern side of the island including Park Hill, Chester Cottage, Sandy Bay and Byera and on the North Western side including Chateaubelair, Coulls Hill, Spring Village and Fitz Hughes. The hurricane injured 2 persons injured, affected about 6100, damaged 1200 homes and destroyed about 20 houses. Damage was also done to schools, community centres and other facilities. The agricultural sector experienced widespread damage especially to bananas and plantains destroying almost 98% in the affected areas. Tree crops and vegetables were also severely affected. Damage was done to water, telecommunications and electricity. SVG also experienced a rainstorm in April 2011 about six month after Hurricane Tomas which caused severe flooding, landslides and the destruction to several bridges in some of the same areas affected by the hurricane. This disaster costed about EC$84 million. On 24th and 25th December, 2013 a tropical trough system produced heavy rains in Saint Vincent and the Grenadines (SVG). Local rainfall stations reported between 200mm and 310mm in a matter of 2 – 3 hours on the north windward side of the island and up to 153.3mm in the north leeward side of the island, which resulted in intense flooding across the island. The ensuing rapid and intense flash flooding resulted in severe damage and 9 confirmed deaths with 3 persons still missing. Additionally, there is widespread damage to road infrastructure, electricity and water infrastructure, housing as well as public and private buildings.

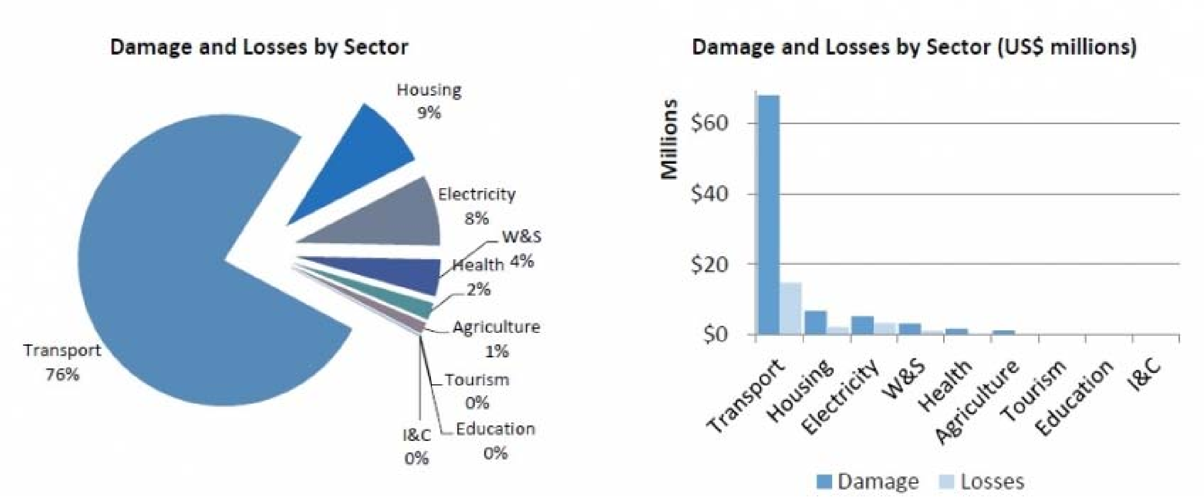

Figure 3-4: Summary of the Damage and Loss report for the 2013 "Christmas Eve trough" event (World Bank, 2014)

According to the summary of the data reported from each affected sector, the December 24-25, 2013 flood event resulted in total damages and losses of US$108.4million (EC$291.4 million), equivalent to 15% of the country's gross domestic product (GDP). Most of the flood damage was sustained in the infrastructure sector (97%) - followed by the social (3%) and productive sectors (<1%). However, as in the case with any rapid assessment following a major event, re-construction/rehabilitation works contingencies – particularly in the transport sector, could potentially increase the total damages reflected in this report by up to 15%

Summary

The preliminary results of the data collection on disaster events are presented in this section and all data are aggregated into a single table (Table 3-5). The data covers a long period starting in the 18th century. For many of the historical events it was possible to reconstruct the date of occurrence. This is important in order to correlate these dates of occurrence with rainfall data for the same period.

Finally, Table 3-5 provides the compiled historical disaster data for Saint Vincent, derived from many sources. The table also indicates for the various events whether there were indications of landslide occurrence, and if so whether the location of the landslides are known. Unfortunately this is not the case for most of the events. We believe that this catalogue is the most comprehensive that was made for Saint Vincent until now.

Table 3-5: Historical disaster events collected from different sources (NI = No Information). C = casualties. Red records (may) have landslides reported.

day	month	Year	Events	Information available	Deaths	Affected	damage	landslides	floods
?	?	1718	Volcanic eruption Soufriere	Major explosive eruption. Unknown number of casualties					
		1812	Volcanic eruption Soufriere	Major explosive eruption. Major damage to sugar industry	80				
9	9	1874	Tropical Storm	Heavy Rain					
1	1	1876	Tropical Storm	Heavy Rain for 2 days					
16	8	1884	Tropical Storm	NI					

15	8	1886	Tropical Storm	110mph from the ENE					
30	7	1887	Tropical Storm	NI					
11	9	1887	Tropical Storm	NI					
6	9	1895	Tropical Storm	NI					
15	9	1895	Tropical Storm	NI					
28	10	1896	Tropical Storm	Heavy Rain					
?	?	1897	Tropical Storm	Cyclone					
11	9	1898	Hurricane	110mph from the ESE killing 100 people	100				
8	5	1902	Earthquakes and volcanic activity Soufriere volcano	Major explosive eruption. !565 deaths. Considerable damage to sugar industry.	1565		US $ 200 Million		
16	10	1916	Tropical Storm	Heavy Rain					
8	9	1921	Hurricane	80mph from the S.E					
		1928	Earthquake	NI					
		1939	Earthquake	NI					
		1946	Earthquake						
		1953	Earthquake						
5	10	1954	Hurricane Hazel	hits just south with 80mph winds from the east					
23	9	1955	Hurricane Janet	levels the area with 115mph winds press 28.90	122			x	
30	5	1957							
5	7	1963	Storm	NI					
24	9	1963	Hurricane Edith	NI					
1	9	1962	Heavy rain	Heavy Rain					
26	6	1962	Tropical Storm	NI					
17	9	1967	Hurricane Behulah	18'' of rain in 12 hours	2		US $ 4.5 million		
17	10	1971	Volcanic activity	Moderate explosive eruption	0	2000 10000 evacuated	40% decline in agricultural production		
13	5	1974	Heavy rains	heavy Rains					
2	10	1974	Tropical Storm	Heavy Rains					
		1975	Drought in period 1970-1975						
18	10	1977	Heavy Rains	Heavy Rains				x	
19	10	1978	NI	NI					
14	4	1979	Volcanic eruption Soufriere volcano	Moderate explosive eruption. No casualties. 20,000 evacuated	2	20000	Us $ 100 million		
11	8	1980	Hurricane Allen	passes just north with 130mph winds on Aug 4th from the ESE	0	20500	US $ 16.3 million		
1	5	1981	Tropical Storm	NI					
8	9	1986	Tropical Storm Danielle	Landslides, damage to pipelines and hydropower projects				x	
?	9	1987			0	1000	5000000	x	
21	9	1987	Hurricane Emily	NI	0	208	5300000	x	
?	11	1987	NI	NI					
22	8	1988	Previous Heavy Rains	Heavy Rains					

22	10	1988	Heavy Rains	Heavy Rains					
28	9	1990	Heavy Rains	Heavy Rains					
26	8	1991	Heavy Rains	NI					
24	10	1991	Torrential Downpours	NI					
21	9	1992	Heavy Rains	NI				x	
29	11	1992	Flood		3				
26	8	1995	Tropical Storm Iris	NI					
8	9	1996	Incessant Rain	NI					
		1997	Earthquake	NI					
8	1	1998	Torrential rainfall	NI					
17	11	1999	Hurricane Lenny	NI					
29	11	2000	Torrential Downpours	NI					
4	10	2001	Tropical Depression Iris	NI					
24	9	2002	Tropical Storm	NI	4				
8	9	2004	Hurricane Ivan	NI	0	1004	EC $ 5 million		
24	11	2004	Tropical Storm	NI					
14	7	2005	Tropical Storm	NI	0	530			
		2008	Tropical Storm/ hurricane Omar	30 boats destroyed, damage along coastline	1		EC $ 5 million		
		2009	Drought	NI					
		2010	Drought	NI					
29	10	2010	Hurricane Tomas	passes just north with 80mph winds. 28 % of population affected, of which 5% severe.	9	6100 1200 in shelters	EC $ 130 million (10.5% GDP)		
8	1	2011	Landslide (17) and flood (21 reports)					17	21
8	2	2011	Landslide (13 reports) and flood (8)					13	8
8	3	2011	Landslide (2 reports)					2	0
13	3	2011	Flood (1 report)					0	1
28	3	2011	Flood (1 report)					0	1
5	4	2011	Flood					0	0
8	4	2011	Landslide & flood (2 reports)					1	1
11	4	2011	Tropical Storm , landslides	NI	0	275			
13	4	2011	Landslide (5) and flood (39 reports)					5	39
14	4	2011	Landslides (7) and flood 39 reports)					7	32
16	4	2011	Landslide (2) and flood (32 reports)					2	15
18	4	2011	Landslide (3) and flood (4 reports)					3	4
19	4	2011	Landslide &flood (2 reports)					1	1
20	4	2011	Flood (1 report)					0	1
21	4	2011	Flood (2 reports)					0	2
23	4	2011	Flood (5 reports)					0	5

24	4	2011	Flood and landslide (2 reports)					1	1
28	4	2011	Flood					0	0
5	5	2011	Flood					0	0
16	6	2011	Landslide (2 reports)					2	0
1	7	2011	Landslide (1 report)					1	0
14	7	2011	Flood (1 report					0	1
16	8	2011	Flood (1 report)					0	1
22	8	2011	Landslide (1 report)					1	0
16	9	2011	Landslide and flood (2 reports)					1	1
17	9	2011	Landslide (1 reports)					1	0
1	10	2011	Landslides (2 reports)					2	0
25	10	2012	landslides	Boat bay, 3					
5	9	2013	flood					x	
5	10	2013	Flooding	E.T. Joshua airport was flooded. Landslides at Belmont, Belair, Calder ridge and La Croix				x	x
25	12	2013	Christmas Eve trough. Tropical Storm, flooding, landslides	Heavy Rain 200 to 300 mm in two hours	12	17422 500 displaced	US $ 108.4 m Million EC $ 330 million	x	x
2	1	2014	Massive floods					x	
2	5	2014	Drought						
22	8	2014	Flood					x	
12	9	2014	flood					x	

1.4. Rainfall frequency analysis

The study area is characterized by a humid tropical climate. The rainy season is normally from May to November, when the rainfall intensity is concentrated over a short period which triggers most of the landslides, flooding, and erosion in the study area.

St Vincent has several stations but of only one station data was obtained in this project: Joshua Airport at Arnos Vale. Of this station, 21 years of daily data (1987-2008) was used in a frequency magnitude analysis, using a Gumbel analysis and Generalized Extreme Value analysis. Because of the limited time series, the maximum return period considered was 1:50 years. This is also consistent with the other islands in the CHARIM project.

A Gumbel distribution was fitted to the data of the station, which is a special case of Generalized Extreme Value distributions, suitable for right hand skewed datasets (such as rainfall, which cannot be less than 0, but can have extreme maxima). The Gumbel distribution assumes a double logarithmic relation between the maximum rainfall R and the return period T. The return period is the inverse of the occurrence probability P. Figure 3-5 shows the Gumbel analysis of the Joshua Airport station with a reasonable linear fit between the log-log values of the return periods and the maximum daily rainfall.

The highest 3 maximum daily rainfall values are related to known tropical storms and hurricanes. Hurricane Ivan in 2004 passed over the island and caused a lot of devastation. Hurricane Lili caused devastation on St Lucia and Dominica, and also St. Vincent and the Grenadines were heavily damaged, especially compared to other islands in the area. Several hundred homes and two schools were damaged, and the Rose Hall Police Station's roof was lost (NOAA hurricane data).

Similar to the other islands a Generalized Extreme Value (GEV) analysis was done to determine return periods. The GEV analysis is better suited to extremely skewed distribution than the Gumbel analysis (Gumbel is a special case of GEV). In the interest of consistency of method, the results are shown in Figure 3-6. The GEV fit parameters of the Joshua Airport station are: mu = 83.0, sigma = 27.7 and k = 0.299.

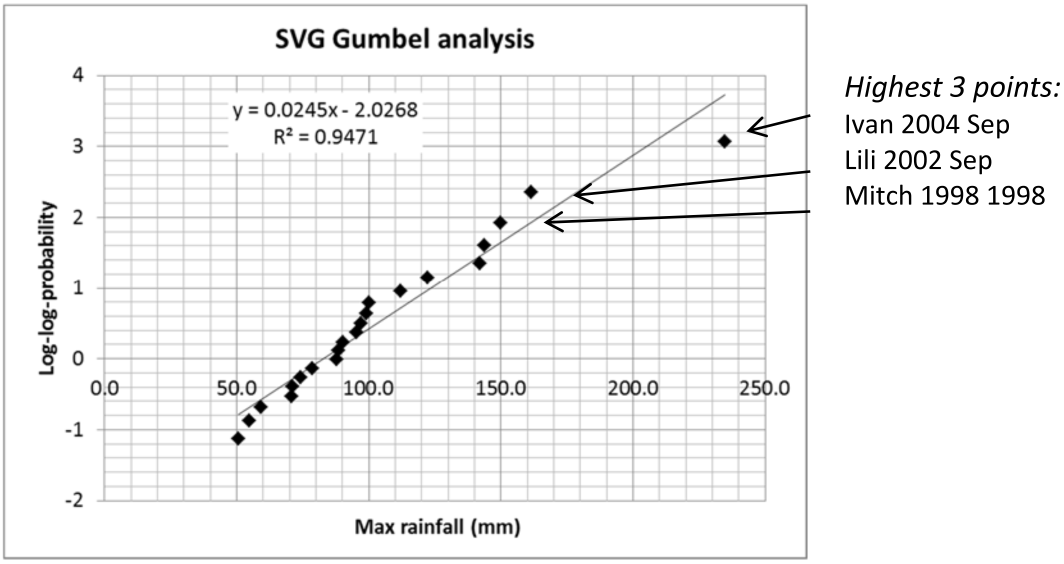

Figure 3-5. Gumbel analysis of maximum daily values of Joshua Airport station (21 years: 1987-2008). The highest 3 maximum daily rainfall are related to known tropical storms and hurricanes.

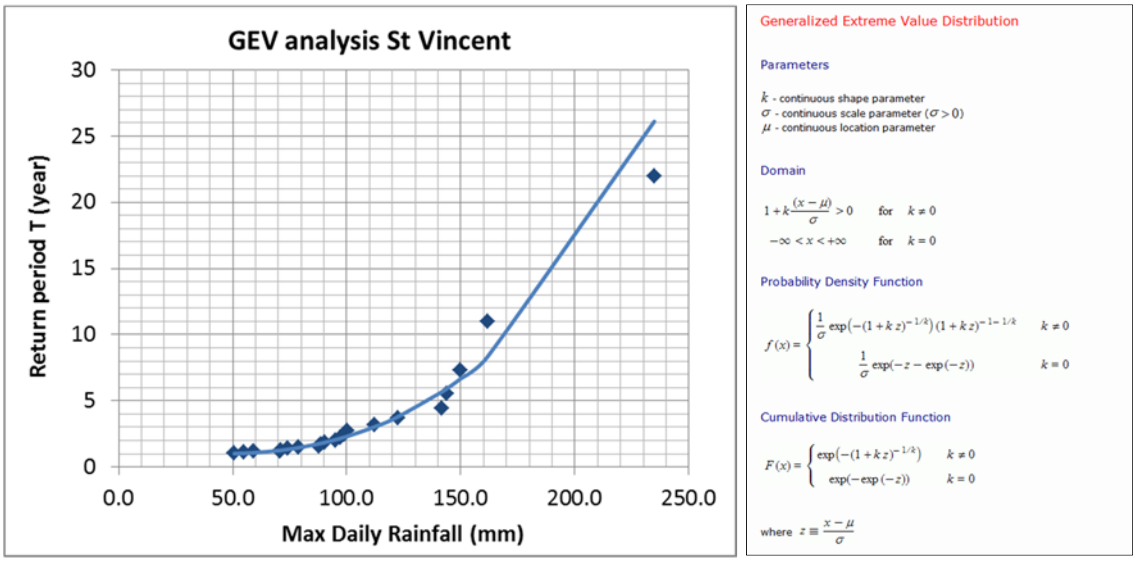

Figure 3-6. GEV analysis of the Arnos Vale station and resulting daily total values.

It is not known if this is representative for the west coast and east coast of the island, although possibly the exposure to hurricanes form the Atlantic might be a reason for higher rainfall at the east coast. This is speculative as the entire weather system of the Caribbean is affected by Hurricanes and tropical storms. On St Lucia and Dominica analysis exist that shows that there is an increasing rainfall towards the interior with the orographic effect of the central mountains, at least for the annual totals. Whether that is also true for individual rainfall events is not known, but some of the hurricanes and tropical storms are far larger than the islands and orographic effects may not be present for these magnitudes.

Looking at the return period analysis of the four islands in CHARIM (Grenada, St Vincent and the Grenadines, St Lucia and Dominica), a north south gradient can be clearly seen in the design storm depth based on the analysis of daily maxima (Figure 3-7). A possible explanation lies in the nature of hurricanes and severe tropical storms, they cross the Atlantic at the equator and veer north due to Coriolis forces. They influence local weather systems as well, which possibly leads to a North-South gradient in amount of rainfall in the Caribbean. However, it should be noted that apart from Saint Lucia, the other islands have only 1 or 2 stations with long records, normally near the airport or the capital. A north-south trend should be seen as a possible indication at best.

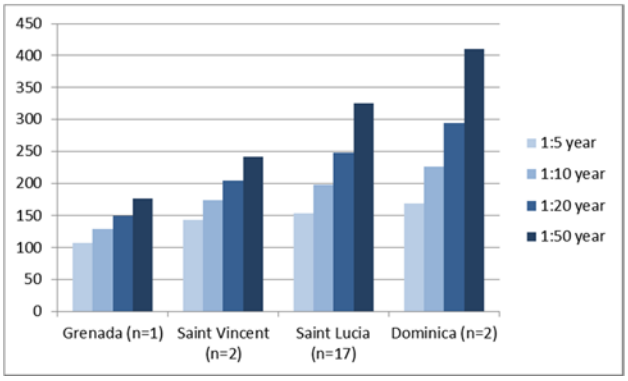

Figure 3-7. Return periods and daily maxima from GEV analyses of rainfall stations at the 4 islands in CHARIM.

As we have seen in other countries (e.g. Dominica) there is a clear relation between elevation and exposure and rainfall amount, as rainfall amounts increase with increasing elevation, and also tend to be higher on the windward side than on the leeward side. Therefore the return periods that have been determined for the rainfall stations at Joshua Airport, may not be representative for those in other elevations and other exposures on the island. Unfortunately there is not enough data to generate magnitude-frequency relations for different parts of the island. In future, this should get more attention, as this has important implications for flood and landslide hazard assessment. Different watersheds in the area might have different magnitude-frequency relations. Also the spatial pattern of rainfall amount during extreme events is important to know as the correlation of causal factors with landslides triggered during these events, could lead to entirely different conclusions when rainfall distribution can be taken into account.

Rainfall thresholds

Rainfall thresholds can be defined on physical (process-based, conceptual) or empirical (historical, statistical) bases (Corominas, 2000; Crosta and Frattini, 2001; Aleotti, 2004; Wieczorek and Glade, 2005). The determination of rainfall thresholds for landslide initiation is considered as a basic task in landslide hazard assessment, and various methods have been proposed to establish rainfall thresholds (Dahal et al., 2008; Guzzetti et al. 2007; Zezere et al. 2005; Giannecchini et al. 2012; Frattini et al. 2009; Crosta 1998; Corominas and Moya 1999; D'Odorico and Fagherazzi 2003; Glade 2000; Godt et al. 2006; Marques et al. 2008; Saito et al. 2010). In general, they can be classified into five threshold groups: (1) empirical; (2) physical-based; (3) intensity duration; (4) normalized intensity-duration; and (5) antecedent rainfall. For rainfall threshold estimation, the four most common variables used in the literature are as follows: daily rainfall (Dahal and Hasegawa, 2008), antecedent rainfall (Glade, 2000), cumulative rainfall (Polemio and Sdao, 1999), and normalized critical rainfall (Aleotti, 2004). The selection of the right parameters in constructing rainfall thresholds is mainly dependent on the landslide type (Martelloni et al., 2011) and on the environmental conditions. One of the largest difficulties when using antecedent rainfall for landslide prediction is to determine the number of days to be used (Guzzetti et al. 2007). A detailed literature review revealed a complex relationship on the correlation between the numbers of days for the antecedent rainfall with the triggering of a landslide. Different authors such as Glade (2000), Aleotti (2004) considered antecedent days ranging from 1 to maximum 15 days. Zezere et al. (2005), Polemio and Sdao (1999) considered until 180-day cumulative daily rainfall data. In summary, antecedent rainfall between 3 and 120 days could be significant for explaining the landslide occurrence (Dahal et al. 2009). The large variability on the number of antecedent rainfall days may be influenced by factors such as (i) diverse lithological, morphological, vegetation, and soil conditions, (ii) different climatic regimes and meteorological circumstances leading to slope instability, (iii) and heterogeneity and incompleteness in the rainfall and landslide data used to determine the thresholds (Guzzetti et al., 2007).

Unfortunately we do not have sufficient landslide dates (See table 3-2) that fall within the period for which rainfall data is available (1986-2014) to be able to evaluate possible rainfall thresholds for landslides in Saint Vincent. Also a correlation between landslide numbers and landslide densities and triggering rainfall characteristics (amount of daily rainfall, and related return period) is not possible, as we basically have only one event that might be represented as a landslide inventory. Even for this event it is not clear whether it captures landslides during Hurricane Ivan (2004) or Hurricane Emily (2005) and therefore the relation with rainfall and return period is also a bit problematic. If we assume a rainfall amount of 256 mm for this event, the landslide triggering event would represent a return period of more than 100 years.

4. Landslide inventory mapping

Landslide inventories are the basis for assessing landslide susceptibility, hazard and risk (Soeters and Van Westen, 1996; Aleotti and Chowdury, 1999; Ardizzone et al., 2002; Dai and Lee, 2008; Galli et al., 2008; Van Westen et al., 2008). They are essential for susceptibility models that predict landslide on the basis of past conditions. If these are not sufficiently available more emphasis should be given on expert assessment and evaluation. Therefore we need to know where landslides happened in the past. The conditions under which landslides happened in the past are analyzed and the relevant combinations are used to predict future ones. We need to understand the causal relations between landslides and the causal factors. These conditions differ for different landslide types, and therefore landslides should be classified into different types. Temporal information is essential to estimate the frequency of landslides. Therefore we need to know when they happened. Landslide inventories are also used to validate landslide susceptibility, hazard and risk maps.

Landslides are generally isolated, rather small events. In a tropical environment such as Saint Vincent they are visible for some time but quickly become difficult to recognize. Fresh landslide scarps become overgrown by vegetation within a few years after they happen. Signs of landslides become also difficult to interpret from images, when the image is taken more than a few months after the landslide occurrence. On the other hand major triggering events such as tropical storms might cause many landslides at the same time, and then it is important to rapidly map the landslides triggered by that event so that we can link the temporal probability of the triggering rainfall to the spatial probability of landslide occurrence.

4.1. Available landslide inventories

In many of the eastern Caribbean countries there is no single agency that has the responsibility for maintaining a landslide database. This is one of the major problems in Saint Vincent as well. No agency feels responsible to collect landslide locations and dates, and keep a database up-to-date. The National Emergency Management Organization (NEMO) seems to maintain a database of emergencies. This is the case both for mapping landslides in the rural areas, as well as for collection landslide data along the road network. The Ministry of Transport and Works doesn't convert the road maintenance reports into an updatable landslide database. Therefore the valuable data on landslide locations and occurrence dates is quickly lost. That is why all landslide inventories have been generated by consultants, organizations and individuals from outside the islands.

For Saint Vincent we have found only one landslide inventory map generated in 1988 by DeGraff (1988). He did this with support from the United States Forest Department, in Dominica, Saint Lucia and Saint Vincent. No attempt is made to discriminate recent from older landslides. Landslides were interpreted from black & white aerial photographs of 1:20,000 scale taken in 1981, covering the entire country except for certain parts of Soufriere volcano. The aerial photography was generally of good quality and allowed to identify and classify landslides. A detailed field investigation was made in 1988 and nearly all roads were traversed. The mapping reflects the situation during the image interpretation of 1981, which was carried out one year after the occurrence of Hurricane Allen (11/8/1980) which passed just north with 130mph winds from the ESE, and during which 20500 person were affected, and resulting in US $ 16.3 million damage. Two years prior to the aerial photographs was an eruption of Soufriere volcano (14/4/1979)/ this moderate explosive eruption caused 2 casualties, 20,000 persons were evacuated, and the damage was estimated at US $ 100 million. The fieldwork in 1988. Between the dates of airphoto acquisition (1981) and fieldwork (1988) there were several major events, especially Tropical Storm Danielle (8/9/1986) which caused reported landslides, damage to pipelines and hydropower projects , and Hurricane Emily (21/9/1987) which caused US $ 5.3 million damage. Given the above, we can conclude that this landslide inventory is not an event-based inventory, but is a compilation of landslides caused by a number of different triggering events. The landslide types were indicated with two degrees of certainty, and with landslide types following the classification of Wieczorek (1984). We checked the landslide locations using visual image interpretation of satellite images and Google Earth. For a number of them it was quite difficult to associate them with landslides. The inventory is shown in Figure 4-1.

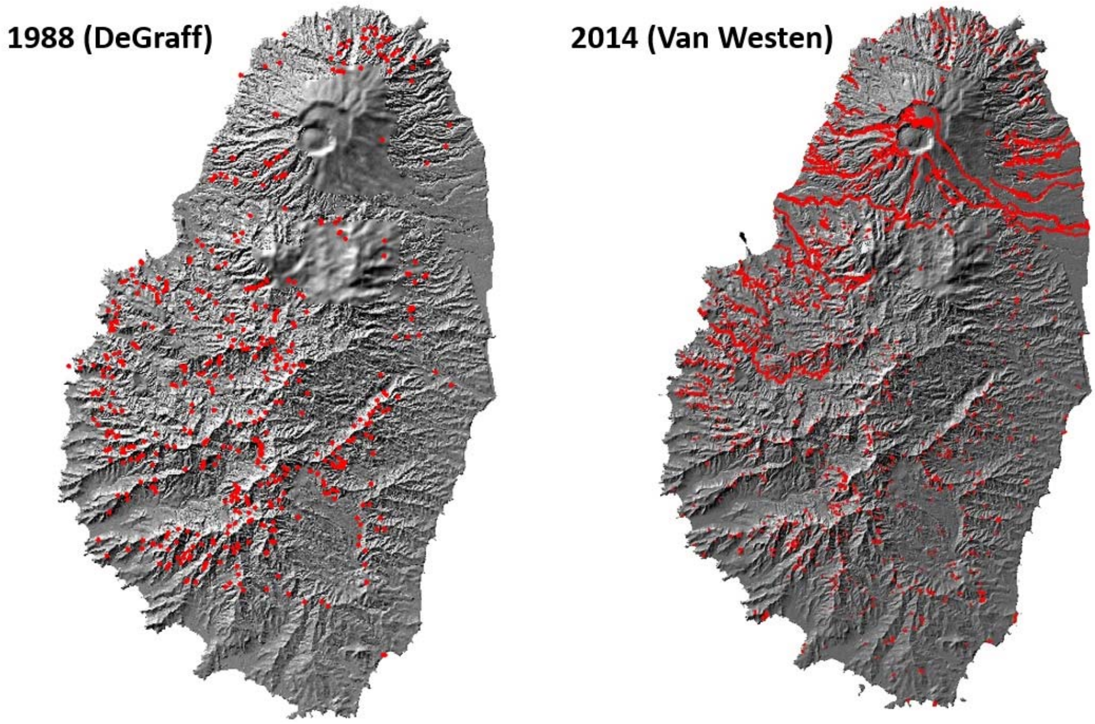

Figure 4-1: Landslide inventory maps for Saint Vincent Left: the map generated by DeGraff (1988). Right: landslide inventory map generated by ITC. .

4.2. New landslide inventory mapping

The available landslide inventory presented in the previous section is quite limited. Landslides are shown as points, and all are concentrated along the road network. Therefore we decided to generate a landslide inventory for the entire island.

The generation of landslide inventories and a landslide database that covers a certain period of time is a tedious procedure. The methods that are considered useful for the generation of landslide inventory maps can be classified into the following main groups (Van Westen et al., 2008):

- **Image interpretation** from aerial photographs, high resolution satellite images, or hillshading images derived from detailed Digital Elevation Models. Also image interpretation using multi-temporal images from Google Earth has become a useful tool for landslide inventory mapping.
- **(Semi) automatic classification** of landslides from satellite images or Digital Elevation Models.
    - o Based on spectral information by detecting fresh landslide areas from multi-spectral satellite images;
    - o Based on altitude information by detecting landslides from multi-temporal high resolution (LiDAR) DEMs, or through radar interferometry
- **Field investigation**, by mapping landslide signs, scarp area, accumulation areas, and verification of landslides mapped through image interpretation and/or classification;
- **Community reporting**, by interviewing local people on locations, dates and impacts of past landslide event;
- **Archive studies**, by studying newspaper archives, old reports, road maintenance reports etc., as explained in chapter 2.

The method used for generating the landslide inventory in Saint Vincent is illustrated in Figure 4-2. We started by collecting all available landslide inventories. But, as these were in most cases not sufficiently, reliable or available, we also decided to collect landslide inventories ourselves. This was done using image interpretation and field work. Image interpretation played a major role in generating updated landslide inventories.

Image interpretation can be defined as the study of the imaged objects of the earth surface, the extraction of those features relevant to the object of study, the analysis of the selected features with the objective to come to a deduction of their significance for the specific field of study (Soeters and Van Westen, 1996). Stereoscopic image interpretation is important tools to recognize and map landslides. The interpretation of images is an empirical and subjective process. It is a systematic scanning of a stereo model assisted by logical and scientific evidences. Stereo image interpretation (API) is an art as much of a science, and it requires well trained, experienced investigators.

We obtained through the EU FP7 Copernicus project INCREO (http://www.increo-fp7.eu/) the possibility to order very high resolution satellite images (Pleiades images, with 0.5 m spatial resolution for panchromatic and 2 m multi-spectral) for Saint Vincent (See Table 4-1). We received the images that were obtained in the 2014. The most important images however, were the various images in Google Earth.

Table 4-1: Available satellite images for Saint Vincent

Satellite	Date	Type	Columns, Rows
Pleiades	2014 02 23	0.5 meter panchromatic 2 meter multispectral. Covers whole island	12507, 16250
Google Earth data	From different years: with oldest one from 1970, and most from 2000 onwards	Covering different parts of the island, with varying degree of cloud cover, resolution and contrast.	

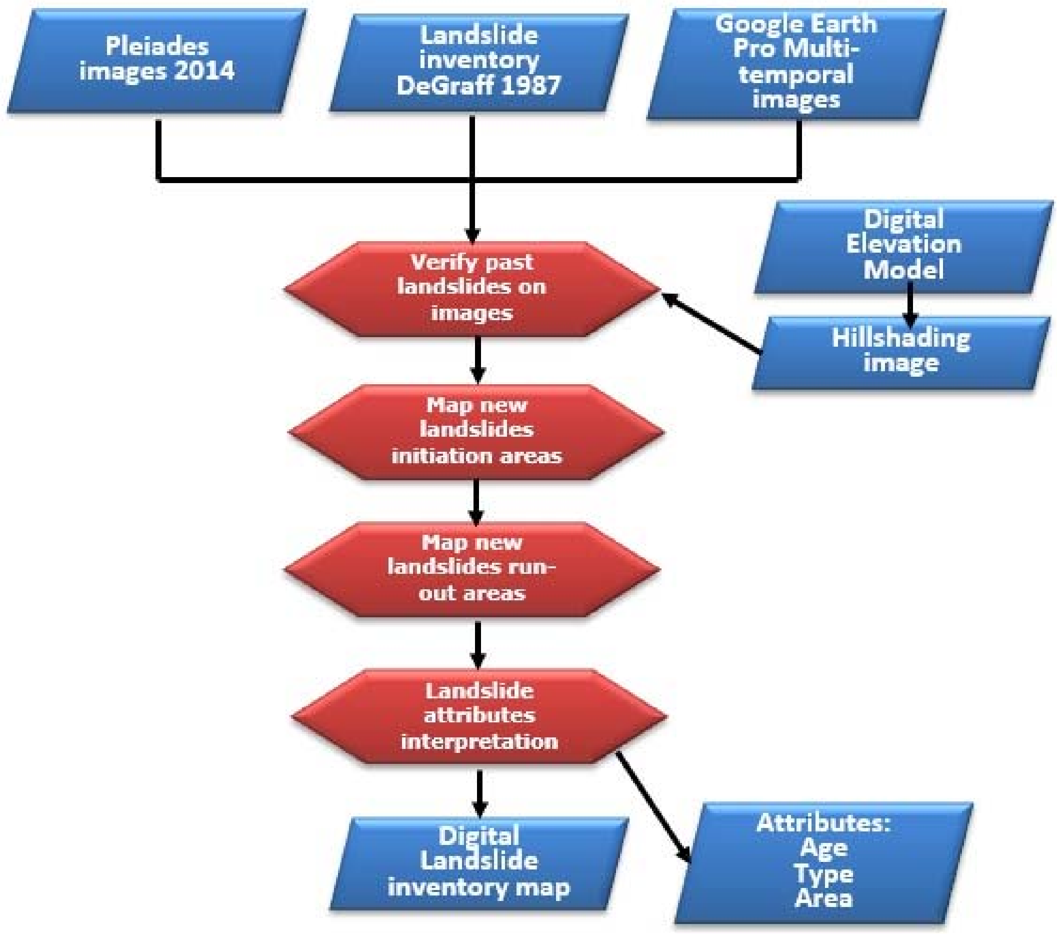

Figure 4-2: Method used for the generation of a landslide inventory map for Saint Vincent

Figure 4-3 gives some examples of image interpretation issues related to the mapping of landslides using images from different periods. Figure 4-3 shows an example of mapping the effect of the 2013 Christmas eve landslide and flood event event for the are around Spring village (St Patrick) where a flashflood / debris flows destroyed a number of components of the hydropower system. Figure 4-3 B shows a number of landslides in the upstream area in the vicinity of Hermitage. Figure 4-3 C shows a series of debrisflow and associated landslides on the flanks of Soufriere volcano near Morne Ronde – Wallibou. The active debris flows fans in the the shore area can be clearly observed. Also the shaded relief map that we produced from the detailed Digital Elevation Model (with pixel size of 5 meters) derived from LiDAR data, turned out to be very useful for mapping older landslide features, that were covered by vegetation but where the bare surface model still showed clear signs of landslide activity.

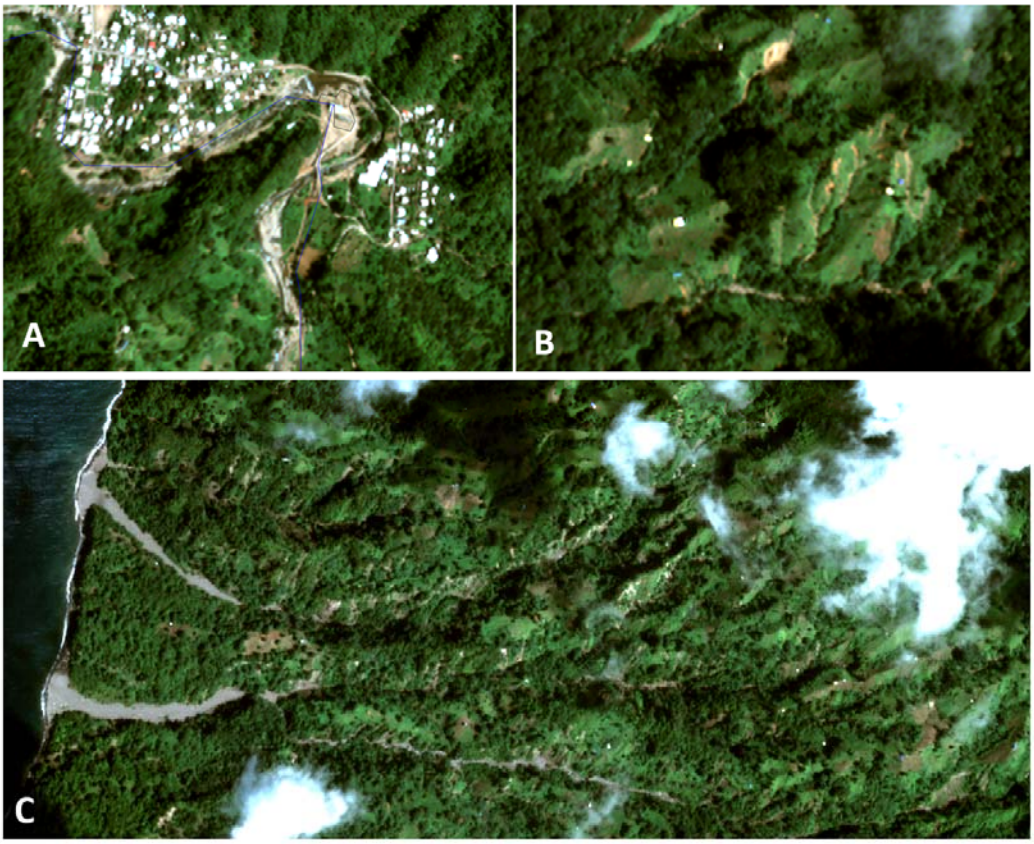

Figure 4-3: Example of high resolution satellite images taken in 2014, to map features from the 2013 Chrismas eve event. A: Spring village, B: area near Hermitage, C: Morne Ronde – Wallibou.

Unfortunately, as will be discussed later, the quality of the DEM was not equally everywhere good due to missing data. We incorporated in our inventory also the landslides from the previous inventories and checked these in the images. Many of these were no longer visible on the images from later years, although when using older images, many of them could still be detected, even though many were revegetated. We interpreted the landslides as polygons, separating between scarp and body, assigning a unique identifier to each landslide and we described each landslide with a number of attributes. We made a complete classification for all landslides. Also the mapping of coastal landslides was carried out. The landslide inventories were checked in the field during a fieldwork period of 1 week in September-October 2014. During the fieldwork several of the features that were identified through image interpretation as potential landslides, were actual bare field or other features. As the interpretation focused not only on the absence of vegetation in potential landslide areas, but more on the morphological characteristics of old landslides, many more landslides were interpreted.
The resulting landslide inventory map is shown in Figure 4-5, and 4-6. Table 4-2 gives a summary of this landslide inventory that includes the previously mapped landslides.

Table 4-2: Summary of landslide inventories with number of landslides indicated.

Type	1988 DeGraff	2014 Mapped	Total
Absent	4	0	4
Debris Flow	390	1011	1401
Debris Landslide	75	383	458
Deep seated Rockslide	59	60	119
Rockslide	26	100	126
Shallow Landslide	0	61	61
Stream Flood Debrisflow	0	17	17
Unknown	0	15	15
Total	554	1647	

4.3. Some examples of landslide characteristics in Saint Vincent

This section gives some illustrations of landslide examples in Saint Vincent.

Landslide at Belmont

The Belmont embankment was constructed in 1970 and it collapsed in September 2013. Water supply to 11 communities was disrupted, and the main road to Mesopotamia and the Windward Highway was blocked. The embankment was constructed with a height of approximately 25 meters, and embankment inclination angle of about 77 degrees. The natural slope profile angle of 65 degrees was measured from the existing slope. The geology along this part of the road embankment is typical of the area, consisting of the alluvial and reworked deposits formation. The embankment was constructed by cut and fill method. Material in the embankment was observed to be typical of the material on the adjacent cut slope. This material consists of slightly humid, brownish red, clayey sandy materials with a few highly weathered corestones. Drainage pipes daylight on the embankment slope face. A channel was dug and buried on top of the remaining road embankment mass structure for a domestic water pipe. Part of the material from this channel has clogged the drainage channel and culverts. This has led to a further recharge of water into the remaining embankment mass. The remaining segment of the road embankment showed a slight tilt towards the slope face. Progressively, this might result into another slide or slip (Figure 4.4). The most important factors for the occurrence of the landslide are the weathering of materials, leading to a deterioration of geotechnical parameters, ground water recharge from precipitation, leaking drainage pipes, and the method of construction and height of the embankment (Mulenga, 2015). The Belmont landslide occurred on a critical spot and interrupted the road connection from Mesopotamia and surrounding densely populated areas with the capital Kingstown, and also the fastest Windward highway connection to Georgetown from Kingstown. The alternative roads are much longer, although the main traffic along the Windward highway now passes by the new Argyle airport. Nevertheless, it is quite important to stabilize the Belmont landslide and re-establish the connection. This is currently being considered using World Bank funding. The procedure for analysing landslide mitigation measures for roads, illustrated with the Example of Belmont landslide, is discussed in http://www.charim.net/use/333

Figure 4-4: The Belmont landslide.

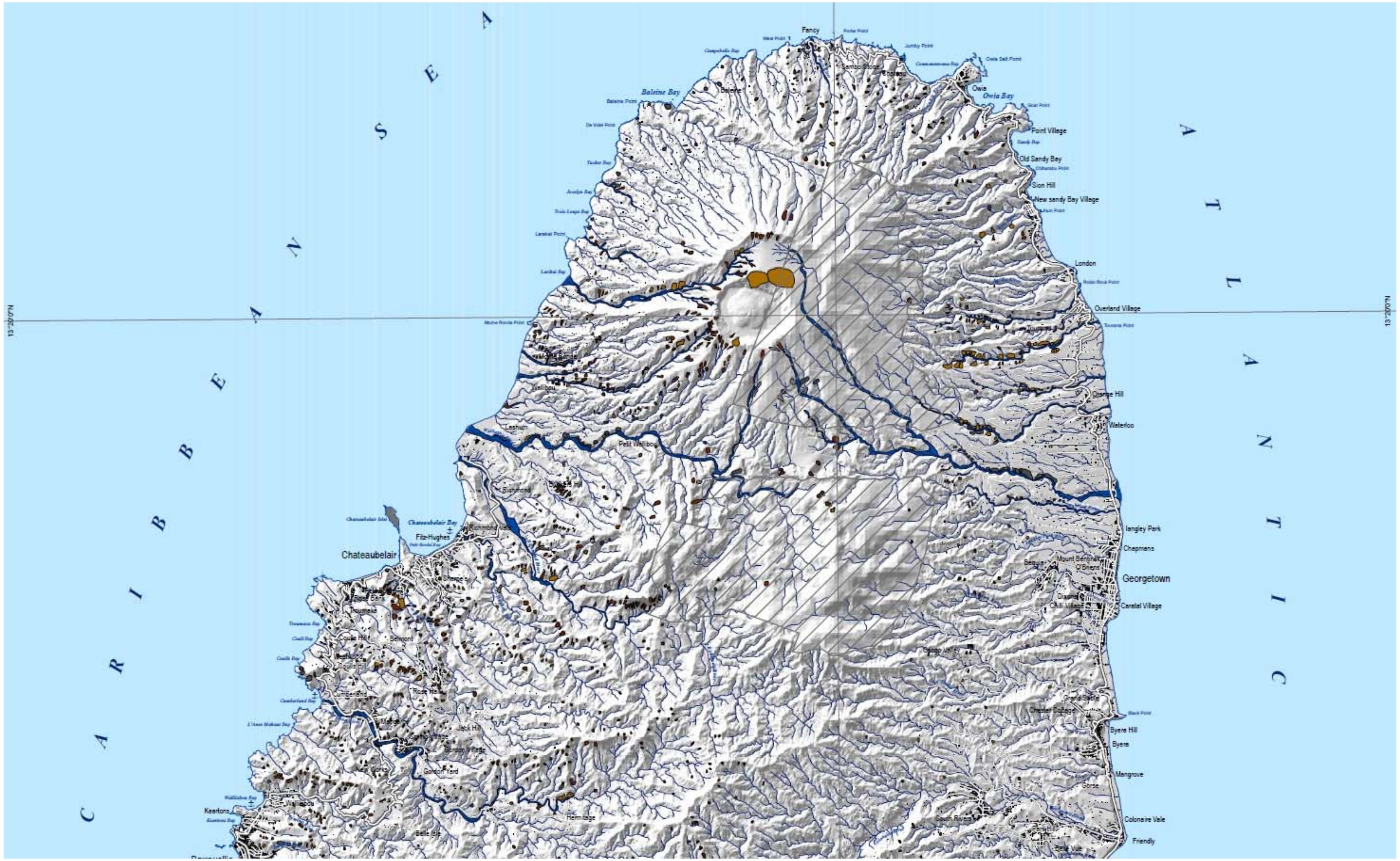

Figure 4-5: Northern part of the landslide inventory map for Saint Vincent. The full map can be downloaded as pdf from the following website: http://www.charim.net/stvincent/maps

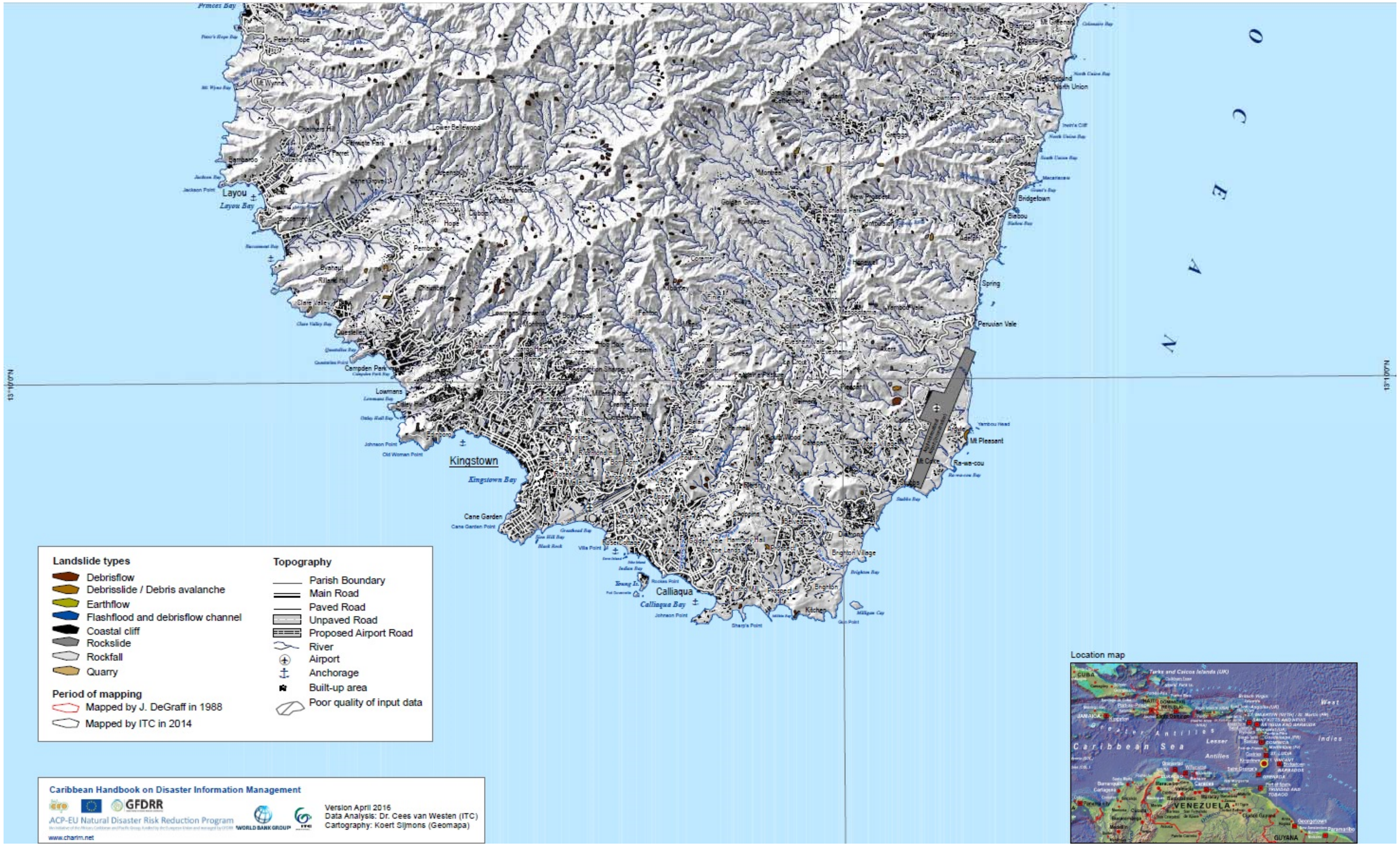

Figure 4-6: Southern part of the landslide inventory map for Saint Vincent. The full map can be downloaded as pdf from the following website: http://www.charim.net/stvincent/maps

Landslides on the slopes of Soufriere volcano

Figures 4-7 and 4-8 show two examples of landslide inventory maps generate for the western (Figure 4-7) and eastern (Figure 4-8) slope of Soufriere volcano, displaying in particular the large number of landslides visible on the 2014 high resolution satellite images (Pleiades) which may be caused by the 2013 Christmas eve rainfall event. The debris slides provide sediment to several debris flow and flash flood channels.

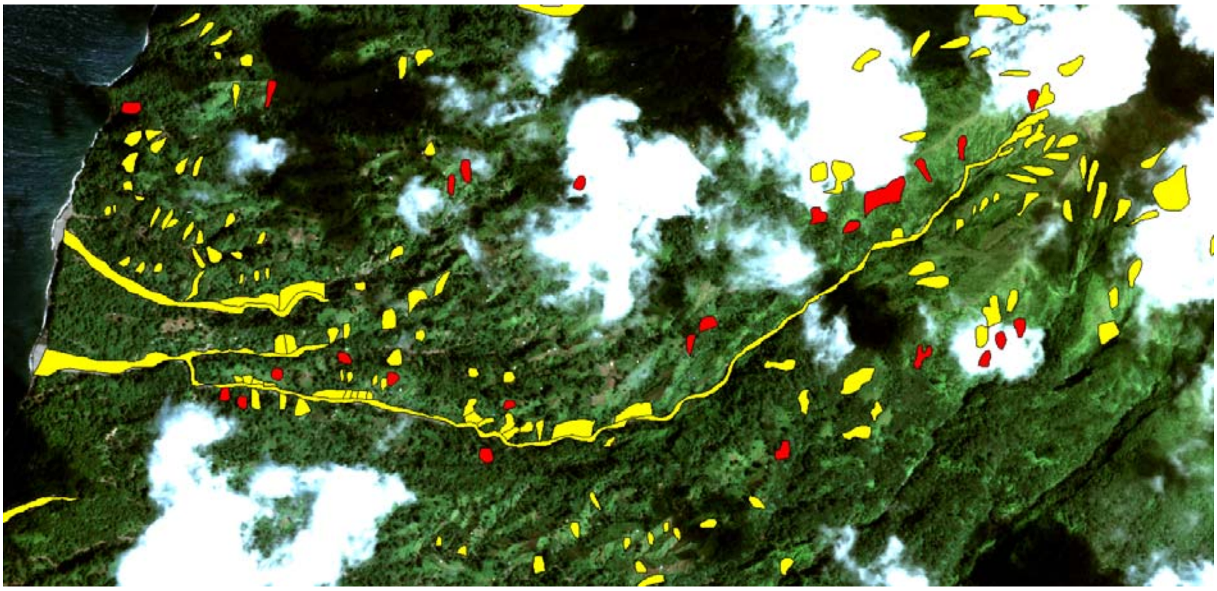

Figure 4-7: Example of interpreted landslides for the western slope of Soufriere volcano in SVG. The red colour are landslides mapped by DeGraff in 1987 and yellow polygons are the landslides mapped by Van Westen in 2014.

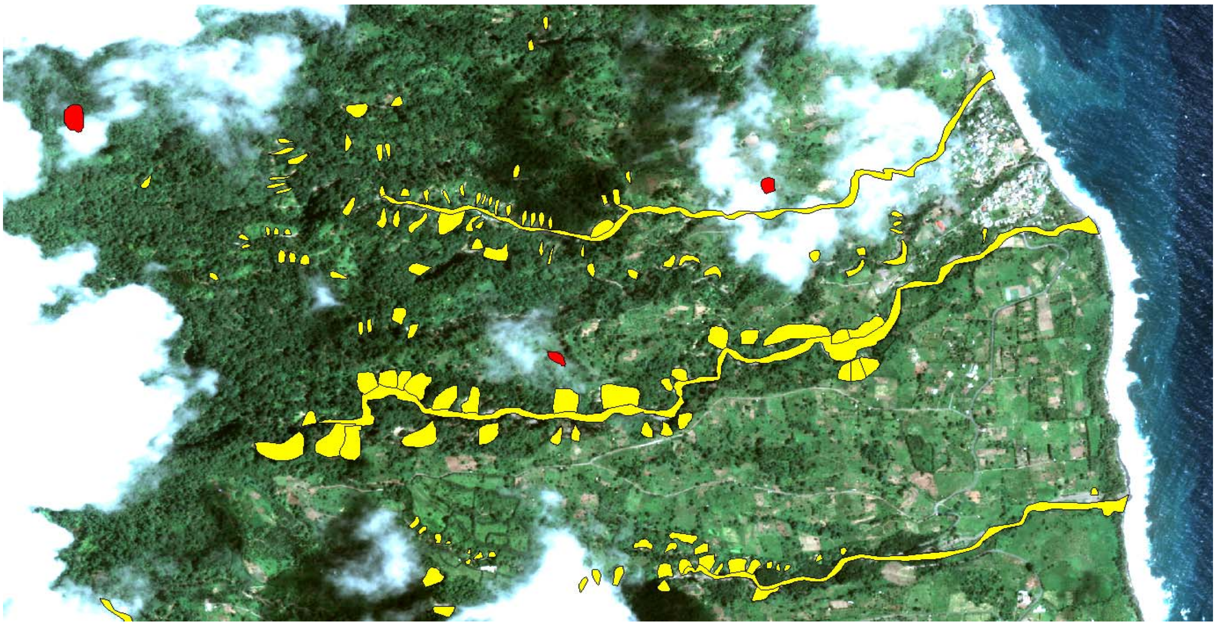

Figure 4-8: Example of interpreted landslides for the eastern slope of Soufriere volcano in SVG towards Overland Village. The red colour are landslides mapped by DeGraff in 1987 and yellow polygons are the landslides mapped by Van Westen in 2014.

Manning village relocation site

Another landslide tragedy that occurred during the 2013 Christmas eve trough, occurred in the village of Manning, which is a relocation site, where residential buildings were constructed to house families that were resettled from a coastal settlement which was too close to the coast, and under threat of storm surge. A landslide from the upper slope, close to the road, had a long runout and hit one house, killing a 62 year old resident in the bedroom. This event exemplified the difficulty of finding completely safe relocation sites, and the need for a detailed hazard assessment of possible relocation sites.

Figure 4-9: Manning village relocation site affected by landslide.

Landslide along the Leeward road

During the 2013 Christmas Eve event five, ranging in age from 18 to 73 people died in a landslide in Rose Bank, which was triggered in a slope above the road, traversed the road and destroyed a building before hitting the road below again.

Figure 4-10: Landslides along the Leeward road, Left: landslide near Upper Vermont village, right: at Rose Bank.

Further events during the Christmas Eve 2013 event

Apart from landslides there were also several flooding problems during the 2013 Christmas Eve event. In Vermont a flash flood affected a number of residential buildings, a stretch of road and several bridges. One person was killed and 15 were injured in the event. Fifteen houses were damaged and 9 destroyed. Also damage occurred in Georgetown, and Fancy, where a debrisflow occurred in the river valley. There was also heavy damage to three of the Central Water and Sewerage Authority distribution systems, and also the national electoral power company Vynlec reported damage to the hydropower system. The Cumberland power plant was severely damaged. Flooding also happened in the main hospital (Milton Cato Memorial hospital) and in the airport (E.T. Joshua airport).

Figure 4-12: Damage due to Christmas eve 2013 rainfall event. .

5. Landslide conditioning factors

In this chapter an evaluation is made of the available factor maps for landslide susceptibility assessment in Saint Vincent. Data was obtained in many different formats, and several different projections, from many different persons and organizations. Most of the spatial data that we obtained from the organizations in Saint Vincent were in different projections. All the data was transformed to UTM WGS84 projection, and is now available as shape files (for vector data), and GeoTIFF (for raster data), through the CHARIM Geonode (http://www.charim-geonode.net/people/profile/svg/?content=layers).
In the description of the data attention is given to the spatial, thematic and temporal accuracy of the data. A summary of the data types is given in table 5-1.

Table 5-1. Overview of input maps for landslide susceptibility assessment, with indication of their quality of the data for the island in green (good), yellow (less good), and orange (not available).

Group	Factor	Layer name	Availability and quality of the data in Saint Vincent
Topographic	Elevation classes	Elevation_Class	It has good quality but it was not updated. Quality was good.
	Distance from cliff	Cliff_dist_cl	It was obtained from a digitalized cliff map.
	Slope steepness classes	Slope_cl	Data were obtained from a DEM which has not been updated. Quality was good.
	Slope direction classes	Aspect_cl	It was available. Data were not updated. Quality was good.
Drainage	Distance from rivers	River_dist_cl	It was obtained from a digitalized stream segments with good quality and detailed level classification.
Geological	Geomorphological units	Geomorphology	It has good quality. It was available.
	Lithological units	Geology	It was available but the classes were not helpful for the analysis in case of soil landslides.
Soil	Soil use limitation	Limitations	It was available but not helpful for the analysis.
	Soil units	Soil_types	It was available and the quality was good.
	Soil erosion classes, indicated in soil legend	Soil_erosion_class	It was available but only the top soil was studied.
Land cover	Distance from coastline	Coast_dist_class	It was not available, so was obtained from the country border.
	Distance from road cuts	Roadcut_dist_cl	It was obtained from a digitalized road cuts map with two classes. It has a good quality.
	Distance from roads	Road_dist_cl	It was obtained from a digitalized road map with good quality.
	Landuse landcover map	Landcover_2014_modified	Land use / land cover generated from Pleiades images by BGS. Some parts have poor data.
	Landuse landcover map	Landcover2005	Land use / land cover generated from Landsat Enhanced Thematic Mapper Plus (ETM+) and SPOT imagery by USGS, USAID, and The Nature Conservancy.
	Landuse landcover map	Landcover2000	

Digital Elevation data

Since topographic information and its various derivatives play an important role in landslide susceptibility analysis, the use of high-resolution digital elevation models (DEMs) is crucial (Corominas et al., 2013). For Saint Vincent a LIDAR derived DEM was available. We do not have metadata for this dataset, so we don't know which consultant made the survey, with which instrument and with which point density. The point map had no data was available for the centre of the island. The points were already filtered out for the terrain elevation, so all vegetation and building points were removed. The point density was not so high (See Figure 5-1). Nevertheless the quality of the resulting DEM was quite good, and displaying the image as a hill shading map in 3-D was very helpful in outlining the landslides. The DEM had one large problem though: the centre and NE of the island was not covered by LiDAR data. We had no other digital elevation data for these areas, so we used SRTM DEM data to fill up the hole in the LiDAR data. As a consequence at the boundaries of the missing LiDAR data there are artefacts (errors in the DEM) that gave problems especially in the modelling (See Figure 5-2).

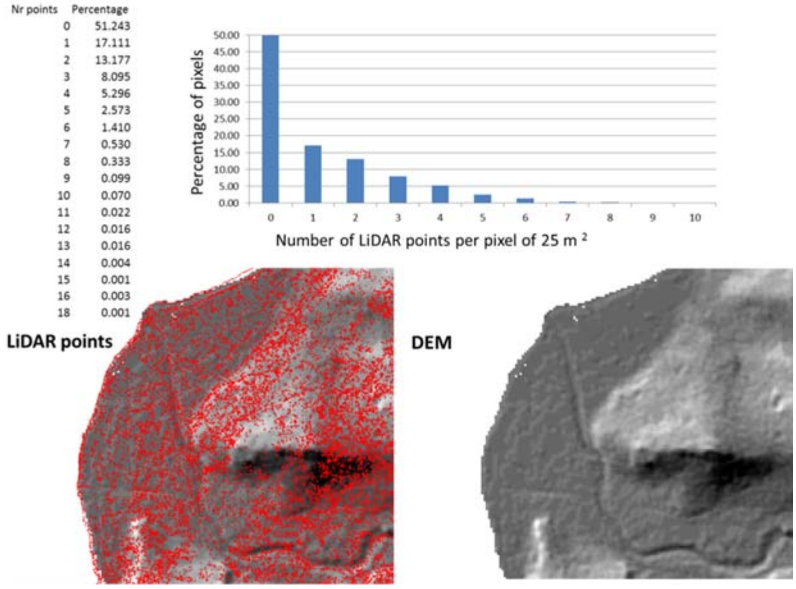

Nr points	Percentage
0	51.243
1	17.111
2	13.177
3	8.095
4	5.296
5	2.573
6	1.410
7	0.530
8	0.333
9	0.099
10	0.070
11	0.022
12	0.016
13	0.016
14	0.004
15	0.001
16	0.003
18	0.001

Figure 5-1: The Digital Elevation Model for Saint Vincent was generated from LiDAR points. The table and graph show the number of points per pixel of 25 m^2 (5 by 5 meter pixel).

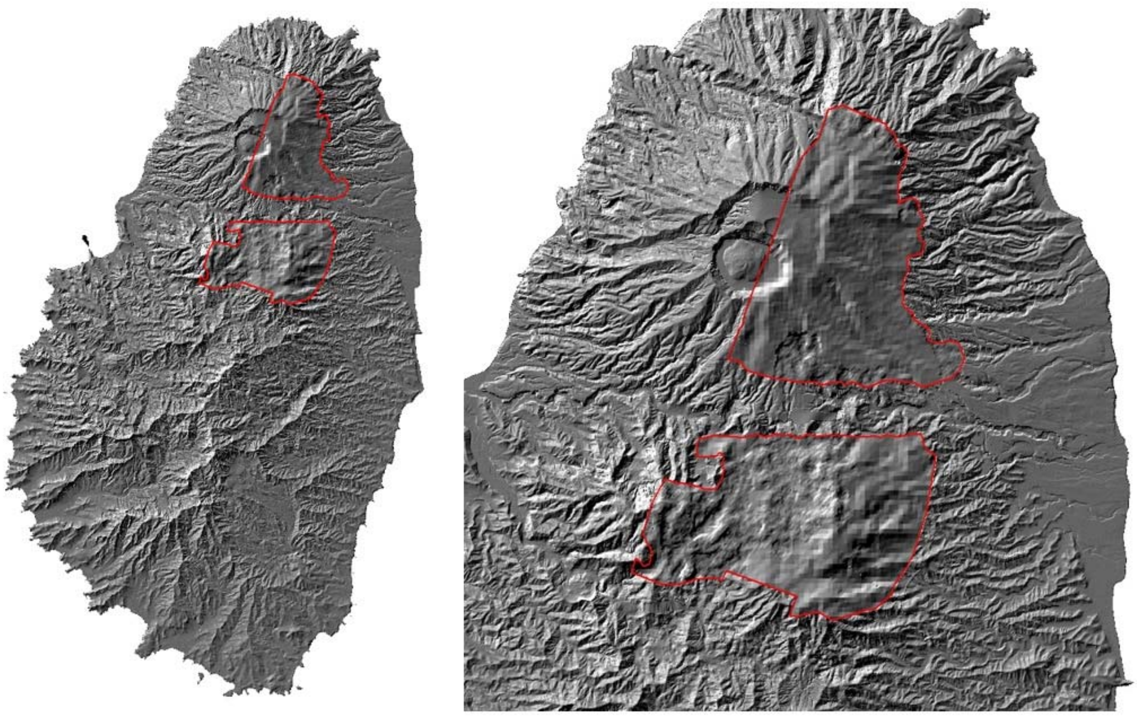

Figure 5-2: The area in the centre of Saint Vincent didn't have LiDAR coverage so we had to fill it with another DEM of lesser quality (SRTM), as can be seen from the detailed hill shading map on the right.

The areas within the red line in Figure 5-2 have a poor data quality. So the landslide susceptibility of this particular zone is less reliable. Users should take this into account when using the map. The outline of the area with lower quality has been included in the final landslide susceptibility map.
The DEM was used as the basis for a number of derivative maps for the landslide susceptibility analysis:

- Elevation classes. This was done because we assumed that there might be a relation between altitude and landslide occurrence, as rainfall amounts strongly increase with increasing altitude.
- Slope steepness classes: an algorithm was used to calculate the slope steepness per pixel in degrees. We assumed that there is a clear relation between slope steepness and landslide occurrence, where the class 20 to 35 degrees might have the highest density of landslides. This will be later analysed in the statistical analysis.
- Slope direction classes: slope direction was calculated using a special algorithm from the DEM. The resulting map was classified into classes with an interval of 45 degrees.
- Part of the island. We subdivided the island in windward and leeward parts because we assumed that there would be more landslides on the windward side of the island.
- Flow accumulation classes. This map was generated from the DEM using a special algorithm, which counts for each pixel how many other pixels are located upslope. We assumed that there is a relation between the locations where streams are initiated, close to water divided, and landslide occurrence.

Geology

The geological map of Saint Vincent is from Robertson (2003). We were not able to access the publication itself, and otherwise it is hard to find descriptions of geology in literature. The geological map contains only 9 units. The volcanic bedrock is composed of basalts and basaltic andesites (Rowley, 1978). It has issued from several eruptive centres as well as Soufriere Volcano (Hay, 1959). Walsh (1985) notes the bedrock of St. Vincent is generally younger that on neighbouring islands. Structurally the island is aligned along a north-south axis. The geology of Saint Vincent is characterized by basalts emplaced during the early phase of volcanic activity in the island and followed by the andesites that occur as dikes, domes or central plugs in the vents of some volcanic centres. Basalts are dominant in the south while andesites are abundant in the northern part of the island. The Southeast Volcanics consist of scoraceous basalts interbedded with massive well-jointed basaltic lava flows. It is intruded by dikes and mostly overlain by fine grained yellow ash associated with the tephra ejected by the Soufriere volcano. The Grand Bonhomme Volcanic Centre is interpreted as a stratovolcano with interbedded sequences of block and ash pyroclastic flow deposits, ash fall deposits, lava flows and subordinate domes. These rocks form a heavily forested landscape with inaccessible interior composed of deeply weathered lavas and volcaniclastic deposits. The Morne Garu volcanic centre is in the north of Grand Bonhomme. The rocks exposed are lava flows, undifferentiated volcaniclastics, red scoria bombs and yellow ash fall deposits.
In terms of age geological unit have been subdivided into South-East Volcanics (2.74±0.07 to 1.54 ±0.62 Ma), Grand Bonhomme Volcanic Center (1.33±0.09 to 1.16±0.08 Ma), Morne Garu Volcanic Center (1.18±0.10 to 0.011±0.014 Ma), Monogenetic red scoria spatter cones, and Soufriere Volcanic Centers (0.69±0.09 Ma to 1979 AD), the deposits of which have been subdivided into Yellow Tephra deposits and Undifferentiated pyroclastic deposits, including the deposits from historic eruptions (1718, 1780?, 1812, 1880?, 1902-03, 1971-72, and 1979 AD) (Robertson, 2003).
St. Vincent has been divided into four major geologic regions: the South-East Volcanics, and the Grand Bonhomme, Morne Garu and Soufrière Volcanic Centres (Robertson 2003); based an examination of the topography field geology, geochemistry and previous work undertaken on the island. In the southeast and northern part of the island are poorly consolidated sequences of clast-supported, pumice lapilli air fall, scoria bombs and ash overlying old lava flows. The abundant scoria bombs that fell close to these centres formed thick and sometimes welded deposits. Ash and small projectiles deposited further from the vents produced discrete beds. Spatter cones are also exposed in the northern part of the island consist of a thick sequence (>20 m) of interbedded grey lapilli-sized ash and red scoria overlain by yellow ash. The red scoria clasts are composed of olivine microphyric basalts but also contain angular basaltic-andesite. The Soufriere stratovolcano occupies the northern half of the island. It is the most active volcano in the Antilles arc. Its last five major eruptions occurred in 1718, 1812, 1902, 1971 and 1979 where basaltic lava domes were extruded in the crater area followed by a phreatomagmatic explosion that produced pyroclastic flows. Other major volcanic centres were identified but these have already become extinct (Heath et al., 1998).
As it could be seen during the fieldwork, the difference between rocks and soils is not clear in engineering terms, due to the relative degree of consolidation of the volcanic deposits, their heterogeneity and the effect of weathering (Cabria, 2015; Mulenga, 2015). The volcanic deposits are usually very thick; they may sustain vertical road-cuts, however, after weathering processes take place such road-cuts may cause problems (See Figure 5-3).

Figure 5-3 Examples of outcrops in volcanic deposits in Saint Vincent. The cut slopes are located along the Windward highway. The upper photos are near the new international airport under construction.

Cabria (2015) and Mulenga (2015) analysed the change in rock mass characteristics related to weathering for a number of the outcrops shown in figure 5-3. The results are shown in Figure 5-4. Volcanic bedrock in tropical climates is susceptible to deep weathering and mass wasting (Prior and Ho, 1972; Hartford and Mehigan, 1984; Rouse, et al. 1986; DeGraff, 1991). Weathered volcanic soil is weaker than the original bedrock and the high precipitation on the island increases pore-water pressure within discontinuities decreasing soil shear strength. The loss of shear strength generates zones of failure in which the mass destabilizes in the form of a landslide or debris flow (Faugeres, 1966; Walsh, 1982; DeGraff, 1991). In order to make the lithological map more realistic we decided to combine it with the slope class map, thus allowing to evaluate the combination of lithological units under different slope classes.

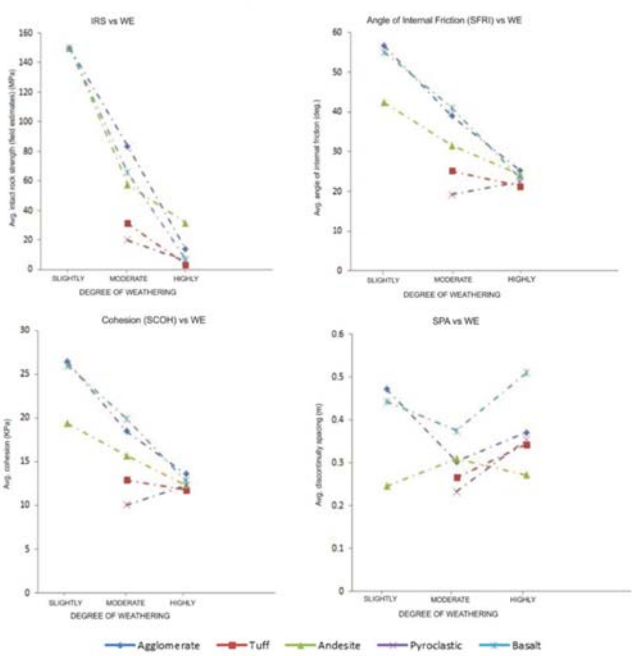

Figure 5-4: Relation of weathering degrees with rockmass characteristics, such as Intact Rock Strength (IRS), Angle of Internal Friction (SFRI), Cohesion (SCOH) and Discontinuity spacing (SPA) for different volcanic rocks (Mulenga, 2015; Cabria, 2015).

Geomorphology

Since the geological map was very general, and the LiDAR DEM allowed to generate a hillshading from which many Geomorphological features could be observed, we decided to generate a Geomorphological map thorugh visual stero image interpretation. The existing geological map was used as reference. The Geomorphological map is shown in Figure 5-5. The digital map can be downloaded as shapefile from http://www.charim-geonode.net/layers/geonode:geomomorphology

The island has an asymmetric profile, with the Leeward side being steeper and shorter, and with deeper valleys than the Windward side, which is also found on other islands (e.g. Grenada). Slope gradients along the west of the central axis of the island are significantly greater than gradients on the east.This in combination with the bathymetry which is much steeper on the western side than on the eastern side suggest a long term tectonic tilting to the West. St. Vincent has been divided into four major geologic regions: the South-East Volcanics, and the Grand Bonhomme, Morne Garu and Soufrière Volcanic Centres (Robertson 2003); based an examination of of the topography field geology, geochemistry and previous work undertaken on the island. No field evidence has been found of faulting but almost all the major river courses on the island appear to be structurally controlled. An emergent coastline found along the east coast has been suggested by Rowley (1978) to be due to Plio-Pleistocene uplift. Erosion has severely dissected the southern volcanic centres and original structures cannot be readily identified. Arcuate scarp features located at Grand Bonhomme, Morne Garu and the Soufrière volcano have been attributed to relict caldera or collapse structures (Rowley, 1978a; Sigurdsson and Carey, 1990; Geotermica Italiana, 1992). A number of cold mineral springs are located in the southern parts of the island but fumarolic activity is confined to the Soufrière volcano. Robertson (2003) gives the following subdivision:

- The **South-East Volcanics** is the most southerly geologic region on the island. It is a dissected landscape of rounded hills with low topography (<210 m), which extends from the Warrawarrow River in the west to the extensive Yambou lava flow in the east. The area is dominated by red scoriaceous basaltic spatter interbedded with and often overlying, massive to well-jointed basaltic lava flows, which are intruded by dykes. It contains the oldest rocks exposed on the island (2.74 ± 0.11 Ma; Briden, et al., 1979) and is mostly overlain by fine-grained yellow ash, which are correlated with late Pleistocene Yellow Tephra erupted by the Soufrière volcano (Hay, 1959, Rowley, 1978b). The youngest deposits exposed in the area are alluvial silt, sand and gravels found in the river valleys.
- The **Grand Bonhomme Volcanic Centre** extends from Argyle to Colonarie in the east and Sion Hill Bay to Chateaubelair in the west. It is the largest geologic region on the island and is interpreted as a large stratovolcano with interbedded sequences of block and ash pyroclastic flow deposits, ashfall deposits, lava flows and subordinate domes. The landscape is heavily forested and the interior inaccessible and composed of deeply weathered lavas and volcaniclastic deposits. This volcanic centre is a composite of several eruptive centres that are now represented by the topographic highs of Grand Bonhomme (970 m), Petit Bonhomme (747 m), Mount St. Andrews (735 m) and an unnamed peak (1021 m). These peaks are central domes or plugs of volcanoes that coalesced to form a large composite volcanic centre. Previous dating of lavas from the western flank of the Grand Bonhomme Volcanic Centre by Briden et al (1979) obtained ages of 1.33 ± 0.09 and 1.18 ± 0.10 Ma respectively for lava flows at Westwood and Chateaubelair.
- The **Morne Garu Volcanic Centre** occurs immediately to the north of Grand Bonhomme and consists of Mount Brisbane (932 m) to the east and Richmond Peak (1074 m) to the west. These two peaks are the remnants of an eroded Morne Garu crater or caldera that is estimated to have been 3 km in diameter (Sigurdsson, et al., in prep). Morne Garu is largely inaccessible and the underlying volcanics are extensively covered with fine-grained yellow ashfall deposits. Recent ages obtained by Heath et al. (1998, 1998) from lavas at Indian Estate (11 ± 14 ka) and Black Point (180 ± 20 ka) on the western flank of Mount Brisbane indicate that volcanism may have been much younger at this centre and may have overlapped with the Soufrière Volcano to the north. The major formations exposed are lava flows, undifferentiated volcaniclastics, red scoria bombs and yellow ashfall deposits. Reworked alluvial deposits occur in the major river valleys.
- **Monogenetic spatter cones**. A number of rounded spatter cones composed of a poorly consolidated sequence of clast-supported, pumice lapilli airfall, scoria bombs and ash resting on old lava flows occur mainly in the southeast of St Vincent although some are found further north. Eruptive centres were identified at Kings Hill, Diamond (S) and Rose Cottage. Eruptions produced abundant scoria bombs, which fell close to these centres and formed thick, and sometimes welded deposits. Ash and small projectiles deposited further from the vents produced discrete beds.

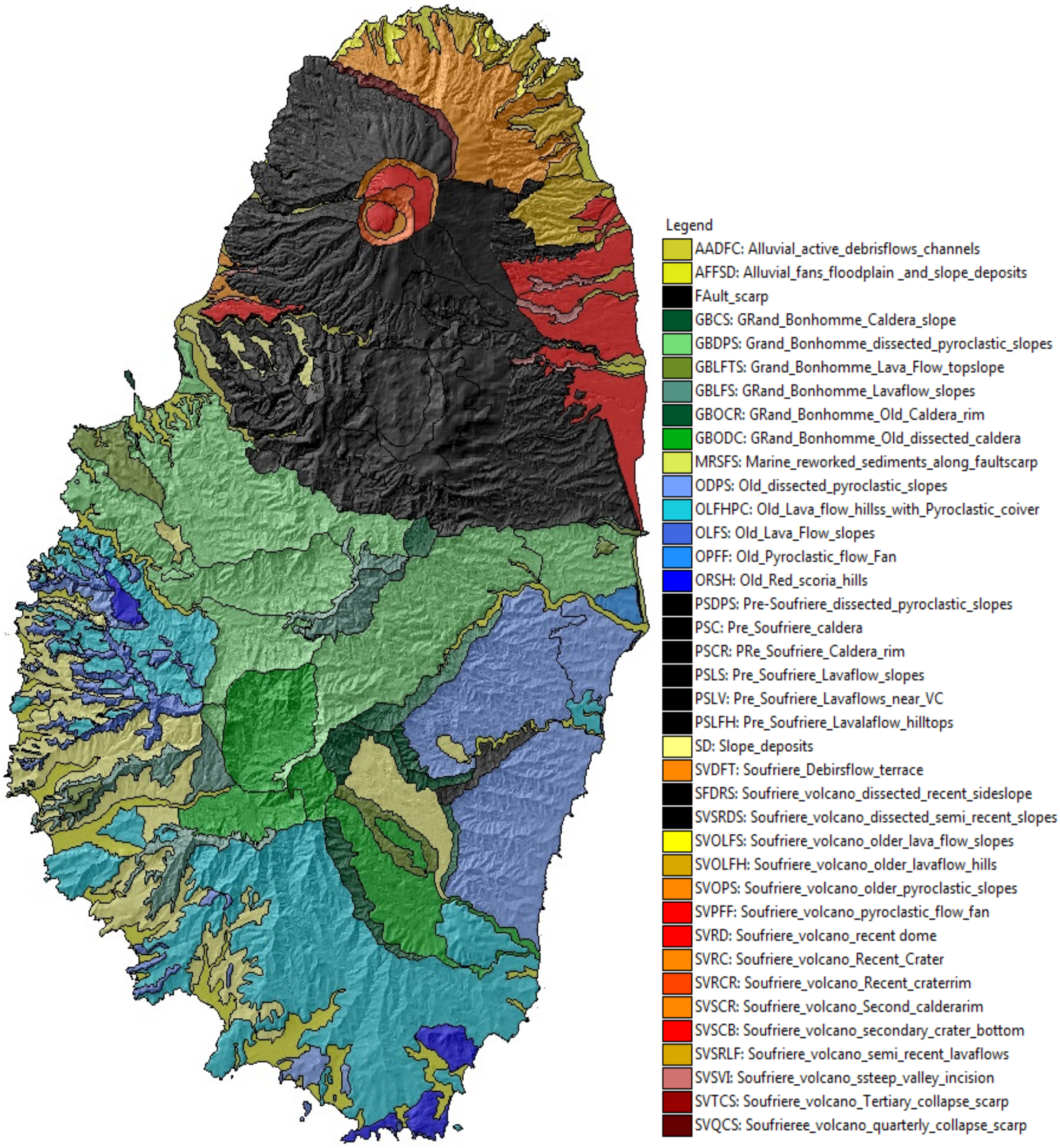

Figure 5-5. Geomorphological interpretation of Saint Vincent (Van Westen) outlining the visible craters, domes, major faults and lineaments.

Soils

The best description on soils in Saint Vincent we could find was given by USAID (1991), which was based on Watson and Jones (1958) who made an island-wide soil survey and mapping exercise . The map was made by the Soil Research Unit of the University of the West Indies, St. Augustine, Trinidad. The soil map was made through physiographic interpretation of aerial photographs, combined with field work and soil testing, and not according to pedology which emphasizes how the soils originated. The map has a very complicated legend. There are 42 different legend classes, and soils are named after a locality (most often an estate), with a suffix related to the parent material. This classification was made in order to identify agricultural fertility problems. For this the degree of weathering was estimated based on field observation data as pH, texture, structure and X-ray analysis on clay mineral content. Other factors were used as well such as parent materials, climate, plant and animal organisms, age of land and topography. The legend units have a large number of attriutes stored in an accompanying table. The most occurring are skeletal soils covering the higher parts of the island.

When topsoil is lost, the formation of replacement soils is an extremely slow process. It may take an estimated 200 to 700 years to form just 2.5 cm of top soil weighing about 360 tons/hectare (USAID, 1991).
The available soil map showed several problems, related to topological errors, and also related to the correlation with other factors. As slope steepness is used as one of the characteristics of the soil units, a mismatch with slope units derived from the DEM was evident. The conversion of this complicated soil map into a GIS layer turned out to be a major challenge. The topology of this map was also problematic, and we had to fix this using a number of GIS operations. The complicated legend would pose a serious problem in the use of this in the landslide susceptibility assessment. We combined the soil map with a slope class map, to make soil classes in relation to the slope classes, which were considered to be better indicators for slope stability than the soil classes alone.

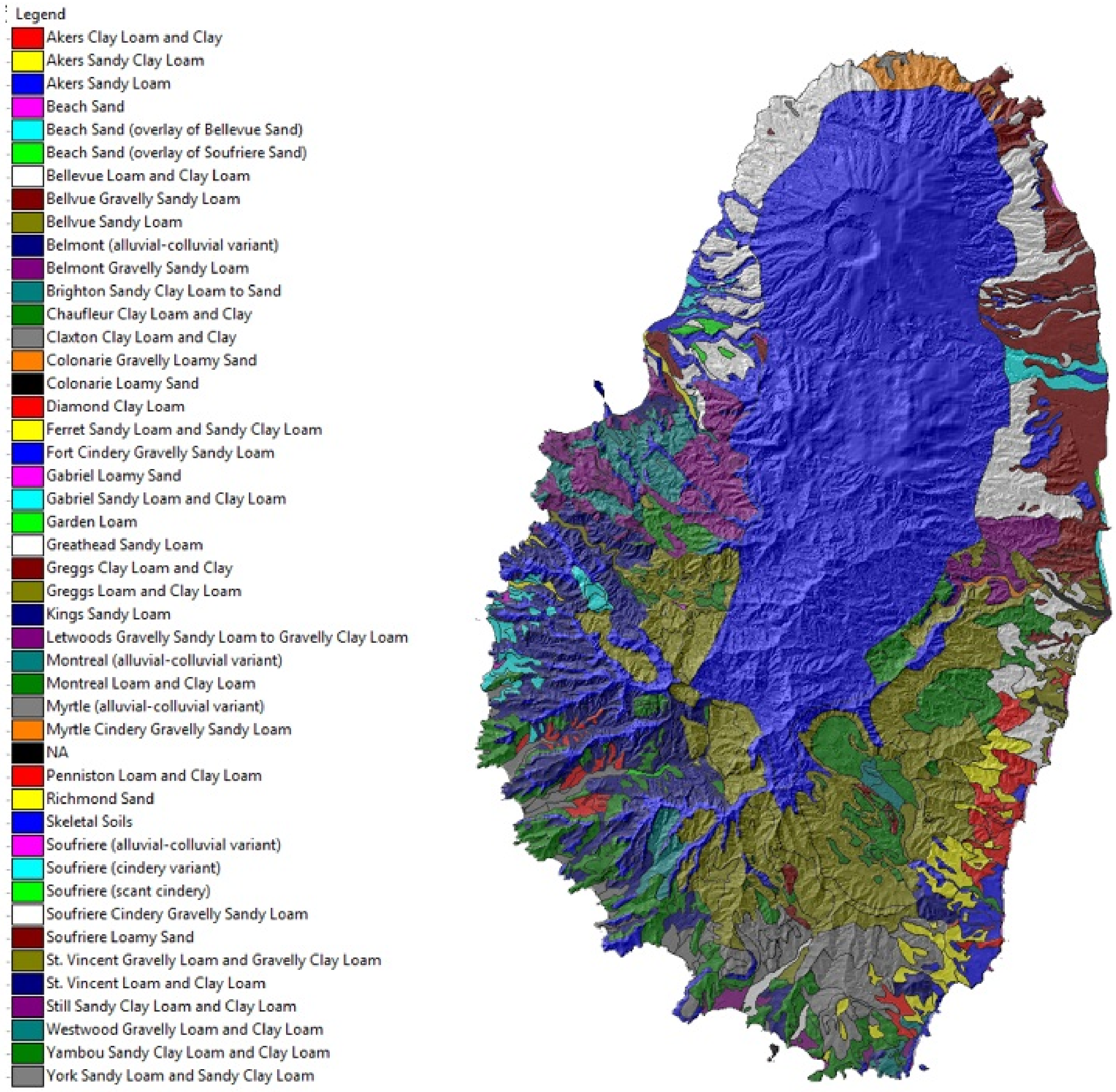

*Figure 5-6: Soil map of Saint Vincent (*Watson and Jones, 1958)

Land-cover

We have three land cover maps for Saint Vincent, two of which without any metadata. However, we found out that one is from 2000 and one from 2005. We understood from the people that gave them to us that these were made using image classification of Landsat ETM+ and Spot images by USGS, USAD and the Nature Conservancy as part of the USAID CarLand project (CarLand, 2000). The maps from 2000 and 2005 are basically the same, except for some differences: Different types of forest to Cultivated land (3.3 km^2).

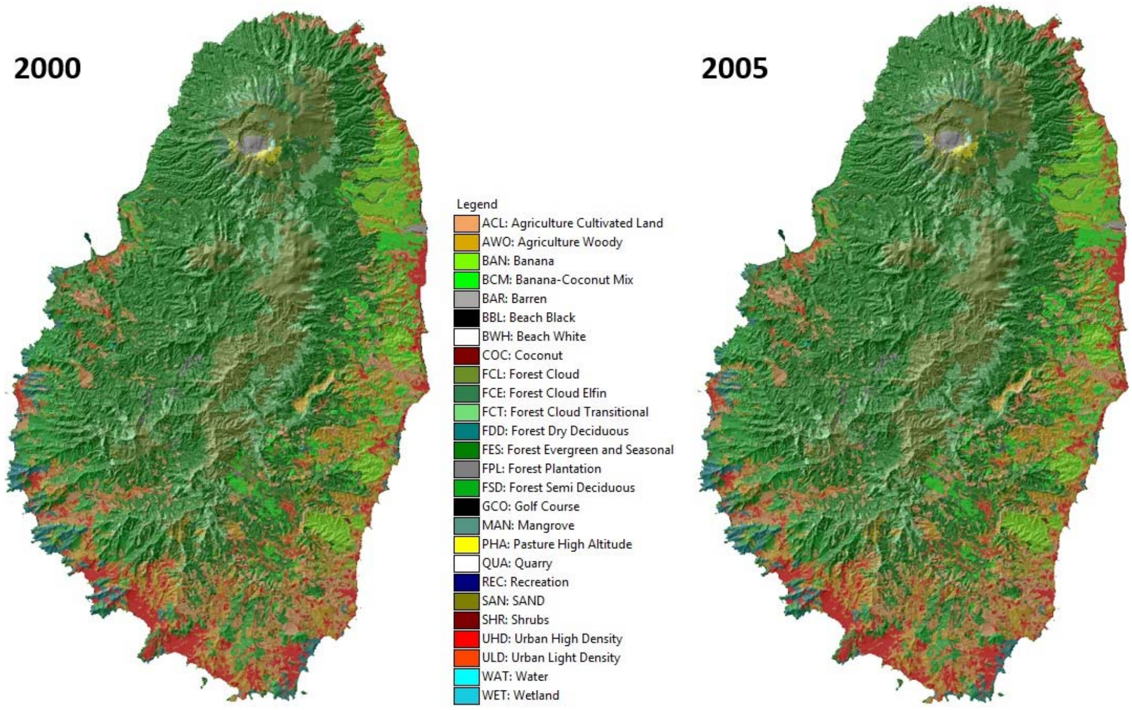

Figure 5-7: Land use/ Land cover maps for 2000 and 2005, generated by the CarLand project (2000)

We also obtained a recent land use map from an international project. The European Space Agency (ESA) and the World Bank (WB) have been collaborating under the umbrella of the "Earth Observation for Development" initiative - branded Eoworld - since 2008. The form of this collaboration has been to develop, produce and deliver examples of EO-based information products that respond specifically to the geo-information requirements of on-going World Bank projects. ESA provided the financial and technical capacity to procure high resolution satellite images which were processed by the British Geological Survey. They used Object-Based Image Classification with Definiens and ENVI software and produced a detailed land cover map for Saint Vincent. Both the detail of this map as well as the legend are so different from the previous land cover maps from 2000 and 2009 that it is difficult to compare them. The large class "Abandoned and underutilized cropland" in 2009 has completely disappeared in 2014. Also the urban areas that were mapped very general in 2009, are much smaller in the detailed land cover map from 2014. Although the new land cover map was a major improvement, it still had a number of problems. One of them is related to cloud cover, where other satellite image data (e.g. Landsat) had to be used to fill these missing parts, leading to large differences in detail (See Figure 5-8). Also the characterization of different vegetation types was problematic so that the new land cover map is less accurate when separating natural forest from plantation areas. Also bare areas, built-up areas, and roads often show large differences with the actual situation (e.g. bare rocks along the coast mapped as buildings, waste disposal site mapped as buildings etc.). Therefore the available building footprint map and road map were used to mask out the areas of buildings and roads. Also airports, seaports, quarries, and waste disposal sites were manually digitized by us, and were masked into the land cover map. Figure 5-8 shows some of the changes that we made to the land cover map of 2014.

Table 5-2 shows the land use / land cover changes from 2005 to 2015, based on the combination of the two landuse maps. When comparing the values for the land use changes, it is clear that a number of the changes do not make much sense, and that both maps have certain problems with accuracy of the land use mapping.

Table 5-2: Land use / landcover changes between the maps from 2005 (CarLand) and 2014 (BGS)

		Land cover 2014																		
		Airport	Sanitary fill	Quarry	Sea	Evergreen Forest	Seasonal forest	Semi-deciduous forest	Pasture, cultivated land	Bare ground	Roads	Building	Drought deciduous, coastal	Water	Elfin	Woody agriculture	Montane non-forest	Blue Mahoe plantation	Golf course	Mangrove	Total
Land use / landcover 2005	Agriculture cultivated land	37	6	0	0	263	5	783	1308	28	66	88	272	1	42	30	0	0	0	0	2929
	Agriculture woody	18	1	6	0	313	9	916	933	31	104	136	384	1	4	71	0	1	0	0	2928
	Banana	0	0	1	0	13	1	137	350	5	18	5	33	0	0	622	0	0	0	0	1185
	Banana-Coconut mix	2	0	1	0	43	2	296	713	2	19	12	69	0	5	187	0	1	0	0	1352
	Barren	0	0	3	0	3	0	4	15	82	1	1	3	1	11	0	4	0	0	0	128
	Beach black	0	0	0	0	3	0	5	6	13	4	5	7	0	0	0	0	0	0	0	43
	Beach White	0	0	0	0	0	0	0	0	0	0	0	0	0	0	0	0	0	0	0	0
	Coconut	0	0	0	0	0	0	5	14	1	1	0	2	0	0	10	0	0	0	0	33
	Forest cloud	0	0	0	0	261	2	80	97	10	1	1	54	2	3357	2	12	1	0	0	3880
	Forest cloud Elfin	0	0	0	0	14	0	10	21	0	0	0	11	0	230	1	3	0	0	0	290
	Forest cloud transitional	0	0	0	0	980	8	181	61	3	2	0	50	1	671	3	2	1	0	0	1963
	Forest dry deciduous	4	0	0	0	35	2	130	151	9	19	24	266	0	0	8	0	0	0	0	648
	Forest evergreen and seasonal	2	0	2	0	6074	352	3535	1348	100	81	66	1003	5	1960	79	5	6	0	0	14618
	Forest plantation	0	0	0	0	46	1	14	4	0	0	0	2	0	1	1	0	33	0	0	102
	Forest semi-deciduous	0	0	5	0	462	10	656	134	5	14	16	280	1	1	45	0	0	0	0	1629
	Golf course	0	0	0	0	0	0	1	1	0	0	0	0	0	0	0	0	0	0	0	2
	Mangrove	0	0	0	0	0	0	1	3	1	0	0	1	0	0	0	0	0	0	1	7
	Pasture high altitude	0	0	0	0	0	0	0	2	7	0	0	1	0	20	0	42	0	0	0	72
	Quarry	0	0	0	0	0	0	0	0	0	0	0	0	0	0	0	0	0	0	0	0
	Recreation	0	0	0	0	0	0	0	0	0	0	0	0	0	0	0	0	0	0	0	0
	Sand	0	0	0	0	0	0	0	0	0	0	0	0	0	0	0	0	0	0	0	0
	Shrubs	0	0	0	0	0	0	0	0	0	0	0	0	0	0	0	0	0	0	0	0
	Urban high density	31	4	1	0	22	1	123	533	33	160	293	158	1	0	6	0	0	0	0	1366
	Urban light density	8	1	1	0	59	2	259	470	17	120	122	169	0	1	22	0	0	0	0	1251
	Water	0	0	0	0	1	0	2	3	3	0	0	2	3	3	0	0	0	0	0	17
	wetland	0	0	0	0	0	0	0	0	0	0	0	0	0	0	0	0	0	0	0	0

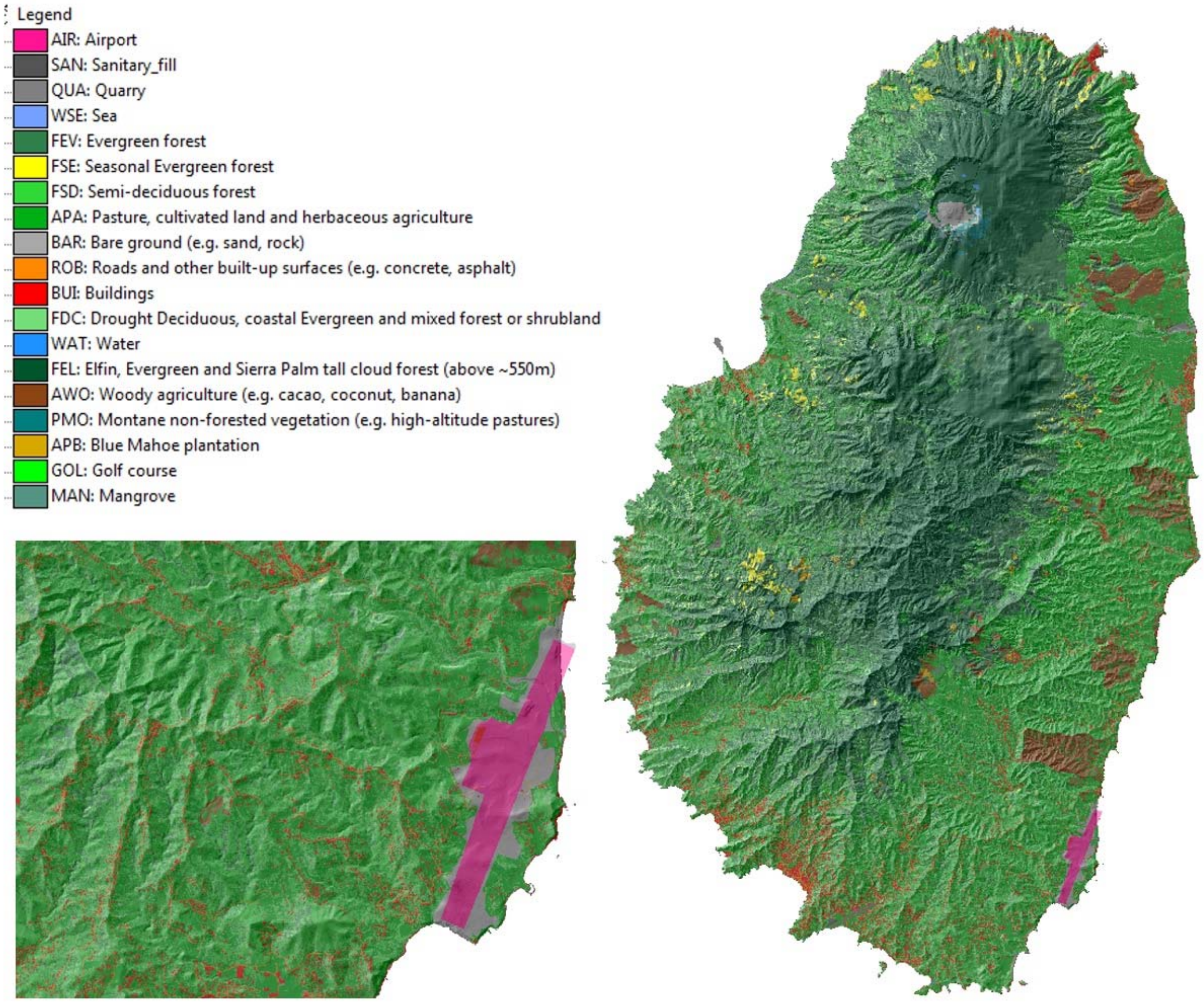

Figure 5-8: Land cover map of Saint Vincent generated by BGS, with detail.

6. Landslide susceptibility assessment

The best approach for landslide initiation susceptibility assessment at a scale of 1:25,000 - 1:50,000 is the use of statistical methods in combination with expert-based weighting approaches. Since we do not have a very reliable landslide data set, we used the available landslides to check the statistical relation with the factor maps, but generate the actual landslide initiation susceptibility map using Spatial Multi-Criteria evaluation. Although we have reconstructed a considerable number of past landslide in the landslide inventory, the factor maps are of poor quality, and therefore the relationships between landslides and these factors are only indicative, and should not be used automatically. Therefore a combination of statistical methods and expert-based methods should be used.

6.1. Evaluation of landslide factors using bi-variate statistical analysis

When enough landslides are available in the landslide inventory, it is advisable to use bi-variate statistical methods as exploratory tool to learn which contributing factors, or combinations of contributing factors are important in the study area. One of the most frequently used methods for bi-variate statistical analysis is the Weights-of-Evidence method, further referred to as WoE. The method is explained in Figure 6-1

	Factor class present (B)	Factor class not present (B)	
Landslides present (S)	180	20	200 (total landslide area)
Landslides not present (S)	3420	6380	9800 (total area free of landslides)
	3600 (total area of factor class)	6400 (total area outside3 factor class)	10000 (total study area)

$$W_i^+ = \log_e \frac{P\{B_i|S\}}{P\{B_i|\overline{S}\}}$$

$$W_i^- = \log_e \frac{P\{\overline{B_i}|S\}}{P\{\overline{B_i}|\overline{S}\}}$$

$P\{B|S\}$ = 180/200 = 0.9

$P\{B|\overline{S}\}$ = (3600-180)/(10000-200) = 3420/9800 = 0.349

$P\{\overline{B}|S\}$ = (200-180)/(200) = 20/200 = 0.1

$P\{\overline{B}|\overline{S}\}$ = (10000-3600-200+180)/(10000-200) = 6380/9800 = 0.6510

Figure 6-1: Illustration of the Weights of Evidence model. Above: Example of a matrix which is calculated for the spatial overlay of a factor class (e.g. a certain slope class, or lithological unit) with landslides. The area for each combination is shown in a hypothetical example. Lower left: equations used for the Weights of Evidence modelling. Lower right: worked out example, based on the values in the matrix above.

The WoE technique was originally developed for quantitative mineral potential mapping to predict the location of possible mineral deposits (Bonham-Carter et al., 1988; Bonham-Carter et al., 1989). However, it has been successfully applied in many landslide susceptibility assessments (van Westen, 1993; Lee et al., 2002; van Westen et al., 2008; Lee and Choi, 2004; Süzen and Doyuran, 2004; Neuhäuser and Terhorst, 2007; Thiery et al., 2007; Blahut et al., 2010;) and is based on the assumption that factors causing landslides in the past will determine the spatial occurrence of future landslide initiation in areas currently free of landslides. A probabilistic Bayesian approach is applied to determine the conditional probability between the presence/absence of each causative factor and the presence/absence of a landslide. For every factor map (e.g. land-cover, lithology, etc.) a weighting table is produced that includes for each class (e.g. grassland, bare rock) the positive weight (W+), which indicates the importance of the "presence" of this class on the occurrence of landslides. The table also has the negative weight (W-) which evaluates the importance of the "absence" of the class on landslide occurrence and the Contrast factor (W+ - W-). The contrast factor is considered a measure of the overall importance of a factor map class on the conditions causing landslide occurrence. The advantages of WoE are its quick and cost effective approach and the capability of combining the subjective choice of the classified factors by the expert with the objective data driven statistical analysis of the GIS. For details on the WoE methodology applied for landslide susceptibility the reader is referred to Lee et al. (2002).

There are several useful tools available that can be used with a conventional GIS system, without the need of external statistical models. These methods basically calculate landslide densities within the contributing factors, or the classes of the contributing factors, and then compare these with the overall density in the map. Also in ArcMap there are extensions for making these calculations, such as ARC-SDM (http://www.ige.unicamp.br/sdm/default_e.htm ; Sawatzky et al., 2009)

The calculation of the Weights of Evidence is carried out using a script in the ILWIS software. A script contains a series of commands that allow the automatic execution of a series of calculation steps for different maps. The script used is indicated in the Figure 6-2.


```
rem ILWIS Script for calculating Weights of Evidence
//The parameter %1 refers to the name of the factor map (e.g. SlopeClass).
// The parameter %2 refers to the domain of the factor map.
//This could be the same as the name of the map but could also be different. So write here the name of the domain.
//The parameter %3 refers to the name of the landslide map, which should be a binary map with 0 and 1 values

//FIRST WE WILL DELETE EXISTING RESULT FILES
// the crosstable c%1%3.tbt
//The attribute table t%1%3.tbt
// and we make a new attribute table t%1%3.tbl

del c%1%3.*
del w%1%3.*
del t%1%3.tbt
crtbl t%1%3 %2

//NOW WE CROSS THE FACTOR MAP WITH THE LANDSLIDEY MAP %3
// The landslide map should have either 0 or 1 values. 1 values mean landslides.
// The cross table is called c%1%3

c%1%3=TableCross(%1.mpr,%3.mpr,IgnoreUndefs)
calc c%1%3.tbt

//Now we calculate one column in the cross table to indicate only the pixels with landslides.

Tabcalc c%1%3 npixact=iff(%3=1,NPix,0)

//NOW WE USE AGGREGATION FUNCTION, WITH OR WITHOUT A KEY TO CALCULATE:
//NCLASS = number of pixels in the class. We sum the values from columns Npix and group them by %1
//nslclass = number of pixels with landslides in the class.We sum the values from columns Npixact and group them by %1
//nmap = number of pixels with landslides in the map. We sum the values from columns Npix and don't group them
//nslide = number of pixels with landslide in the map. We sum the values from columns Npixact and don't group them
//THE RESULTS ARE NOT STORED IN THE CROSS TABLE S%1 BUT IN THE ATTRIBUTE TABLE %1

Tabcalc c%1%3 t%1%3.nclass  = ColumnJoinSum(c%1%3.tbt,Npix,%1,1)
Tabcalc c%1%3 t%1%3.nslclass = ColumnJoinSum(c%1%3.tbt,Npixact,%1,1)
Tabcalc c%1%3 t%1%3.nmap = ColumnJoinSum(c%1%3.tbt,Npix,,1)
Tabcalc c%1%3 t%1%3.nslide = ColumnJoinSum(c%1%3.tbt,Npixact,,1)

//NOW WE CALCULATE THE FOUR VALUES NPIX1 - NPIX4 OF A MATRIX THAT COMBINES THE FACTOR CLASS WITH LANDSLIDES
// We correct for the situation when Npix1 - Npix3 might be 0 pixels, and change it into 1 pixel

Tabcalc t%1%3 npix1 {dom=value.dom; vr=0:10000000:0.001} =IFF((nslclass>0),nslclass,0.001)
Tabcalc t%1%3 npix2 {dom=value.dom; vr=0:10000000:0.001}= IFF((nslide-nslclass)=0,0.001,nslide-nslclass)
Tabcalc t%1%3 npix3 {dom=value.dom; vr=0:10000000:0.001}= IFF((nclass-nslclass)=0,0.001,nclass-nslclass)
Tabcalc t%1%3 npix4 {dom=value.dom; vr=0:10000000:0.001}= nmap-nslide-nclass+nslclass

//NOW WE CALCULATE THE WEIGHTS IN THE ATTRIBUTE TABLE
Tabcalc t%1%3 wplus {dom=value.dom; vr=-100:100:0.00001} = LN((npix1/(npix1+npix2))/(npix3/(npix3+npix4)))
Tabcalc t%1%3 wminus {dom=value.dom; vr=-100:100:0.000001}  = LN((npix2/(npix1+npix2))/(npix4/(npix3+npix4)))

//NOW WE CALCULATE THE CONTRAST FACTOR
Tabcalc t%1%3 Cw = wplus-wminus

//NOW WE CALCULATE THE FINAL WEIGHT
//The final weight is the sum of the positive weight and the negative weights of the other classes
Tabcalc t%1%3 WminSum=aggsum(wminus)
Tabcalc t%1%3 Wmap=wplus+Wminsum-Wminus

//NOW WE MAKE AN ATTRIBUTE MAP OF THE FINAL WEIGHTS
w%1%3.mpr = MapAttribute(%1,t%1%3.Wmap)
calc w%1%3.mpr
```

Figure 6-2: Weights of evidence script used in the ILWIS software.

When executing the script an input screen will ask for the input data (See Figure 6-3)

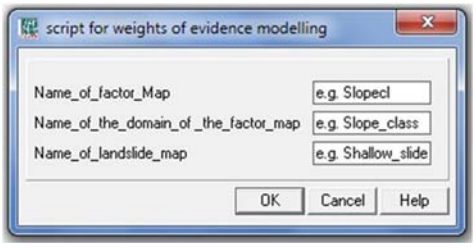

Figure 6-3: Input screen for the Weights-of-Evidence script used in the analysis. The script needs three inputs: name of the factor map (e.g. slope class, lithology), name of the domain of the factor map, and name of the landslide map, which should be a binary map (0= no landslide, 1= landslide).

The script was analysed for each of the factor maps in combination with two landslide input maps: one for shallow soil slides, and one for rockslides and rock falls. After running the script a table is made for each factor map with the Weights of Evidence for all classes of the factor map and also the Contrast Factor, which is the absolute difference between W+ and W-.

The results from the Weights of Evidence modelling were used to evaluate the relative contribution of the various factor maps, and the classes of the factor maps, to landslide occurrence. We also tested out whether specific combinations of factors had a better relation with landslides, e.g. by combining lithology with slope classes.

6.2. Results of the statistical analysis for Saint Vincent

The landslides described in chapter 4 were subdivided into two datasets: one group consisting of rockslides and rock falls, and the other group consisting of soil-related landslides. This was done because these two main groups were expected to have occurred under different conditions, and the analysis of the various contributing factor was therefore done for these groups separately. Figure 6-4 shows the two landslide input maps, which were converted into binary maps (1= landslide, 0= no landslide). The type of landslides that was included in the rock related group were rock slides and deep-seated-rock slides. While for the soil slides it included debris slide, debris flow, and shallow landslides. We excluded the class Stream flood Debris Flow, as this relates to the accumulation section of landslides, whereas the analysis is done for initiation areas.

Table 6-1: Summary of landslide inventories, separated by main group of landslides classified.

Rock related landslides		
	1988	2014
Number	85	160
Area of landslides m^2	22.86	56.28
Study area (km^2)		344.58
Density	0.00066	0.00163
Percent	0.07	0.16
Nr/km2	0.25	0.46

Soil related landslides		
	1988	2014
Number	524	1472
Area of landslides	111.13	611.30
Study area		344.58
Density	0.00323	0.01774
Percent	0.32	1.77
Nr/km2	1.52	4.27

Figure 6-4 illustrates the two main groups that the landslides were divided. For Saint Vincent the following factor maps were analysed using the Weights of Evidence method (Table 6-2).

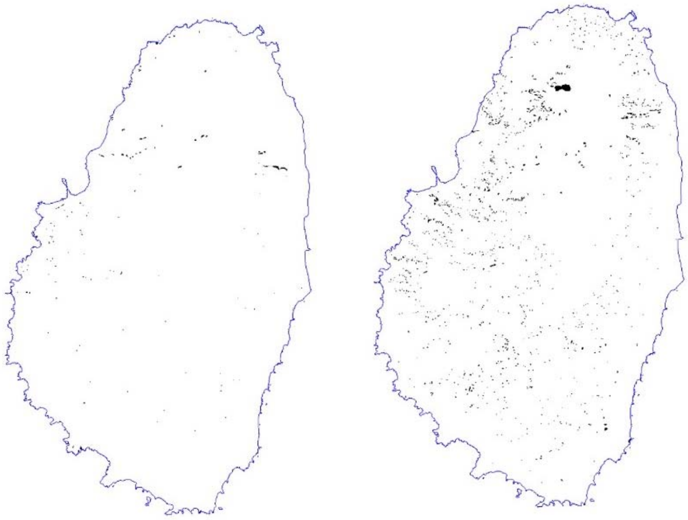

Figure 6-4: Landslide inventory maps for rockslides and soil-related landslides that were used in the analysis.

Table 6-2: Overview of the factor maps used for the statistical analysis for Saint Vincent.

Name of factor map	Explanation	Classes
Geology_Slopecl	Combination of geology and slope classes	50 classes combining the 10 geological units with 5 slope classes.
Landuse_Slopecl	Combination of land use and slope classes	83 classes combining 19 land use classes with 5 slope classes.
SoilType_Slopecl	Combination of soil types and slope classes	230 classes combining 46 soil classes with 5 slope classes.
ElevCL_SlopeCL	Combination of elevation and slope steepness	30 classes, combining with 6 elevation classes and 5 steepness classes
River_dist_cl	Distance from rivers	4 classes (0_25, 25_50, 50_100, >100 meter)
Geomorphology	Geomorphological units	35 geomorphology units
Geology	Lithological units	10 geological units, without clear differentiation between lithological types.
Coast_dist_class	Distance from coastline	8 classes (0-50, 50_100, 100_150, 150_200, 200_250, 250_350, 350_500, >500 m)
Roadcut_dist_cl	Distance from road cuts	5 classes (0-40, 40-80, 80-150, 150-250, >250)
Road_dist_cl	Distance from roads	4 classes (0-2, 25-50, 50-100, > 100 meter)
Landcover_2014_modified	Landuse/landcover map	19 land use and land cover classes
Limitations	Soil use limitation	5 soil use limitation
Soil_types	Soil units	46 Main classes, but many subdivisions. Very complicated legend
Soil_erosion_class	Soil erosion classes, indicated in soil legend	6 simplified classes ranging from non to severe.
Elevation_Class	Elevation classes	6 classes (0 - 100, 100 – 265, 265 – 500 500 – 825, 825 - 1000, >1000 m.a.s.l.)
Cliff_dist_cl	Distance from cliff	8 classes (0-25 , 25_50, 50_75, 75_100, 100_150, 150_200, 200_300, >300 meter)
Slope_cl	Slope steepness classes	5 classes (0 - 10 , 10 - 20, 20 - 35 , 35 – 50, >50)
Aspect_cl	Slope direction classes	9 classes (N, NE, E, SE,S,SW, W, NW, Flat)

Slope steepness.

Both rockslides and soil slides show a relation with slope steepness (Figure 6-5), with negative weights for the lower slope steepness classes, and increasing weights for the steeper slope classes. Both show a similar behaviour although rockslides occur more on very steep slopes.

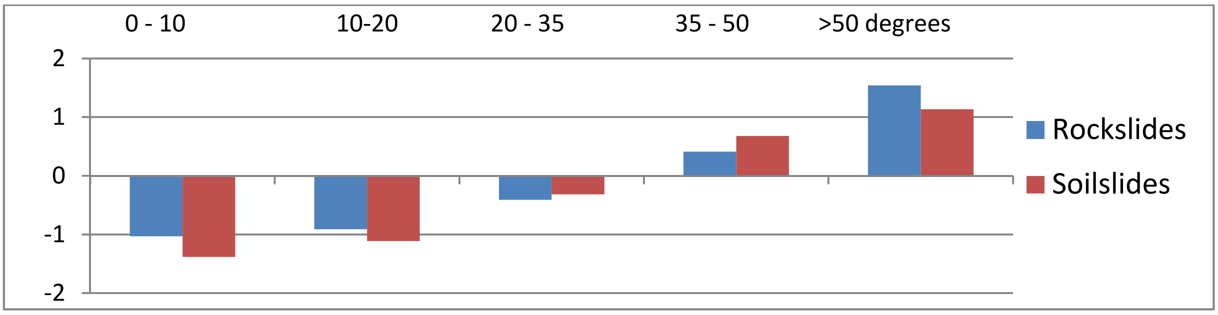

Figure 6-5: Contrast factors for slope steepness classes for rockslides and soil slides.

Slope direction.

When using slope direction directly from the Digital Elevation Model (See Figure 6-6) the relation is less clear than when using the major subdivision in windward and leeward sides of the island. The South and East oriented classes are relatively more important for both types of landslides.

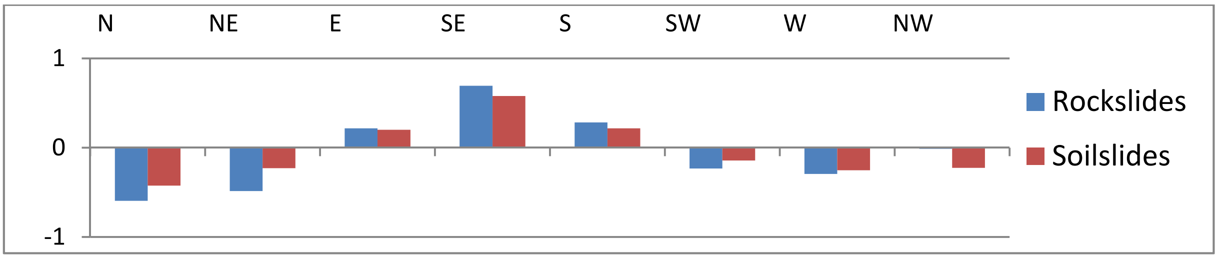

Figure 6-6: Contrast factors for slope direction classes for rockslides and soil slides.

Elevation

The factor elevation plays a different role for rockslides and soil slides. As can be seen in Figure 6-7, rockslides are most prominent at low elevation, whereas soil slides have a relation with increasing elevation, meaning that the slope of Soufriere volcano are particularly landslide prone.

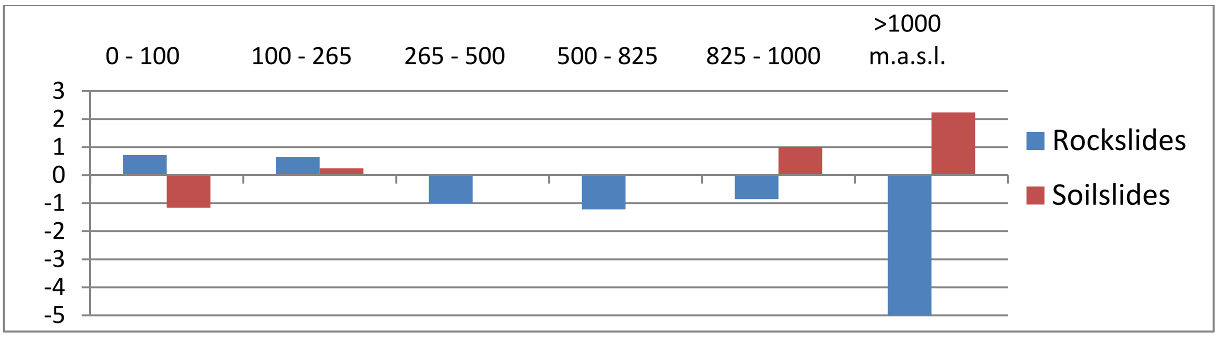

Figure 6-7: Contrast factors for elevation classes for rockslides and soil slides.

Distance from the coast

There is a clear relation between rockslides and distance from the coast. As many rockslides occur along the coastal cliffs there is an obvious relation (See Figure 6-8). Soil slides do not have such a clear relation with the distance from the coast.

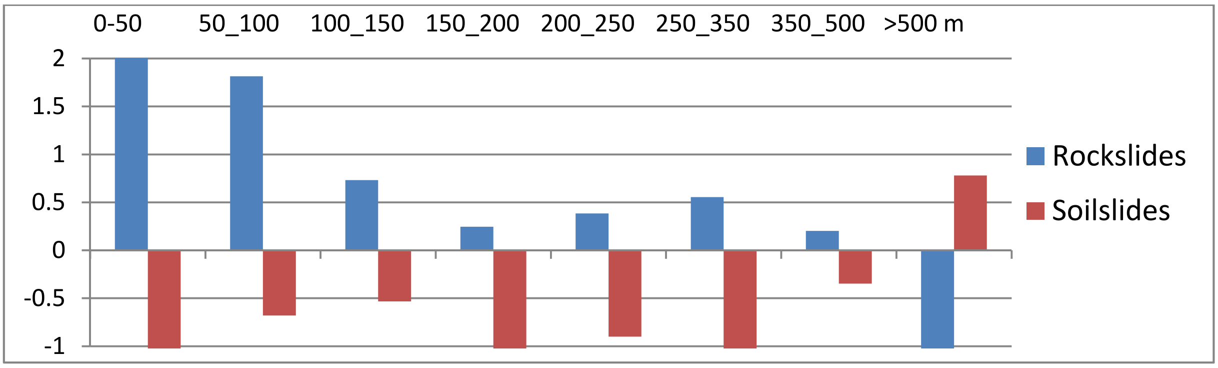

Figure 6-8: Contrast factors for distance to the coast for rockslides and soil slides.

Distance from cliffs.

There was a separate layer available with cliffs, derived from the LiDAR based survey. There is a clear relation between the distances from cliffs for both type of landslides.

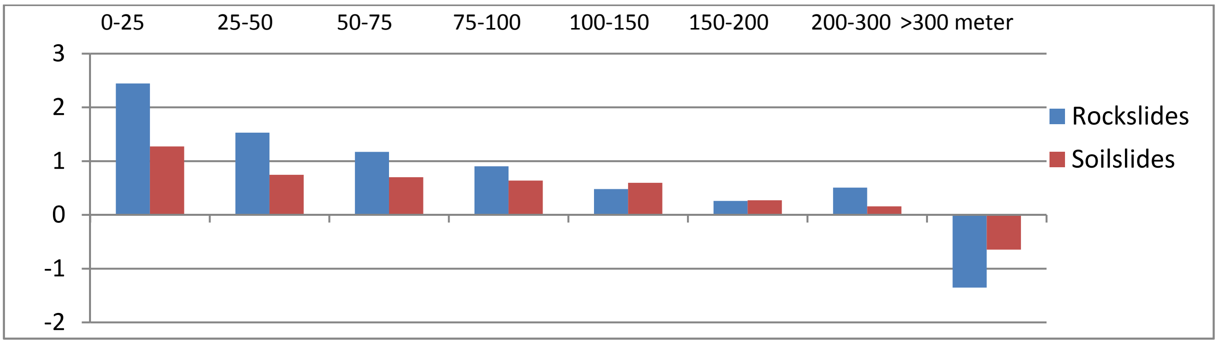

Figure 6-9: Contrast factors for distance from cliff classes for rock slides and soil slides.

Distance from rivers

We calculated the distance from rivers and made a buffer of 25-50 meters. The results are shown in Figure 6-10. Both soilslides and rock slides have no clear relation with the distance to rivers.

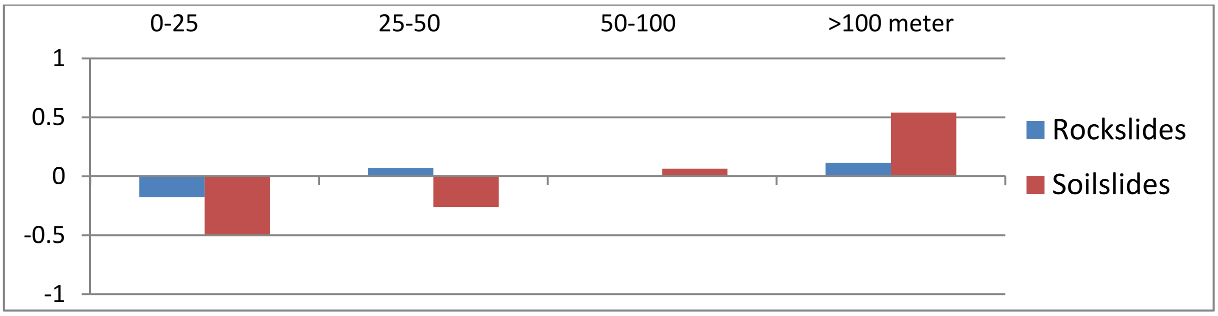

Figure 6-10: Contrast factors for distance to rivers for rockslides and soilslides.

Distance from roads

For analysing the relations between landslides and the distance to roads we generate distance classes from the main roads. The results (Figure 6-11) show that both rockslides and soil slides have a rather poor relationship with the distance to roads.

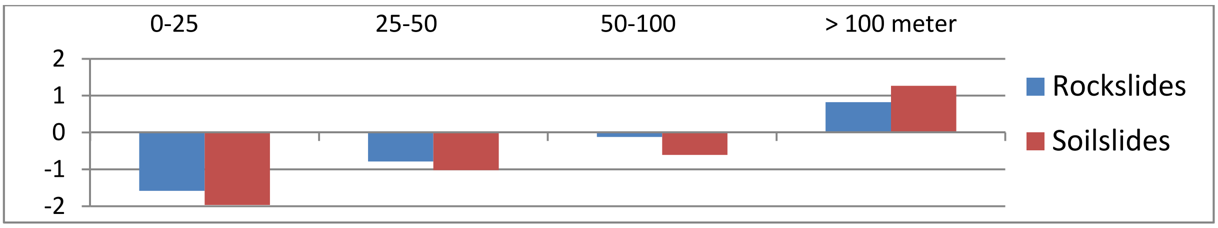

Figure 6-11: Contrast factors for distance to roads for rockslides and soilslides.

Geological units

The relationship between landslides and geological units is rather complex. From Figure 6-12 it can be seen that the contrast factors are only positive for two geological units in the case of rock slides: lava flows, domes and associated deposits, and pyroclastic deposits of Soufriere volcanic centres. The latter is also susceptible to soil slides, together with the class eruptive centres, and major scarp features. All other geological units show negative contrast factors.

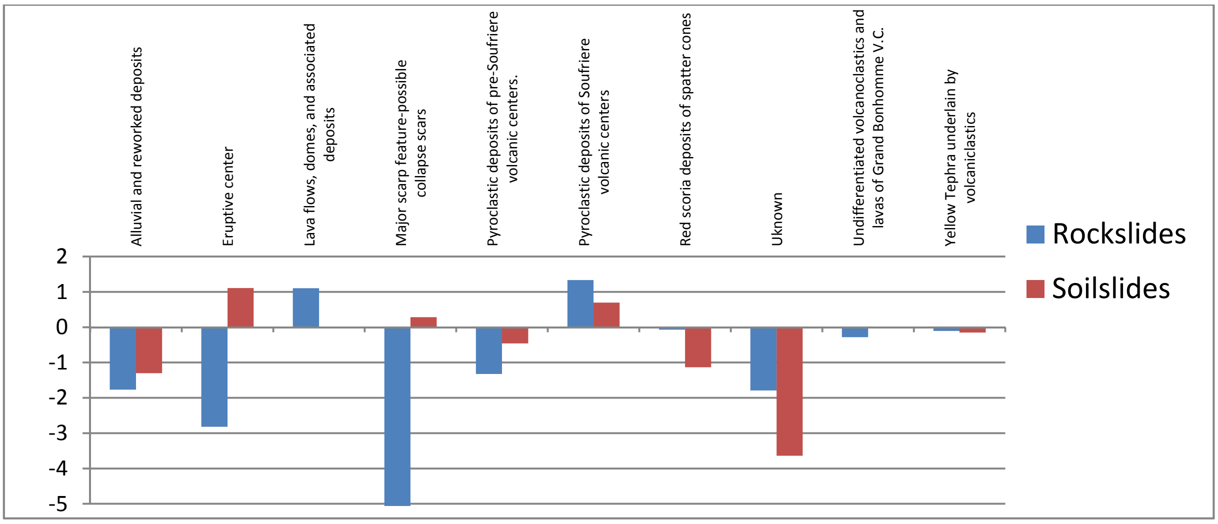

Figure 6-12: Contrast factors for geological units classes for rock slides and soil slides.

Soil types

The soil map which is available has a very complicated legend. Therefore it was decided to split this map into several sub-maps that show different aspects of the soil characteristics. The first one is the classification of the soil parent materials. The relation is shown in Figure 6-13. The relationship is actual rather good, as there are a limited number of soil units with positive contrast factors for both soilslides and rock slides.

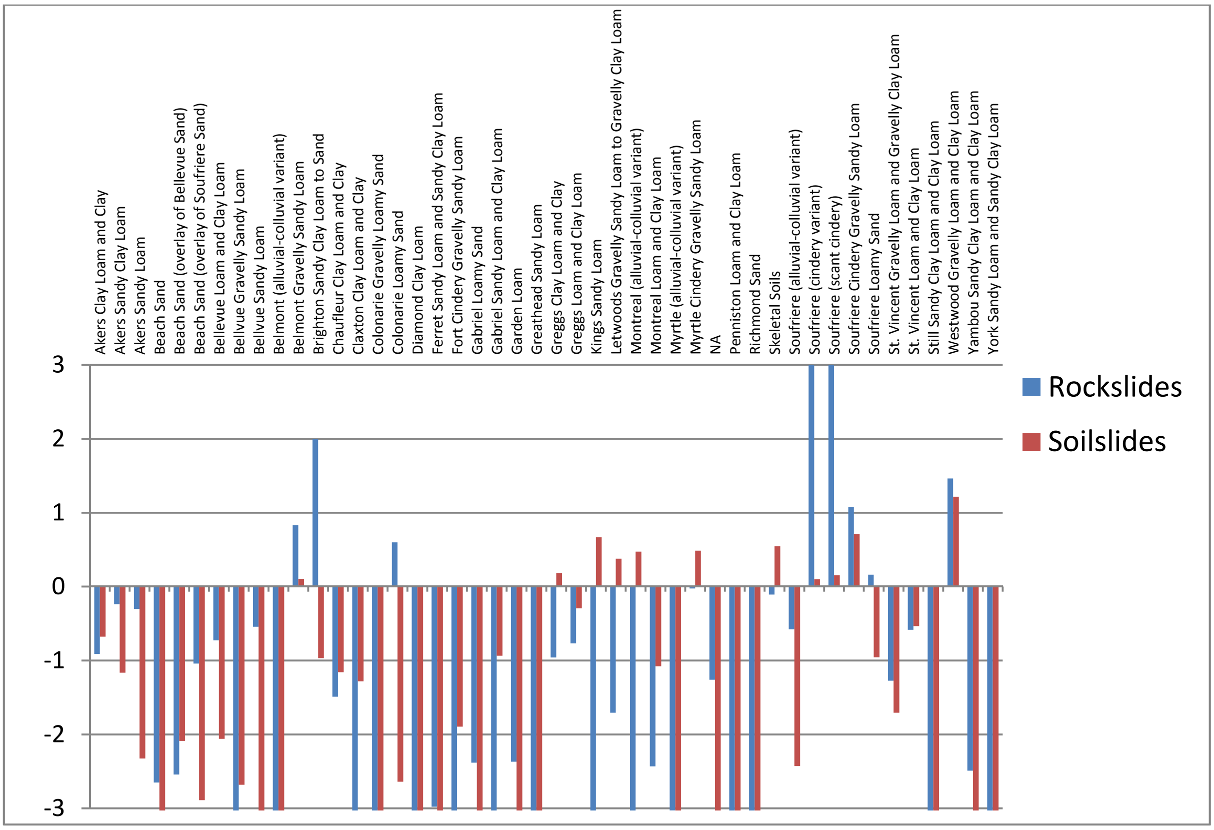

Figure 6-13: Contrast factors for soil type classes for rock slides and soil slides.

Soil erosion.
We also analysed the relation between specific soil characteristics and landslides. The relation of the soil erosion classes and landslides does not seem very logical, as the class without erosion seems to have a positive relation with landslides.

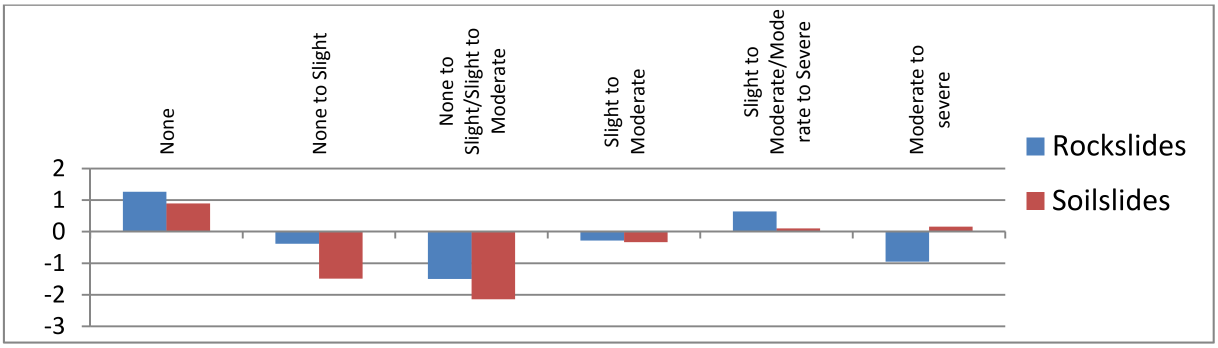

Figure 6-14: Contrast factors for soil erosion classes for rock slides and soil slides.

Soil limitation.
Another attribute of the soil map was called "Soil limitations". There were some classes with a relation with the two types of landslide. In case of rock slides the class "boulders and stones" had a positive relation, while for soil slides the most related factors are "Erosion hazards", which is in contradiction to Figure 6-14.

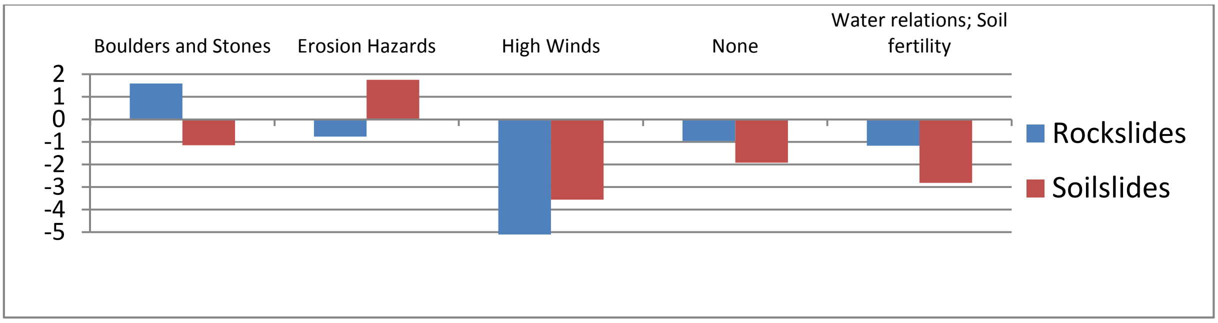

Figure 6-14: Contrast factors for soil limitation classes for rock slides and soil slides.

Land cover/ land use
The results for the relation between land cover and landslide types are summarized in Figure 6-15. The data has been ordered from high to low for rockslides.

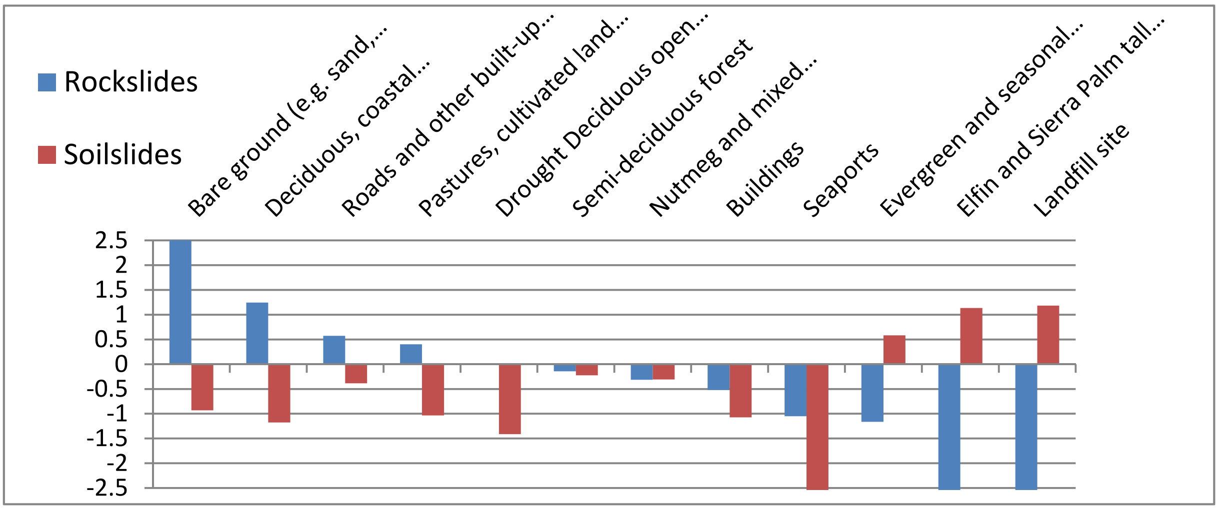

Figure 6-15: Contrast factors for land use classes for rockslides and soil slides.

As can be assumed bare areas have the highest relation with rockslides, however this is a "chicken-and-egg" problem: are the landslides there because the land cover was bare, or is the area bare due to the landslides? Fortunately both rockslides and soil slides have a negative relationship with buildings. Rock slides have a positive relationship with roads in this case as well (meaning that a number of roads are located in rockslide areas, like Mabouya). The positive relation of soil slides with landfill site is due to a single, but fairly large landslide that affected the landfill site at Perseverance, which is not very large in size.

6.3. Summary

Finally, after evaluation all the factor maps and combinations of factor maps, we have drawn conclusions on the usefulness of the various maps for the susceptibility assessment for rockslides and for soil slides. The results are summarized in Table 6-3.

There is a clear difference between the factor maps that are considered useful for the susceptibility assessment of soil slides and rockslides. Obviously soil related factors are less useful as factor maps for the analysis of the susceptibility of rockslides, which are much deeper, and where soil type doesn't play an important role as causal factor. The soil related factors are only relatively useful for soil slides as well, as the relations that we obtained through the statistical analysis are often rather confusing. Also the geological map is perhaps more useful as a factor map for the rockslides, which show a clearer relation with the geological units, than the soil slides, as landslides seem to occur in nearly all units. Nevertheless we will use this factor, but only in combination with slope classes, to avoid illogical combinations. We also do the same for other factor maps, such as soil types, and land use types.

Table 6-5: Summary of the usefulness of the various factor maps used for the statistical analysis for Saint Vincent

Group factor	Factor	Name layer	Rock slides	Soil landslides
Topographic	Elevation classes	Elevation_Class	Somewhat useful	Useful
	Distance from cliff	Cliff_dist_cl	Very useful	Useful
	Slope steepness classes	Slope_cl	Useful	Useful
	Slope direction classes	Aspect_cl	Somehow Useful	Somehow Useful
Drainage	Distance from rivers	River_dist_cl	Not useful	Not useful
Geological	Geomorphological units	Geomorphology	Very useful	Useful
	Lithological units	Geology	Useful	Somewhat useful
Soil map	Soil use limitation	Limitations	Not useful	Not useful
	Soil units	Soil_types	Somewhat useful	Useful
	Soil erosion classes, indicated in soil legend	Soil_erosion_class	Not useful	Not useful
Land cover	Distance from coastline	Coast_dist_class	Very useful	Not useful
	Distance from road cuts	Roadcut_dist_cl	Not useful	Not useful
	Landuse/landcover map	Landcover_2014_modified	Not useful	Somehow Useful
	Distance from roads	Road_dist_cl	Not useful	Not useful
Crossed maps	Combination of geology and slope classes	Geology_Slope_cl	Not useful	Not useful
	Combination of cliffs and slope classes	Cliff_dist_cl_Slope_cl	Not useful	Not useful
	Combination of distance from coast and slope	Coast_dist_class_Slope_cl	Not useful	Not useful
	Combination of landuse and slope classes	Landcr_2014_mod_Slope_cl	Not useful	Not useful

The weights obtained from the Weights-of-evidence modelling are a useful indication for the importance of the various factor classes and factor maps. However, the bottom-line is that an expert should be able to explain why a certain factor class contributes to the occurrence of landslides from a process point of view. This is difficult in many cases, and the weights for a given factor class might be actually due to other factors that are related. As the factor maps have problems with positional, thematic, and temporal accuracy and with lineage as well, we do not want to use the weights from the Weights-of-evidence simply as they are, but will adjust them in an expert based method for combining the factor maps, which will be discussed in the next section.

6.4. Landslide initiation assessment using SMCE

For the actual landslide susceptibility assessment we have chosen to use the results of the bi-variate statistical analysis in an expert-based weighting approach, using Spatial Multi-Criteria Evaluation.
Spatial multi criteria evaluation is a technique that assists stakeholders in decision making with respect to a particular goal (in this case a qualitative landslide susceptibility assessment). It is a spatial tool for transparent decision making, using spatial criteria (in the form of maps), which are combined and weighted with respect to the overall goal, based on expert opinion. In this analysis we decided to use the SMCE module of the ILWIS software as it is one of the best tools for SMCE. The theoretical background for the multi-criteria evaluation is based on the Analytical Hierarchical Process (AHP) developed by Saaty (1980).

The input is a set of maps that are the spatial representation of the criteria, which are grouped, standardised and weighted in a 'criteria tree.' The output is one or more 'composite index map(s),' which indicates the realisation of the model implemented. See Figure 6-16
.

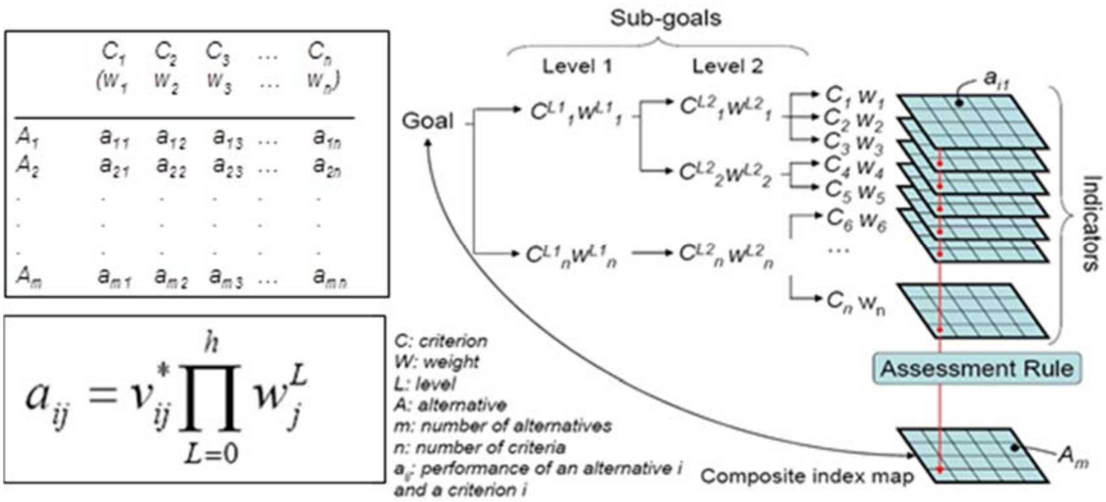

Figure 6-16: Schematic procedure for spatial multi-criteria evaluation based on the analytical hierarchical process

From a decision-making perspective, multi-criteria evaluation can be expressed in a matrix as shown in the Figure 6-17. The matrix A contains the criteria in one axis (C_1 to C_n), and a list of possible alternatives, from which a decision has to be taken on the other axis (A_1 to A_m). Each cell in the matrix (a_{ij}) indicates the performance of a particular alternative in terms of a particular criterion. The value of each cell in the matrix is composed of the multiplication of the standardised value (between 0 and 1) of the criterion for the particular alternative, multiplied by the weight (W_1 to W_n) related to the criterion. Once the matrix has been filled, the final value can be obtained by adding up all cell values of the different criteria for the particular alternative (e.g. a_{11} to a_{1n} for alternative A_1).
For implementing this matrix according to the AHP, three principles steps need to be considered. The first one decomposes the problem (and the weights) into a hierarchical structure. The second one considers the weighting process, employing the pairwise comparisons of the criteria, and the synthesis is related to the multiplications among the hierarchical levels. Additionally, in the spatial implementation of this procedure, every criterion (C_j) becomes a raster layer, and every pixel (or set of pixels) of the final composite index map eventually becomes an alternative A_j. The goal (risk index) has been decomposed into criteria levels C^{L1} and C^{L2}.
The intermediate levels are often indicated as sub-goals or objectives (e.g. in level 1, the sub-goals are a 'topographic index' and a 'soil index'). Each criterion of each level will also have an assigned weight. Therefore, the values for the layers of the intermediate levels are obtained through the summation of the performance for the alternative at lower levels. As the criteria consist of raster maps, their spatial performance (a_{ij}) and the alternative (A_i) will be identified for particular raster cells
The composite risk index map is obtained by an assessment rule (sometimes also called decision rule), which is calculated by adding up the performance of all cell values of the different criteria (aij) for the particular

alternative. However, the performance of every element in the matrix (aij) is obtained in a different way (See equation in Figure 6-16).
In this equation, v_{ij} refers to the standardised value of criterion (C_j) for alternative (A_i), and weight w^L_j refers to the weight of criterion (C_j) for level L (0–h levels). During the analysis, it could be desirable (and sometimes necessary for a better definition of the weights wLj) to produce the intermediate criteria maps.
The general steps in the process are:

- **Definition of the problem**. Structuring of the problem into a criteria tree, with several branches or groups, and a number of factors and/or constraints.
- **Standardization of the factors**. All factors may be in different format (nominal, ordinal, interval etc.) and should be normalized to a range of 0-1. SMCE has some very handy tools for that especially for value data, making use of different transformation graphs.
- **Weighting of the factors within one group**. SMCE has some very handy tools for that derived from Analytical Hierarchical Processing (AHP), such as pair wise comparison and rank ordering. The weights that are derived from the statistical analysis are used as the basis for the weighting. However, users can deviate from that based on their expert opinion.
- **Weighting of the groups**, in order to come to an overall weight value.
- **Classification of the results**.

6.5. Generation of the susceptibility maps for Saint Vincent

Based on the results from the statistical analysis, which were presented in the previous section, two criteria trees were constructed: one for rock slides and one for soil slides. The selection of the criteria, and the grouping, the standardization of the criteria and the weighing of the individual factors was done iteratively. Each time the resulting susceptibility maps were compared with the existing landslide inventory pattern to evaluate whether the areas representing high susceptible zones were in agreement with the expert opinion derived from the image interpretation of the island. A second method to check the quality of the resulting landslide susceptibility maps was made using the application of success rate curves, which will be explained later.
The resulting criteria trees for the generation of susceptibility maps for rockslides and soil slides are shown in Figure 6-17.

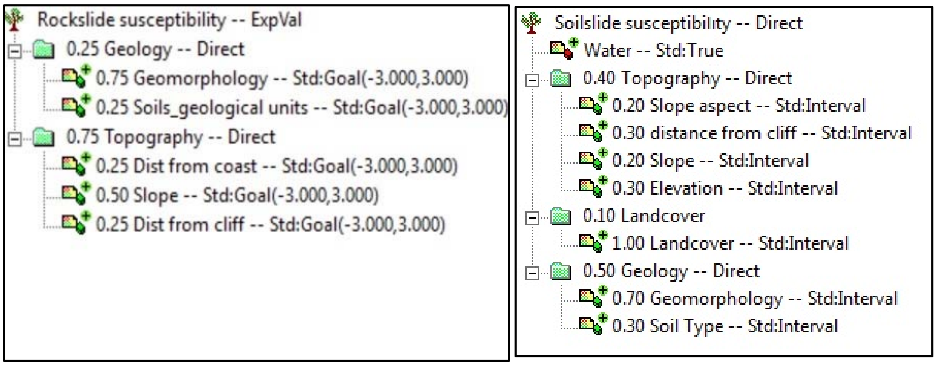

Figure 6-17: Criteria trees used for the susceptibility assessment of rockslides (left) and soil slides (right)

For the criteria selection the results from the bi-variate statistical analysis were leading, however not decisive. For several of the criteria we decided to substitute the weights derived from the statistical analysis with expert-derived weights. This was done for the following reasons:
Many of the factor maps used are rather poor in quality, and have problems in relation to:

- Positional accuracy: due to digitizing problems and projection problems the boundary lines of some of the maps are not always logical. It was not possible to re-digitize all these factor maps, as we didn't have the original maps and this would also take too much time.
- Thematic accuracy: the actual thematic content of the maps is often problematic. Either the units used are too general (e.g. for the geological map, and the land use map) or are not matching internally with the units from other maps, therefore giving a number of rather illogical combinations. These were removed when assigning weights. However, this may not actually improve the final result, as the maps themselves were not improved.

- Temporal accuracy: the maps may not present the situation under which the landslides actually occurred. This is the main problem for the landuse map, for which we have no metadata, and therefore do not know from which year this map is. The land use situation may have changed considerably since the time the map was made.

Since we are not using the weights of the statistical analysis directly as they were, we didn't separate the available landslide data set into a test data set and a training data set, which is customary in statistical landslide susceptibility assessment. We used all the landslides in the exploratory statistical analysis, in order to be able to get a complete picture of the importance of the various factors classes.
We then used the statistically derived weights as a guidance for assigning the expert-based weights in the SMCE. And after generating the final susceptibility maps we calculated the success rates with all landslides of the same type.
.

6.6. Validation of the final susceptibility maps

In the iterative process of using the Spatial Multi-Criteria Evaluation for the generation of the landslide susceptibility maps, two methods were used to evaluate the quality of the resulting maps":

- Visual inspection of the resulting susceptibility classes in relation with the landslide inventory pattern. We overlaid the landslide inventories for rockslides and soil slides on the respective susceptibility maps and evaluated the patterns. Are most of the landslide on or near to highly susceptible area? If not, what are the factors that occur in these landslides, and could these factors be weighted more without making too much other, currently landslide free areas, also highly susceptible? What are the reasons that some landslides are not in the susceptible zones? This is clearly an iterative procedure, and many runs were carried out using different configurations of the criteria trees in SMCE to adjust the result until an optimal result was obtained.
- The generation of so-called *success rate curves*. A success rate curve is made by overlaying the susceptibility map (before classification) with the landslide inventory map. The percentage of the susceptibility map with values ranging from the highest to the lowest is plotted on the X-Axis, and the percentage of the number of landslides on the Y-axis. The steeper the curve is and the more it deviates from the diagonal, the better the prediction is.

The resulting success rate curves are shown in Figure 6-18. We have shown two success rate curves for each landslide type.

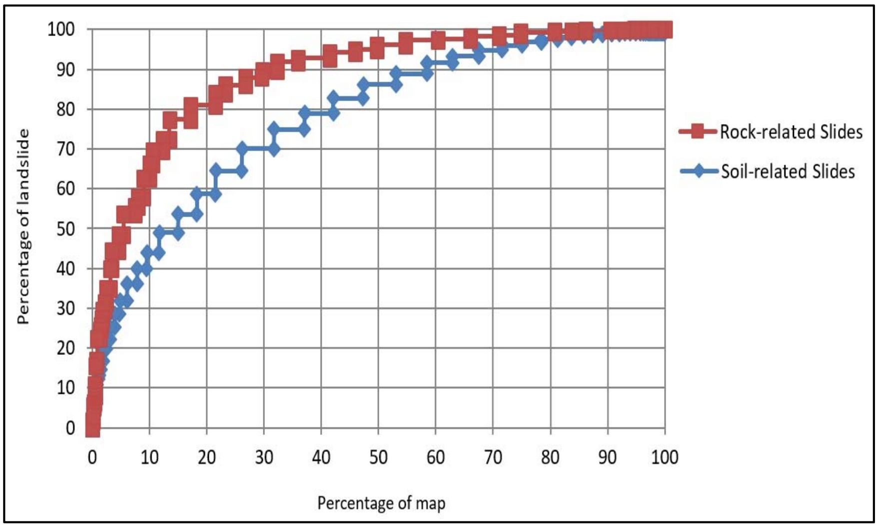

Figure 6-18: Success rate curves for the susceptibility maps for rockslides and soil slides.

From the figures it is clear that the susceptibility map for rockslides is better than the one for soil slides. Rock slides have a more narrowly defined set of conditions under which they occur, and soil slides may occur to a wide variety of conditions, that are not always well depicted in the factor maps.
Success rate is one of the methods to evaluate the quality of the resulting susceptibility map, but not the only one. Previous work has shown that with different combinations of factors, susceptibility maps could be generated with similar success rate curves but very different spatial patterns. Therefore the combination of the two methods is the best in generating the best maps given the limitations in the input data.

6.7. Combining the susceptibility maps

The success rates can also be used to classify the susceptibility maps into a limited number of classes. It is generally best to use only a few classes as this gives the best information for decision makers, and more classes might lead to confusion. After consultation with planners and engineers from Saint Vincent and the other target countries in the CHARIM project, we have decided to classify the susceptibility maps into the following three classes:

- **Low landslide susceptibility class**: this class generally is landslide free, although under very special circumstances it may be possible that a landslide might occur in this zone, but the density and frequency will be extremely low.
- **Moderate susceptibility**: the intermediate zone is actually the most problematic for use in spatial planning and planning/maintenance of infrastructure. This zone has some probability that landslides might occur, although not very frequent and not with a high density. In the process of susceptibility assessment the analysist should make sure to make the size of the moderate class as low as possible, as it is the intermediate, or "left-over" class, which is not as meaningful as the other two classes.
- **High susceptibility**: this class has the highest density and frequency of landslides. Density is derived from previous inventory and frequency by combining it with the frequency of triggering factors.

The criteria that were used for subdividing the landslide susceptibility maps are given in Table 6.6. It is clear that the results for rockslides are better than those for soil slides. However, even these are rather good, with 70% of the landslides in the high susceptibility class, which covers 30% of the island, resulting in a landslide density of 2.84 %.

Table 6-6: Criteria for subdividing the unclassified susceptibility maps into three classes: high, moderate and low

		Rockslides	Soil slides
High susceptibility	Cut-off value	0.49	0.53
	Percentage of the map	20%	30%
	Percentage landslides	83%	70%
	Landslide density	0.60%	2.84%
Moderate susceptibility	Cut-off value	0.38	0.48
	Percentage of the map	40%	28%
	Percentage landslides	14%	22%
	Landslide density	0.06%	0.10%
Low susceptibility	Cut-off value	0	0
	Percentage of the map	40%	42%
	Percentage landslides	3%	8%
	Landslide density	0.01%	0.01%

The resulting landslide susceptibility maps for rockslides and soil slides are shown in Figure 6-19.
For decision makers it is not useful to have two individual landslide susceptibility maps. Therefore we have combined them into one single map, using the following combination table (Table 6-7)

Table 6-7: Combination table for generating the final susceptibility map.

		Soil slide susceptibility map		
Rockslide susceptibility map		Low	Moderate	High
	Low	Low	Moderate	High
	Moderate	Moderate	Moderate	High
	High	High	High	High

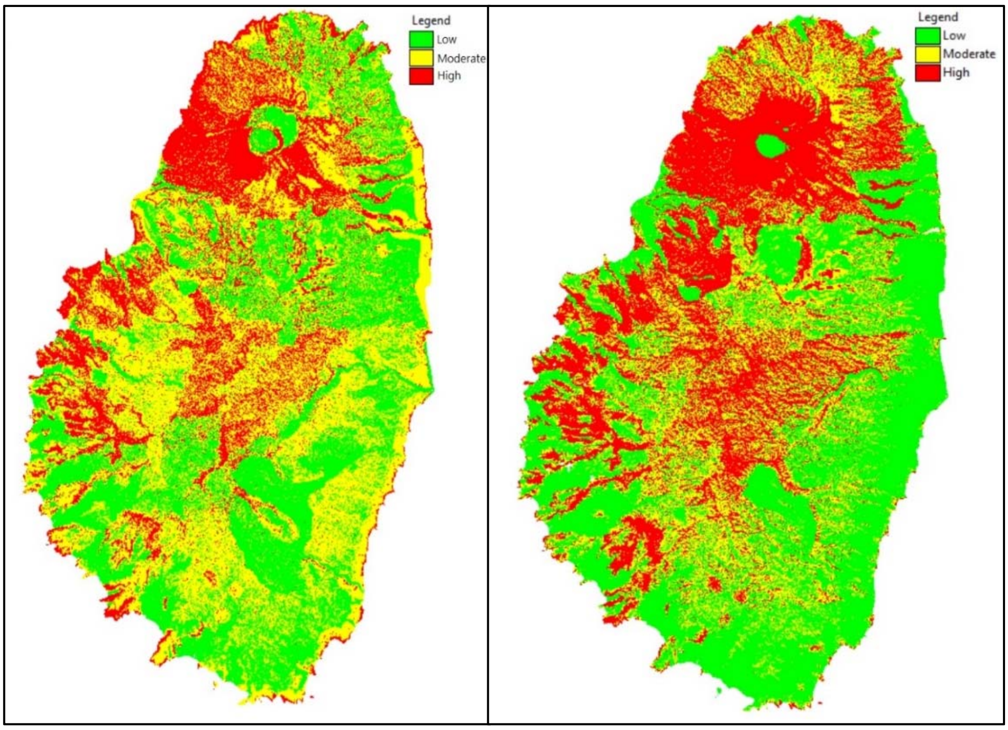

Figure 6-19: Classified landslide susceptibility maps for rockslides (left) and soil slides (right)

After generating the susceptibility map, we still found a number of inconsistencies between the pattern of the mapped landslide and the landslide susceptibility classes. There are several reasons for that:

- First of all related to the landslide locations. We have carefully checked the locations of the landslides during the image interpretation phase, but we are able to check whether the landslides mapped by others are located in the right location. Even a shift of 10 meters might result in a change in landslide susceptibility when making the map overlay between landslides and susceptibility map.
- Secondly, the landslides are mostly mapped as either single polygons, or points. When they are mapped as single polygons, most of the polygon will consist of the runout and accumulation areas of the landslides, which may not correspond well with the landslide initiation susceptibility classes represented on the map.
- Thirdly, the factor maps with which the analysis has been carried out, may be the cause. As was mentioned in chapter 5, the digital elevation model was derived from LiDAR data, and the slope data is very detailed. Therefore local variations in slope steepness may be seen in the map as a mottled pattern of high and moderate pixels mixed together in certain locations. We tried to avoid the mottled pattern in the final landslides map (See Figure 6-20).
- The effect of using such problematic data in combination with landslide locations that are also uncertain is that the resulting weights calculated in the bivariate statistical analysis, often have a lot of noise, and are difficult to interpret.
- Finally, the method used in this chapter thus far generalizes the situation as it brings it back to a combination of a number of factor maps, without paying much attention to the local conditions. For instance when landslides are in general more frequent along the coast, and one would use a certain distance buffer as factor map, this may also have influence on the susceptibility of places that are near the coast but are not susceptible due to other reasons.

In order to improve the final map we carried out steps 10 to 13 as described in section 2.1. First we masked with GIS all historical landslides in the susceptibility map as class “high”, as it is possible that landslides may happen again in these conditions, unless remedial measures have been adopted after the landslide occurrence (See Figure 6-20). The next step was to check and edit the susceptibility map. This was done by exporting the map to an external photo-editing software (CorelPhotoPaint) where it is possible to edit the three classes using the Paint tool. We did this using a dual screen, by comparing the map with a Google Earth image and with a hill shading image overlain with the landslide susceptibility map, plus topographic information, like rivers, roads, buildings etc. This way each part of the area was visually checked, and the modelled zones of high, moderate and low susceptibility were adapted when necessary, so that they reflect the best situation according to the mapping geomorphologist. This was a rather time consuming activity, but it allowed to analyse the different parts of the map separately, and therefore obtain results that also are valid for a local scale, and not only for a national scale. The manual editing of the susceptibility map was also done to simplify the susceptibility units (See Figure 6-20). After running the statistical analysis and spatial multi-criteria analysis, the resulting landslide susceptibility raster map shows many small areas with different degrees of susceptibility. Sometimes the susceptibility differs from pixel to pixel, due to variations in the input maps (e.g. slope classes may differ very locally). In order to be able to use the resulting map as a basis for planning, the area should be subdivided into zones with different likelihood of landslide occurrence. Therefore during the manual editing phases, areas are simplified, and classified into one of the three classes, removing the large local variation. Also after completing the manual editing process, still many locations with isolated pixels remain. These were subsequently removed in GIS using a majority filter. The resulting landslide susceptibility map can also be converted into a polygon map.

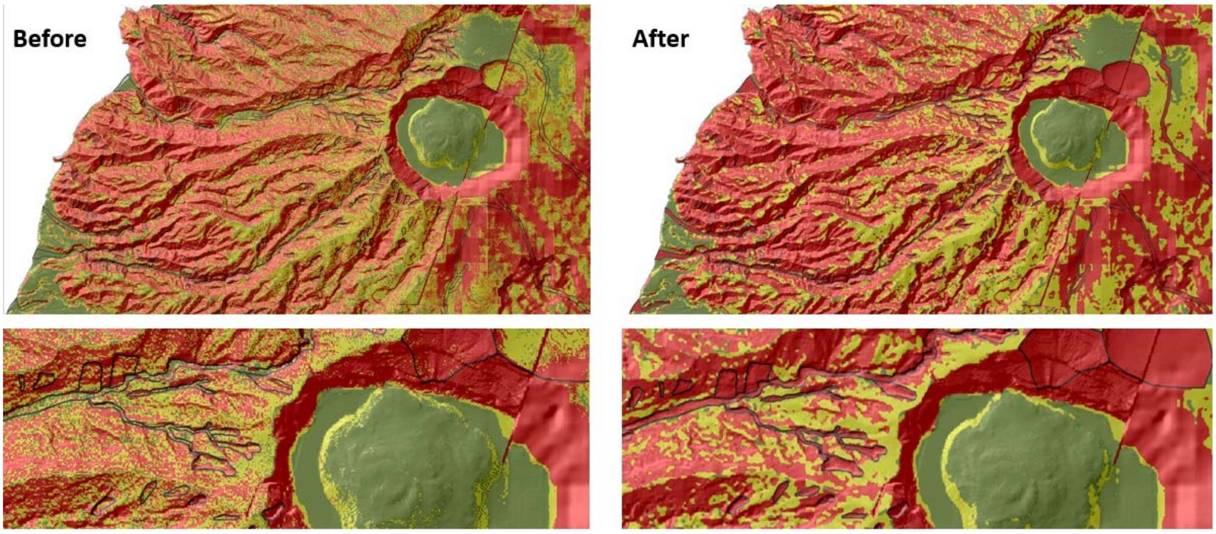

Figure 6-20: The effect of editing the final susceptibility map, shown for an example are near the crater of the Soufriere volcano. Left: before editing and right is after editing. The colours show the susceptibility classes (red= high, yellow= moderate, and green=low). The influence of the poor quality DEM is also visible as the right side of the map, where the straight line forms the boundary between the area covered by the LiDAR DEM (wester part) and by the coarse SRTM DEM (East).

The final landslide susceptibility map is shown in Figure 6-21 (northern part) and Figure 6-22 (southern part). The resulting data for the final susceptibility map is shown in Table 6-8. These maps are available as PDF's on the CHARIM webpage (http://www.charim.net/stvincent/maps). Also the digital versions of the landslide inventories and the landslide susceptibility maps were made available through the GeoNode (http://charim-geonode.net/maps/244).

Table 6-8: Summary information for the final landslide susceptibility map of Saint Vincent.

	Low susceptibility	Moderate susceptibility	High susceptibility
Area in square kilometres	145.11	108.18	89.67
Percentage of total area	42.31	31.54	26.15

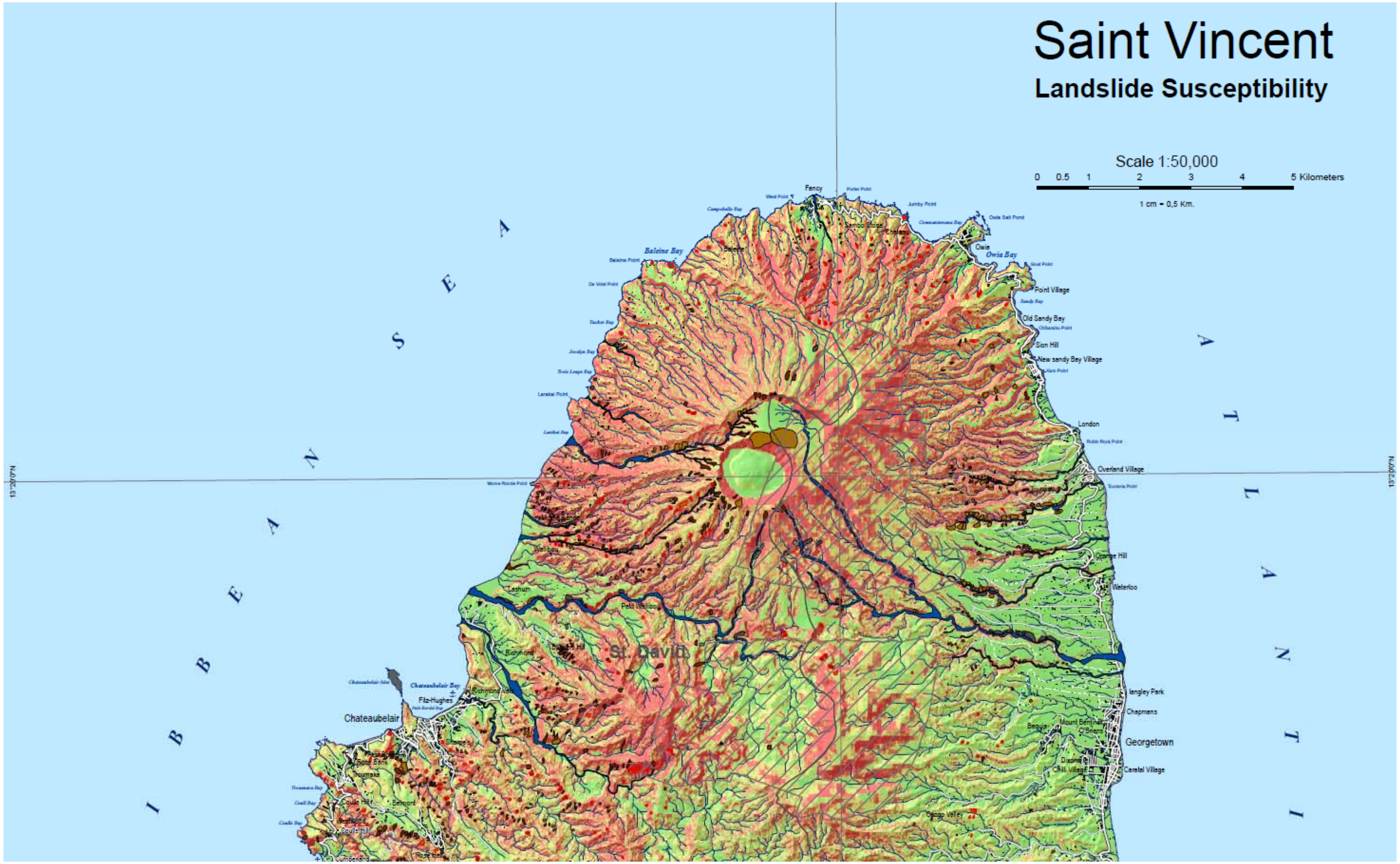

Figure 6-22: Final landslide susceptibility map for Saint Vincent (North part). The full map can be downloaded as pdf from the following website: http://www.charim.net/stvincent/maps

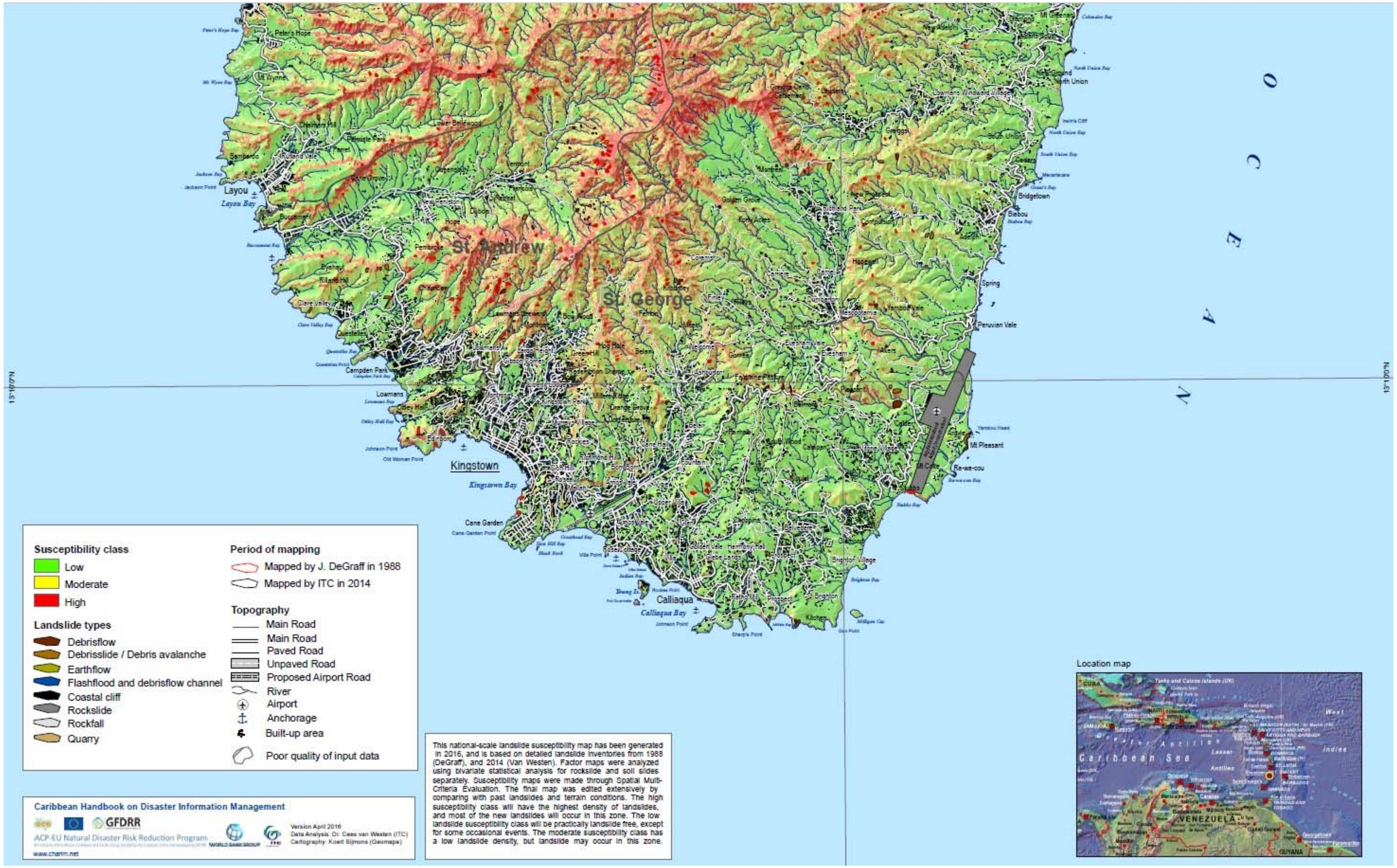

Figure 6-23: Final landslide susceptibility map for Saint Vincent (South part). The full map can be downloaded as pdf from the following website: http://www.charim.net/stvincent/maps

7. Characterizing the susceptibility classes

This chapter aims to show how the landslide susceptibility classes could be characterized in terms of the expected landslide density (in area and number) for different frequencies, and also how many buildings are located in the various susceptibility classes.

7.1. Density and frequency information

Conversion of landslide susceptibility maps into landslide hazard maps requires estimates of spatial, temporal and magnitude probabilities of landslides (Guzzetti et al., 1999; Glade et al., 2005; Fell et al., 2008; Van Asch et al., 2007; Corominas and Moya, 2008; van Westen et al., 2008). The difference between susceptibility and hazard is the inclusion of probability (temporal, spatial and size probability). Temporal probability can be established using different methods. A relation between triggering events (rainfall events) and landslide occurrences is needed in order to be able to assess the temporal probability. Temporal probability assessment of landslides is either done using rainfall threshold estimation, and through the use of multi-temporal data sets. Rainfall threshold estimation is mostly carried out using antecedent rainfall analysis, for which the availability of a sufficient number of landslide occurrence dates is essential. If distribution maps are available of landslides that have been generated during the same triggering event, a useful approach is to derive susceptibility maps using statistical or heuristic methods, and link the resulting classes to the temporal probability of the triggering events. For the Caribbean countries the event-based landslide inventories play a crucial role in characterizing the landslide susceptibility classes with density and frequency information. The number and quality of these maps will determine whether this can be based on a quantitative analysis or also on an expert-based estimation of landslide densities in relation with return periods. For the classified landslide initiation susceptibility map, the historical landslides are used to characterize the classes.

In the previous chapter the landslides susceptibility map was presented for the entire island. This map shows the relative likelihood that a certain area may be affected by landslides. However, for a hazard assessment it is also important to indicate how severe and frequent an area might be affected. In table 7-1 landslide densities are given for the various susceptibility classes. Unfortunately for the study area very limited information is available in terms of event-based landslide inventories for different return periods. We only have the inventory that was generated through image interpretation, and the inventory from DeGraff (1988). We do not have enough information to link these inventories to particular rainfall events, and therefore we cannot include return periods.

Table 7-1. Summary information of different landslide inventories within the low, moderate and high susceptibility classes

		Landslide susceptibility		
Source	**Characteristics**	**Low**	**Moderate**	**High**
The study area	Area in square kilometres	145.11	108.18	89.67
	Percentage of total area	42.31	31.54	26.15
De Graff 1988	Landslide area (m^2)	93450	364325	749350
	Number of landslides	194	441	488
	Landslide density (percentage)	0.00064	0.00338	0.00843
	Landslide density (nr/km^2)	1.34	4.08	5.44
This study (2015)	Landslide area	155925	319600	639125
	Number of landslides	423	810	939
	Landslide density (percentage)	0.00108	0.00296	0.00718
	Landslide density (nr/km^2)	2.92	7.49	10.47
Total	Landslide area	249375	683925	1388475
	Number of landslides	617	1251	1427
	Landslide density (percentage)	0.00172	0.00636	0.01573
	Landslide density (nr/km^2)	4.25	11.56	15.91

7.2. Exposure analysis

The final susceptibility map can be used for calculation the exposure of buildings, roads and other infrastructure. Building data was available for Saint Vincent. However, the data was not editable in a GIS due to many digitizing and topological errors, with overlapping boundaries and double digitized boundaries of building footprints. The buildings also didn't have any attribute data. The building footprint map was also not updated, and the new situation in the international airport was not yet included in the building footprint map. High resolution imagery of the satellite Pléiades was available for the whole island. The resolution of multi-spectral image is 2 meters whereas, panchromatic is 0.5 meters. Both images were fused to get highest possible resolution with colour. This provided a good quality data that could be used together with building footprints to update buildings. The building footprints were subsequently overlain with the landslide susceptibility map and with the Parish map.
The results of the building exposure analysis is shown in Table 7-2. The results show that in the entire country 400 buildings (0.8 % of the total) are located in high landslide susceptibility zones, 2508 (4.8 %) in moderate susceptibility zones and the vast majority of 48950 buildings (94.4 %) in low landslide susceptibility zones.
When we evaluate these values per Parish, Saint David parish has the largest percentage of buildings located in high susceptibility zones (187 buildings, which is 5.2 %). Many of these buildings are semi-illegal informal buildings located on the slopes of Soufriere volcano, related to marihuana plantations.

Table 7-2. Buildings exposed to low, moderate and high susceptibility classes for the whole country and for individual Parishes.

	Landslide susceptibility			
Parish	**Low**	**Moderate**	**High**	
Charlotte	15352	481	41	15874
St Andrew	6248	391	51	6690
St David	2911	466	187	3564
St George	20402	944	30	21376
St Patrick	4037	226	91	4354
Total	48950	2508	400	

Table 7-3: Percentage of buildings located in low, moderate and high landslide susceptibility zones per parish.

	Landslide susceptibility			
Parish	**Low**	**Moderate**	**High**	
Charlotte	96.7	3.0	0.3	
St Andrew	93.4	5.8	0.8	
St David	81.7	13.1	5.2	
St George	95.4	4.4	0.1	
St Patrick	92.7	5.2	2.1	

One should be careful when using the national-scale landslide susceptibility and hazard map for evaluating the landslide hazard of individual buildings and critical infrastructure. The scale of this map is not appropriate to utilize it for local or detailed scale analysis. Other, more detailed landslide hazard methods should be used for these scales, which also require more detailed information on soil characteristics, such as soil depth, hydrological and geotechnical properties.

8. Conclusions and recommendations

8.1. Conclusions

The original aim of this study was to generate a national-scale landslide susceptibility and hazard map using the available data for Saint Vincent. However, the available data turned out to be insufficient to generate reliable results. We therefore generated several new data layers, and adjusted quite some of the existing data:

- We generated a new database of disaster events for Saint Vincent using all available data, making use of many different sources, which was presented in Table 3-2. This is the most complete inventory up to our knowledge.
- We also compiled all available landslide data from different sources, and generated a completely new landslide inventory using multi-temporal visual image interpretation, and generated an extensive landslide database for Saint Vincent.
- We generated a geomorphological map.
- We improved the land use map as much as possible.
- We improved the national building footprint map and added information on occupancy types, and number of people, based on census data.

We analyzed the triggering conditions for landslides as far as was possible given the available data, and generated rainfall magnitude-frequency relations. Rainfall magnitude-frequency relations for different landslide densities might not be required for a landslide susceptibility assessment, but they are important to convert susceptibility into hazards. However, there were not enough data (both in terms of landslide dates and date-related inventories) to be able to calculate magnitude-frequency relations for landslides, in terms of the number or density of landslide per different frequencies.

We applied a method for landslide susceptibility assessment that is the best possible, given the availability of data. The bi-variate statistical analysis provided indications on the importance of the possible contributing factors, but the actual combination of the factor maps was done using a subjective expert-based iterative weighing approach using Spatial Multi-Criteria Evaluation. The method is transparent, as the stakeholders (e.g. the engineers and planners from the four countries) and other consultants can consult the criteria trees and evaluate the standardization and weights, and make adjustments.

It is important to state here that this method doesn't propose to come to a fixed number of contributing factors or to fixed weights that should be used. In each country or situation the experts that do the analysis should decide what the main contributing factors are, what their relative importance is, and assign the weights.
We also generated different landslide susceptibility maps for different landslide types, as they were related to different combinations of causal factors. The two susceptibility maps made for rockslides/rockfall and for soil-related landslides were combined into one single map, which is more easy to use by the end users.

We initially were also planning to generate both initiation and accumulation (run-out) susceptibility. However, given the small scale of the analysis and the large area covered (and the related large computation time using an empirical run-out model like FLOW-R) we decided not to do that. In more local scale assessments such runout analysis should be incorporated though.

The national scale landslide susceptibility and hazard assessment should not be used to evaluate local scale or site-investigation problems. The analysis was done using raster maps with a spatial resolution of 5 meters. Most of the input data was obtained from 1:25000 or even 1:50000 scale maps. Also given the relatively poor quality of the factor maps (especially the Digital Elevation Model, the geological map and the land use map) the local variations are not properly depicted in the final map.

For these scales the optimal approach is the use of physically-based landslide susceptibility assessment methods. These methods are based on modelling the processes of landslides using physically-based slope stability models. An overview of physically based models and their application for landslide susceptibility assessment is given in Brunsden (1999), Casadei et al. (2003), Van Asch et al. (2007) and Simoni et al., (2008). Most of the physically-based GIS models that are applied at a local scale (SINMAP, TRIGRS, SHALSTAB, STARWARS, PROBSTAB) make use of the infinite slope model and are therefore only applicable to modelling shallow translational landslides. At site investigation scale it is possible to apply 2-D Limit equilibrium methods with groundwater flow and stress analysis (E.g., SLOPE/W, SLIDE, GALENA, GSLOPE), 3-D slope stability analysis (e.g. CLARA-W, TSLOPE3, SVSLOPE) or numerical modelling (e.g. continuum modeling (e.g. finite element, finite difference) , like FLAC3D, VISAGE, or discontinuum modeling (e.g. distinct element, discrete element), e.g. UDEC).

The final national landslide susceptibility and hazard map is called that because it is basically a landslide susceptibility map, which divides the country in three zones with a different likelihood of landslide occurrence. However, based on the available data we also tried to express information on the magnitude of landslides (in terms of the expected landslide density) and the related frequency, which are both related to the hazard component. The final legend of the susceptibility map is given in Table 8-1. These maps are available as PDF's on the CHARIM webpage (http://www.charim.net/stvincent/maps). Also the digital versions of the landslide inventories and the landslide susceptibility maps were made available through the GeoNode (http://charim-geonode.net/maps/244).

Table 8-1. Characterization of the landslide susceptibility classes.

Susceptibility	Explanation	Characteristics
Low	This class generally is landslide free, although under special circumstances it may be possible that a landslide might occur in this zone, but the density and frequency will be low.	Area: 145.11 km^2 Landslide area: 25 hectares Number of landslides: 617 Spatial probability: 0.00172 Landslide density: 4.25 landslides /km^2
Moderate	This class has some probability that landslides might occur, although not very frequent and not with a high density.	Area: 108.18 km^2 Landslide area: 68 hectares Number of landslides: 1251 Spatial probability: 0.00636 Landslide density: 11.6 landslides /km^2
High	This class has the highest density and frequency of landslides.	Area: 89.67 km^2 Landslide area: 139 hectares Number of landslides: 1427 Spatial probability: 0.01573 Landslide density: 15.9 landslides /km^2

8.2. Recommendations

This study tried to generate the best possible landslide susceptibility and hazard map at a national scale gievne the limitations of data availability and time. Nevertheless, in order to be able to make a reliable landslide hazard map that also represents future changes the following recommendations are given:

1. **Establishment of a national landslide database**.

Currently there is no single organizations responsible for generating and maintaining landslide data in Saint Vincent. The Ministry of Transport, Works, Urban Development & Local Government, and the Ministry of Housing, Informal Human Settlements, Lands & Surveys and Physical Planning, should collaborate with NEMO to store the landslide information into a landslide database. However, the current situation is that these data get lost after some years. NEMO receives information about emergencies, which also include landslide events. Also the physical planning division requires landslide data for generating land use plans, and for building permit issuing. The current practice is that landslide data is collected by external parties within international projects. There is a need to develop a national landslide database, which requires that one organization is made responsible for generating and maintaining such a database, and where several other organizations should contribute. This will require additional funding from a donor agency to set it up. The landslide inventory should be stored in a web-mapping application, with a Google Earth or other background, where various national and international organizations can consult the existing landslide information, and where new landslide events can be added by government organizations, local people, news media, NGO's etc. A close collaboration with the online news media in Saint Vincent is highly recommended, as they are reported many landslide events, with additional photo or video footage, which could be easily linked to a geolocation, and stored in such a database so that the information is not lost. It is very important to get better data on the location, type, damage and especially the date of landslide events, so that in future a correlation between rainfall characteristics and landslide incidences, and the establishment of rainfall thresholds, and frequency/magnitude relationships can be properly carried out. These reported events would be stored in a separate database, which is used by the national responsible organization for landslide inventory mapping, as the basis for checking. These are added to the actual database only after they have been checking by an expert. This will also allow the continuation of the landslide database in future. It is essential that there is a close collaboration between the various national organizations that have to deal with landslides. However, one organization should be the nodal agency responsible for setting-up the national landslide database.

Figure 8-1: Screenshot of a web-based hazard reporting system developed for another country

2. **Generating landslide susceptibility map along the road network.**

Landslide information along the national road network was not available as a geo-coded dataset, so we could not use these in a landslide susceptibility assessment along the road network. Therefore we didn't perform this analysis for Saint Vincent. The method used is presented in Figure 8-2. Such approaches were used by other authors for similar studies and they are proved to be significant factors for road related landslides (e.g., Das et al, 2010; Jaiswal et al, 2011; Jaiswal and Van Westen, 2013).

Road segmentation and characterization refers to subdividing the road network into smaller segments that possess the same spatial characteristics. This can be done using available road map, with a subdivision of the roads into the following categories: primary road, secondary road, tertiary road and road under construction

For such a study only the primary road network should be considered. Normally in such type of project a road database from the Ministry of Works should be used. Such a road database should be updated after major changes in the road network. Such a database should contain information on the following items: drainage type and drainage width both on the left and right side of the road, indication whether the roadside is a cutslope, valley or flat, indication of landslide mitigation measures along the road, indication of historical landslide locations along the road, and land use of the area around the road section.

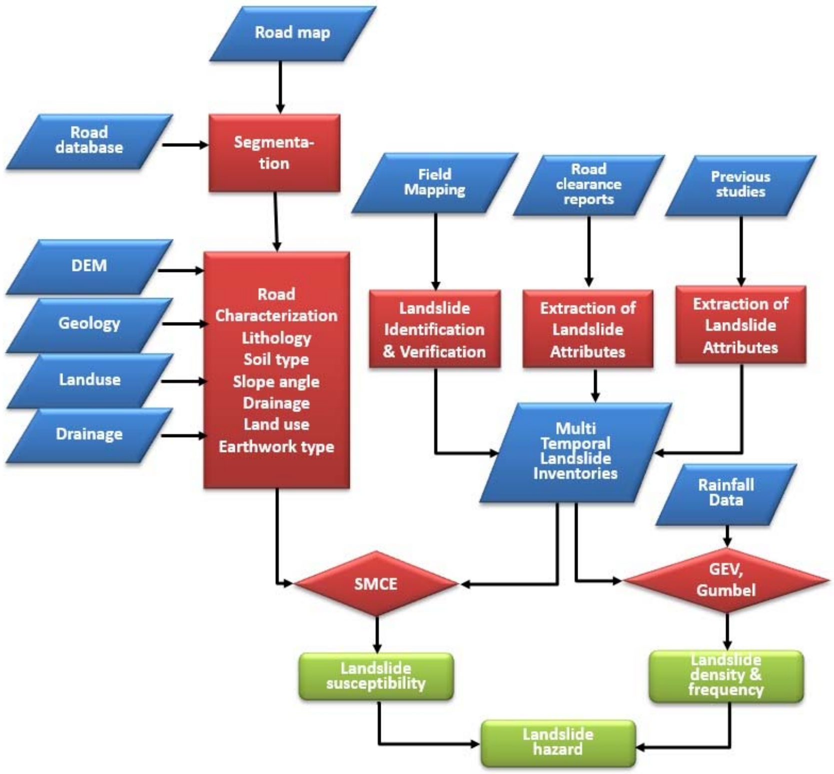

Figure 8-2: Method used for assessing the landslide susceptibility along the national road network in Saint Vincent.

These data should be made available for road homogenous road section that have a length preferably of less than 1 km. In the database the road sections should be indicated by their starting and end points, and should be linked to a GIS layer which has the same codes. The lithology, soil type and slope angle of the road segments can be extracted from the available geological map, soil map and digital elevation model (DEM) respectively. For this purpose buffer maps along the road network can be prepared taking a 50 m buffer distances on both sides. For each road segment the upslope side buffer should be identified based on the information obtained from the road database and image interpretation.
Road maintenance and clearance reports should be prepared by the Road Department after each rainfall event that leads to landslides and flooding. Unfortunately no information was available in Saint Vincent for such events, except one in 2005. The results should be stored in the road database, and should also be located with GPS, so a link should be made with a point file of these incidents.
The landslide susceptibility assessment along the road network can also be carried out using Spatial Multi-Criteria Evaluation (SMCE). The basic units are the road segments that are generated from the road database. The criteria tree for Saint Vincent could contain factors such as slope conditions along the road, drainage, material and land use attributes as spatial factors. Under the slope factor, slope type of adjacent ground left and right and slope angle can be included. The slope type of the adjacent ground indicates whether the road segment is a cut-slope, valley or flat section. In the drainage spatial factor, side ditch type left and right can be included. To check the validity of the analysis results also success rate calculations could be made using available landslide inventories along the road. In future such results could be improved when a consistent landslide database would be maintained on the island. Based on the success rate results, the susceptibility map can be classified into three classes of susceptibility level i.e. high, moderate and low.

3. Improve the LiDAR derived DEM for Saint Vincent

Although Saint Vincent has a Digital Elevation Model derived from LiDAR data the data quality of the LiDAR-derived DEM varies considerably. The DEM had one large problem though: the centre of the island was not covered by LiDAR data. We had another raster dataset (also for this we had no metadata) that we used to fill up the hole in the LiDAR data. However, at the boundaries of the missing LiDAR data there are a number of artefacts (errors in the DEM) that gave problems especially in the modelling. The areas within the red line in Figure 5-2 have a poor data quality. So the landslide susceptibility of this particular zone is less reliable. Users should take this into account when using the map.

A detailed bare-surface model would allow for interpretation of geomorphological evidence of old landslides, and other relevant geological and geomorphological features much better (Razak et al., 2013). DEM derivatives such as slope steepness, slope direction, local drain direction, flow accumulation, slope convexity and slope length would be much more accurate than they are now. LiDAR-derived DEMs are also essential for other applications, such as for flood hazard assessment, where very local topographic differences are important, and also for many other application related to hazard and risk assessment, forestry, agriculture, and tourism. LiDAR data would also allow to generate building footprint maps in an automatic way, and would also allow to record building heights, which are very useful for exposure and risk assessment, but also for a large number of other planning and management activities related to housing, schooling, shelter planning, health, social aspects etc. And LiDAR survey would also allow to generate an improved land use map, in combination with the optical images that are normally collected simultaneously with a LiDAR survey. Vegetation characteristics (height of vegetation, density etc.) can be derived from LiDAR data.

4. Updated engineering geological map for Saint Vincent

The available soil map was made a long time ago without the new technology that is now available. The available map is also focusing on pedologic soils, which makes it less useful for landslide applications, where we are more interested in engineering soils and their characteristics. The existing geological map focuses on the description of the age and origin of the rocks rather than on their engineering characteristics. Therefore there is a need to generate an engineering geological map for Saint Vincent that would describe engineering soil and rock types. Engineering soils need to be described with respect to their origin (e.g. weathering soil, colluvial soil, alluvial etc), grainsize composition, depth, geotechnical characteristics (soil strength, atterberg limits etc) and hydrological characteristics (infiltration capacity, hydraulic conductivity, pore space etc). Engineering rock types should focus on their lithology, depth of weathering zones, and geotechnical characteristics (rock strength, discontinuities etc) (Chacon et al., 2006). The updated engineering geological map should be generated on the basis of a detailed terrain mapping, which should be done using the LiDAR-based hillshading image as a basis, by an experienced geomorphologist. Based on the terrain classification, individual material units are outlined, which are subsequently described in term of material types, vertical sequences and depths of soil layers. Based on the classification of the material types a stratified sampling scheme should be designed to sample the various types of materials and test them in the field for infiltration capacity, and in the laboratory for saturated hydrological conductivity, density, porosity, swelling clay potential, cohesion and angle of internal friction.

5. Updating the landslide susceptibility map

It is advisable to update the landslide susceptibility map regularly, as land cover and other relevant contributing factors related to landslide occurrences might change. We advise to update the landslide susceptibility map at least once every five years. We also advise to update the map after every major extreme rainfall event that has triggered a substantial (>15) number of landslides. The updating could be done by organizations in the country, although it is advisable to ask consultants or University of the West Indies to do this work. The landslide susceptibility map should have small high and moderate classes, and as high as possible low susceptibility classes. This means that it is important to incorporate new landslide in the high susceptible class and re-analyse the factors using the method indicated in this report. In the classification of the final susceptibility zones, it is then important to check with success rate curves and adjust the modelling until the highest success rate possible is obtained, which is then used to determine the thresholds between the high, moderate and low classes. It is also important to manually edit the final susceptibility map, as indicated earlier on in this report.

6. Including runout assessment in the susceptibility assessment

This report only discussed the generation of an initiation susceptibility map at a national scale, which was classified into three classes. At this scale it is not yet possible to also analyse runout susceptibility for the entire country, as this would be extremely time consuming with the existing methods. In local scale studies it would be relevant to extract the high susceptible initiation areas, and use these in a regional scale run-out model. One of these models is the Flow-R model, which was developed by the University of Lausanne, and is freely available from the following website: http://www.flow-r.org/ Flow-R (Horton et al., 2013) is a modelling software that uses a GIS empirical distribution model to probabilistically estimate the flow path and run-out extent of gravitational mass movements over larger areas. It was successfully applied to different case studies in various countries. Flow-R first requires the identification of source areas before the actual run-out can be modelled. Two parameters are required to model the run-outs for each return period in the Flow-R model: (1) the minimum

travel angle and (2) the maximum velocity. These two parameters can be estimated based on literature review or back calibrated based detailed run-out models. It is possible to use different travel angles and maximum stopping velocity for different return periods, assuming that larger triggering events will result in larger landslides with longer travel angles.
The software calculates probably flow paths from source points based on energy line calculations. The energy calculation is illustrated by the below example. Initially the potential energy is converted into kinetic energy, and the most likely flow paths are determined, until the runout reaches a certain distance where the line between the starting points and the end point is characterised by the reach angle, related to the H/L ratio, and the process stops. The method doesn't require source volumes, or rheological parameters. It also doesn't consider entrainment. It can calculate the flow paths from many different source zones at the same time. This makes the model suitable for use at a regional to medium scale. The results are indicative, but previous work has shown that the calculated distances correlate well with more detailed run-out models. The model can also be applied for different types of movement, e.g. debris flows, flow slides, and rockfall, by varying the reach angles.

7. Improvement of the HydroMet system for Saint Vincent

We were only able to obtain daily rainfall data for a one station (E.T. Joshua Airport) in Saint Vincent that covers a substantial number of years of data. We have cleaned the data and made them available to the organizations in Saint Vincent. There are also some other rain gauges that have shorter records and some project-related rainfall data (e.g. JICA Early Warning Project). In order to be able to make better predictions for landslides as well as floods, and droughts it is essential that the HydroMet system is improved. Continuous recording stations should be installed in more locations, and the data should be made available through the web. Given the small size of Saint Vincent it may be desirable that the CIMH would take the lead in this. Weather radar will be extremely important as this will allow to measure the spatial distribution of rainfall over the islands, and therefore have better inputs into the flood modelling, and a better correlation of causal factors with landslides.

8. Further training and discussion

The current version of the landslide susceptibility and hazard map should be discussed extensively with the experts in the various government departments, but especially with the Physical Planning Unit and the Roads Unit of the Ministry of Communications, Works, Physical Development, Public Utilities, ICT & Community Development. The use of this map in land use planning, building permit issuing and land subdivision process should be further discussed. Also recommendations with respect to landslide hazard assessment at the local and detailed level should be discussed with the local organizations. Further training on the use of the maps and the method for generating them would also be important, especially when one government organization would be give the responsibility for generating and maintaining a national landslide database, this organization should also be trained in using that data for updating the national and local scale landslide hazard maps. Further training is also required in the use of spatial data and the sharing of spatial data through the GeoNode: http://charim-geonode.net/people/profile/svg/?content=layers
We recommend that the landside susceptibility and hazard map is updated once more detailed input data become available (e.g. the LiDAR data) or after a major triggering event. We have generated the datasets and calculation script for updating the landslide susceptibility maps for each of the countries, and will make these available to interested parties, and possibly also through the GeoNode. The analysis was carried out using the Open software ILWIS, which is also made available.

9. Implications of the susceptibility classes for planning

The landslide susceptibility map should be used by planners and other professionals as the source of information on where landslide problems can be expected in future. Although the map is a national scale map, in the preparation also local situations were taken into account during the map editing stage. However, the map is still a national scale map and cannot be used for local or site specific planning.

We recommend the following use of the susceptibility classes:

- **Low susceptibility**: For planners there is no limitation with respect to expected landslide problems in the development of these areas. No special care should be taken by engineers with respect to planning and maintaining infrastructure in these areas with respect to landslides. Of course it is important to also check the other hazard maps for these areas. Of course it is important to also check the flood hazard maps for these areas, as areas that are flat and near a river or coast might be still flood prone.

- **Moderate susceptibility**: It is advised to carry out a more detailed landslide study for residential development and for critical infrastructure. There is no need to avoid these areas altogether, but care should be taken that landslides might occur. This class is actually the most problematic for use in spatial planning and planning/maintenance of infrastructure, as it is an intermediate class.
- **High susceptibility**: There are severe restrictions with respect to expected landslide problems in these areas. The best is to avoid these areas in the development of future residential areas or critical infrastructure whenever possible. Development plans should always incorporate a more detailed study of landslide hazard in these areas. Engineers should consider the high landslide hazard when designing or maintaining infrastructure. Further evaluations would have to be carried out before allowing new constructions – be that an expert inspection of the site, detailed slope stability evaluations – that may depend on the importance of the asset (e.g. a private building would be dealt with differently than a hospital)

One could argue that it is not possible to make the underlying implications for planning, given the high level of uncertainty, related to the poor quality of data, and that making restrictions based on this map can generate an immediate conflict with the inhabitants of the areas that are located in areas of "high sensitivity". However, the alternative is not to use any guidance map and wait until more detailed maps are available with the utopy that these will be without uncertainty. It is better to act now, even based on maps that are uncertain, than to increase the risk in potentially dangerous area, leading to losses of life and investments.

9. References:

Aleotti P (2004) A warning system for rainfall-induced shallow failures. Eng Geol 73: 247–265.

Aleotti, P. and Chowdury, R. 1999. Landslide hazard assessment: summary review and new perspectives. Bull. Eng. Geol. Env. (1999): 21-44, pp 21- 44

Andereck, Z. D. (2007). Mapping Vulnerability of Infrastructure to Destruction by Slope Failures on the Island of Dominica, Wi : A Case Study Of Grand Fond, Petite Soufriere, And Mourne Jaune. Faculty of Miami University.

Anderson, M. G., Holcombe, E., Blanke, J.R., Ghesquir, F., Holm-Nielsen, N., & Fisseha, T. (2011). Reducing landslide Risk in communities: evidence from the Eastern Caribbean. Applied Geography, 31(2), 590-599.

Arculus, Richard John (1973). The alkali basalt andesite association of Grenada Lesser Antilles, Durham theses, Durham University. Available at Durham E-Theses Online: http://etheses.dur.ac.uk/10510/

Ardizzone, F., Cardinali, M., Carrara, A., Guzzetti, F. and Reichenbach, P.: Impact of mapping errors on the reliability of landslide hazard maps, NHESS, 2(1/2), 3–14, 2002.

Benavot, A. and Riddle P., 1988. The Expansion of Primary Education, 1870-1940: Trends and Issues. Sociology of Education, Vol. 61, No. 3 pp. 191-210.

Blahut, J., van Westen, C.J., Sterlacchini, S., 2010. Analysis of landslide inventories for accurate prediction of debris-flow source areas. Geomorphology, 119(1–2), 36-51.

Bonham-Carter, G.F., Agterberg, F.P., Wright, D.F., 1988. Integration of geological datasets for gold exploration in Nova Scotia. Photogrammetric Engineering and Remote Sensing, 54(11), 1585-1592.

Bonham-Carter, G.F., Agterberg, F.P., Wright, D.F., 1989. Weights of evidence modelling: a new approach to mapping mineral potential. In: D.F. Agterberg, G.F. Bonham-Carter (Eds.), Statistical Applications in Earth Sciences. Geological Survey of Canada, Ottawa.

Boruff, B.J. and Cutter, S.L. (2007). The Environmental Vulnerability Of Caribbean Island Nations. The Geographical Review 97 (1): 24-45,

Brunsden, D. (1999). Some geomorphological considerations for the future development of landslide models: Geomorphology. 30(1-2), p. 13-24.

Cabria, X. (2015). Effects of weathering in the rock and rock mass properties and the influence of salts in the coastal road cuts in St. Vincent and Dominica. MSc thesis, Faculty of Geo-Information Science and Earth Observation (ITC), University of Twente. https://www.itc.nl/library/papers_2015/msc/aes/cabria.pdf

CarLand (2000). Caribbean Land cover Analyses. USGS. http://lca.usgs.gov/lca/carland/dataproducts.php

Casadei, M., Dietrich, W.E., and Miller, N.L. (2003). Testing a model for predicting the timing and location of shallow landslide initiation on soil mantled landscapes: Earth Surface Processes and Landforms. 28(9), p. 925-950.

CDMP [Caribbean Disaster Mitigation Project]. 1999. The TAOS/L Storm Hazard Model and CDMP TAOS/L Applications. Implemented by the Organization of American States, Unit of Sustainable Development and Environment for the USAID Office of Foreign Disaster Assistance and the Caribbean. Regional Program. http://www.oas.org/CDMP/hazmap/taos/taosdoc/taosfull.htm

CDMP (Caribbean Disaster Mitigation Project) 2000. Atlas of Probable Storm Effects in the Caribbean Sea. Implemented by the Organization of American States, Unit of Sustainable Development and Environment for the USAID Office of Foreign Disaster Assistance and the Caribbean Regional Program

Chacon J, Irigaray C, Fernandez T, El Hamdouni R (2006) Engineering geology maps: landslides and geographical information systems. Bull Eng Geol Environ 65:341–411.

Charveriat, C. (2000) Natural disasters in Latin America and the Caribbean: an overview of Risk. Interamerican Development Bank (IDB). http://papers.ssrn.com/sol3/papers.cfm?abstract_id=1817233

Corominas J, Moya J (1999) Reconstructing recent landslide activity in relation to rainfall in the Llobregat River basin, Eastern Pyrenees, Spain. Geomorphology 30(1–2):79–93. doi:10.1016/s0169- 555x(99)00046-x

Corominas J (2000) Landslides and climate. Keynote lecture- In: Proceedings 8th International Symposium on Landslides, (Bromhead E, Dixon N, Ibsen ML, eds). Cardiff: A.A. Balkema, 4: 1–33

Corominas, J. C.J. van Westen, P. Frattini, L. Cascini, J.-P. Malet, S. Fotopoulou, F. Catani, M. Van Den Eeckhaut, O. Mavrouli, F. Agliardi, K. Pitilakis, M. G. Winter, M. Pastor, S. Ferlisi, V. Tofani, J. Hervas, and J. T. Smith (2014) Recommendations for the quantitative analysis of landslide risk. Bulletin of Engineering Geology and the Environment, V 73, N 2, pp 209–263.

Crosta G (1998) Regionalization of rainfall thresholds: an aid to landslide hazard evaluation. Environ Geol 35(2):131–145. doi:10.1007/s002540050300

Cross, J.A. (1992). Natural Hazards within the West Indies. Journal of Geography, Volume 91, 5, 190-199

Crosta GB, Frattini P (2001) Rainfall thresholds for triggering soil slips and debris flow. In: Proceedings 2nd EGS Plinius Conference on Mediterranean Storms (Mugnai A, Guzzetti F, Roth G, eds). Siena: 463– 487

Crowards, T. (2000) Comparative Vulnerability to Natural disaster in the Caribbean. CARIBBEAN DEVELOPMENT BANK, Staff Working Paper No. 1/00.

Crozier, M.J. (2005). Multiple occurrence regional landslide events in New Zealand: hazard management issues. Landslides,2: 247-256

Dahal RK, Hasegawa S (2008) Representative rainfall thresholds for landslides in the Nepal Himalaya. Geomorphology 100(3–4):429–443. doi:10.1016/j.geomorph.2008.01.014

Dai, F.C., Lee, C.F. and Ngai, Y.Y. (2008). Landslide risk assessment and management: an overview . Engineering Geology, 64 (1), 65-87

Das, I., Sahoo, S., van Westen, C.J., Stein, A. and Hack, H.R.G.K. (2010) Landslide susceptibility assessment using logistic regression and its comparison with a rock mass classification system along a road section in the northern Himalayas. In: Geomorphology, 114 (2010)4 pp. 627-637

DeGraff, J.V., 1988. Landslide hazard on St. Vincent, West Indies-Final Report. Washington, D.C., Organization of American States. 20 pages

DeGraff, J.V., Bryce, R., Jibson, R.W., Mora, S., and Rogers, C.T. 1989. Landslides: Their extent and significance in the Caribbean. In E.E. Brabb and B.L. Harrod (eds), Landslides: Extent and Economic Significance. p. 51-80. Rotterdam: A.A. BalkemaDeGraff, J. V., 1991: Determining the significance of landslide activity: Examples from the Eastern Caribbean. Caribb. Geogr., 3, 31–42.

DeGraff, J.V., Romesburg, H.C., Ahmad, R, and McCalpin, J. 2012. Producing landslide-susceptibility maps for regional planning in data-scarce regions. Nat Hazards (2012) 64:729–749

DipEcho, 2014 Saint Vincent country profile for disaster risk reduction. http://dipecholac.net/docs/files/789-cd-svg.pdf

D'Odorico P, Fagherazzi S (2003) A probabilistic model of rainfall-triggered shallow landslides in hollows: a long-term analysis. Water Resour Res 39(9). doi:10.1029/2002wr001595

DOMEX project. : http://www.domex2011.com/rain-gauge-network

Fairbridge, R.W., 1975c. Windward Islands. In R.W. Fairbridge (ed.), The Encyclopedia of World Regional Geology, Part 1: Western Hemisphere, p. 667. Stroudburg, Dowden, Hutchinson and Ross.

Faugeres, M.L., 1966. Observations dur le modele des versants dans la region des Pitons du Carbet (Martinique). Assoc. Geographes Francaise Bull. 342-343: 52-63

Fell,R., Corominas, J., Bonnard, C., Cascini, L., Leroi, E., Savage, W.Z., and on behalf of the JTC-1 Joint Technical Committee on Landslides and Engineered Slopes (2008): Guidelines for landslide susceptibility, hazard and risk zoning for land use planning. Engineering Geology, Vol. 102, Issues 3-4, 1 Dec., pp 85-98. DOI:10.1016/j.enggeo.2008.03.022

Fiske, R.S., and Sigurdsson, H., 1982, Soufriere volcano, St. Vincent: Observations of its 1979 eruption from the ground, aircraft, and satellites: Science, v. 216, p. 1105-1126

Franklin, J. E. and Brown, D.P. , 2006. Tropical Cyclone Report, Hurricane Emily 11-21 July 2005. National Hurricane Center. http://www.nhc.noaa.gov/data/tcr/AL052005_Emily.pdf

Frattini P, Crosta G, Sosio R (2009) Approaches for defining thresholds and return periods for rainfalltriggered shallow landslides. Hydrol Process 23(10):1444–1460. doi:10.1002/hyp.7269

Galli, M., Ardizzone, F., Cardinali, M., Guzzetti, F. and Reichenbach, P.: Comparing landslide inventory maps, Geomorphology, 94(3-4), 268–289, 2008.

Gilleland, E. (2015). Package " extRemes " (p. 115).

Glade T (2000) Applying probability determination to refine landslide-triggering rainfall thresholds using an empirical ''antecedent daily rainfall model''. Pure Appl Geophys 157(6):1059–1079. doi:10.1007/ s000240050017

Glade T., Anderson M. & Crozier M.J. (Eds) (2005): Landslide hazard and risk.- Wiley. 803 p

Godt JW, Baum RL, Chleborad AF (2006) Rainfall characteristics for shallow landsliding in Seattle, Washington, USA. Earth Surf Proc Land 31(1):97–110. doi:10.1002/esp.1237

Guha-Sapir, D., Below,R., Hoyois, P. - EM-DAT: International Disaster Database – www.emdat.be – Université Catholique de Louvain – Brussels – Belgium.

Guzzetti, F., Carrara, A., Cardinali, M. and Reichenbach, P., (1999). Landslide hazard evaluation: a review of current techniques and their application in a multi-scale study, Central Italy. Geomorphology, 31(1-4): 181-216.

Guzzetti F, Peruccacci S, Rossi M, Stark CP (2007) Rainfall thresholds for the initiation of landslides in central and southern Europe. Meteorol Atmos Phys 98(3):239–267. doi:10.1007/s00703-007-0262-7

Hartford, D., and Mehigan, P.J., 1984, Rain -induced slope failures in the Commonwealth of Dominica, West Indies: 5th International Symposium on Landslides, vol.3, p.87-89

Hay, R. L. (1959). Origin and weathering of Late Pleistocene ash deposits on St. Vincent, B.W.I. The Journal of Geology, 67(1), 65 – 87. doi:10.1086/626558

Heath, E., Macdonald, R., Belkin, H., Hawkesworth, C., & Sigurdsson, H. (1998). Magmagenesis at Soufriere Volcano, St Vincent, Lesser Antilles Arc. Journal of Petrology, 39(10), 1721–1764. doi:10.1093/petroj/39.10.1721

Hurricane City (http://www.hurricanecity.com/city/)

INCREO (http://www.increo-fp7.eu/)

Iverson, R. M., 2000: Landslide triggered by rain infiltration. Water Resour. Res., 36, 1897–1910.

Jaiswal, P., van Westen, C.J. and Jetten, V.G. (2011) Quantitative assessment of landslide hazard along transportation lines using historical records. In: Landslides: journal of the International Consortium on Landslides, 8 (2011)3 pp. 279-291.

Jaiswal, P. and van Westen, C.J. (2013) Use of quantitative landslide hazard and risk information for local disaster risk reduction along a transportation corridor: a case study from Nilgiri district, India. In: Natural hazards : journal of the international society for the prevention and mitigation of natural hazards, 65 (2013)1 pp. 887-913

Jones, P.D.; Harris, I. (2008). Climatic Research Unit (CRU) time-series datasets of variations in climate with variations in other phenomena. NCAS British Atmospheric Data Centre, date of citation. http://catalogue.ceda.ac.uk/uuid/3f8944800cc48e1cbc29a5ee12d8542d

Kappes MS, Keiler M, Von Elverfeldt K, Glade T, (2012). Challenges of analyzing multi-hazard Risk: A Review. Natural Hazards 64(2), 1925-1958

Larsen, M. C., and A. Simon, 1993: A rainfall intensity-duration threshold for landslides in a humid-tropical environment, Puerto Rico. Geogr. Ann., A75, 13–23.
Lee, S., Choi, J., 2004. Landslide susceptibility mapping using GIS and the weight-of-evidence model. International Journal of Geographical Information Science, 18(8), 789-814.
Lee, S., Choi, J., Min, K., 2002. Landslide susceptibility analysis and verification using the Bayesian probability model. Environmental Geology, 43(1-2), 120-131.
Lindsay, J.M., Robertson, R.E.A., Shepherd, J.B. and Ali, S. (2005) Volcanic Hazard Atlas of the Lesser Antilles. University Of The West Indies
Lindsay, J. M., A. L. Smith, M. J. Roobol, and M. V. Stasuik (2005), Dominica, in Volcanic Hazard Atlas of the Lesser Antilles, edited by J. M. Lindsay et al., pp. 1–48, Seismic Res. Unit, Univ. of the West Indies, St. Augustine, Trinidad and Tobago.
Lockhart, A. L. 1879. Leeward Islands Almanack. Roseau: Official Gazette Office
Lowe, C.J. (2010). Analysing vulnerability to Volcanic Hazards: application to St Vincent. PhD thesis, University college London. http://discovery.ucl.ac.uk/20466/1/20466.pdf
Lozano Zafra, D. P. (2015) National Scale Landslide Susceptibility Assessment for Dominica And Saint Vincent. MSc thesis, Faculty of Geo-Information Science and Earth Observation (ITC), University of Twente. https://www.itc.nl/library/papers_2015/msc/aes/lozano-zafra.pdf
Marques R, Zeˆzere J, Trigo R, Gaspar J, Trigo I (2008) Rainfall patterns and critical values associated with landslides in Povoaçao County (Sa˜o Miguel Island, Azores): relationships with the North Atlantic Oscillation. Hydrol Process 22(4):478–494. doi:10.1002/hyp.6879
Martelloni G, Segoni S, Fanti R, Catani F (2011) Rainfall thresholds for the forecasting of landslide occurrence at regional scale. Landslides:1–11. doi:10.1007/s10346-011-0308-2
Martin-Kaye, P.H.A. 1956-61. Geological survey of the Windward Islands. Progress Reports. Castries
McGuire, W. J. (1996), Volcano instability: A review of contemporary themes, in Volcano Instability on the Earth and Other Planets, edited by W. J. McGuire, A. P. Jones, and J. Neuberg, Geol. Soc. Spec. Publ., 110, 1–23
Mehigan, P.J. & D.N.D.Hartford l-985. Aspects of slope stability in relation to road design in the Commonwealth of Dominica. Proc. llth Internat. Conf. Soil Mech. Found. Eng. L: 2339-2343
Mulenga, C. (2015). Influence of weathering and stress relief on geotechnical properties of roadcut mass and embankment fill on St. Vincent and St. Lucia. MSc thesis, Faculty of Geo-Information Science and Earth Observation (ITC), University of Twente. http://www.charim.net/sites/default/files/handbook/otherpages/MSC/Chishala%20Mulenga-s6011799.pdf
Natural Hazard and Disasters: Landslides (1999).Retrieved July 27, 2014 from http://www.mona.uwi.edu/uds/Landslides.html
Neuhäuser, B., Terhorst, B., 2007. Landslide susceptibility assessment using "weights-of-evidence" applied to a study area at the Jurassic escarpment (SW-Germany). Geomorphology, 86(1–2), 12-24.
NGDC [National Geophysical Data Center]. 2003. Tsunami Data at NGDC. Boulder, Colo.: National Geophysical Data Center. [www.ngdc.noaa.gov/seg/hazard/tsu.shtml].
OAS, USAID/OFDA (2002) Caribbean Disaster Mitigation Project. Online. Available at: http://www.oas.org/CDMP/document/seismap/
Office of Disaster Management (http://odm.gov.dm/)
O'Keefe, P. and Conway, C. (1977). Natural Hazards in the Windward Islands. University of Bradford, Disaster Research Unit, Occasional Paper Nr, 14. http://www.ilankelman.org/miscellany/BDRU14.pdf
OAS (1996).History of Storms on Dominica: HURSTAT. Caribbean disaster Mitigation Project. http://www.oas.org/cdmp/document/dominica_waves/2_History/History.htm
Parsons, T. and Geist, E.L. 2009. Tsunami Probability in the Caribbean Region. Pure appl. geophys. 165 (2009) 2089–2116. Available from :http://woodshole.er.usgs.gov/project-pages/caribbean/pdf/Parson_Geist_PAGeoph2009.pdf
Polemio M, Sdao F (1999). The role of rainfall in the landslide hazard: the case of the Avigliano urban area (Southern Apennines, Italy). Eng Geol 53(3–4):297–309. doi:10.1016/s0013-7952(98)00083-0
Prior, D.B. and C. Ho, 1972. Coastal and mountain slope instability on the islands of St. Lucia and Barbados. Eng. Geol. 6:1-18.
Razak, K.A., Santangelo, M., van Westen, C.J., Straatsma, M.W. and de Jong, S.M. (2013) Generating an optimal DTM from airborne laser scanning data for landslide mapping in a tropical forest environment. In: Geomorphology, 190 (2013) pp. 112-125.
Richardson, B. C. 1989. Catastrophes and Change on St. Vincent. National Geographic Research 5 (1): 111-125.
Richardson, B. C. 2004. Igniting the Caribbean's Past: Fire in British West Indian History. Chapel Hill: University of North Carolina Press.
Robertson, R. E. A. 1995. An Assessment of the Risk from Future Eruptions of the Soufriere Volcano of St.Vincent, Natural Hazards 11 (2) : 163-19
Robertson, R.E.A. (2003). The Volcanic Geology of the Pre-Soufrière rocks of St Vincent, West Indies. PhD, Department of Geography and Geology, University of the West Indies, Mona.
Robertson, R.E.A. (2003). Making Use of Geology - the Relevance of Geology and Geological Information to the Development Process in St Vincent and the Grenadines. http://www.open.uwi.edu/sites/default/files/bnccde/svg/conference/papers/robertson.html
Rouse, C., 1990. The mechanics of small tropical flowslides in Dominica, West Indies. Eng. Geol., 29:227-239.
Rouse, W.C., A.J. Reading, and R.P.D. Walsh, 1986. Volcanic soil properties in Dominica, tr]est Indies : Eng. Geol . 23: 1- 28.

Rowley, K. 1978. Late Pleistocene pyroclastic deposits of Soufriere volcano, St. Vincent, West Indies: Geological Society of America Bulletin, Vol. 89, p. 825-835.

Saaty. T.L. 1980. The Analytic Hierarchy Process, Planning, Piority Setting, Resource Allocation. McGraw-Hill, New york, 1980.

Saito H, Nakayama D, Matsuyama H (2010) Relationship between the initiation of a shallow landslide and rainfall intensity–duration thresholds in Japan. Geomorphology 118(1–2):167–175. doi:10.1016/ j.geomorph.2009.12.016

Sawatzky, D.L., Raines, G.L., Bonham-Carter, G.F., Looney, C.G., 2009. Spatial Data Modeller (SDM): ArcMAP 9.3 geoprocessing tools for spatial data modelling using weights of evidence, logistic regression, fuzzy logic and neural networks.

Shepard, J.B., Aspinall, W.P., Rowley, K.C., and others, 1979, The eruption of Soufriere volcano, St. Vincent, April-June, 1979: Nature, v. 282, p. 24-28.

Shepard, J.B., and Sigurdsson, H., 1982, Mechanism of the 1979 explosive eruption of Soufriere volcano, St. Vincent: Journal of Volcanology and Geothermal Research, v. 13, p. 119-130.

Sigurdsson H, Carey SN (1991) Caribbean Volcanoes: A Field Guide to Martinique, Dominica and St. Vincent. Geological Association of Canada, Toronto 1991 eld trip guidebooks, pp 1-101.

Simoni, S., Zanotti, F., Bertoldi, G., and Rigon, R., (2008). Modelling the probability of occurrence of shallow landslides and channelized debris flows using GEOtop-FS: Hydrological Processes. 22(4), p. 532-545.

Smith, M. S., and J. R. Shepherd. 1993. Preliminary Investigations of the Tsunami Hazard of the Kick'em Jenny Submarine Volcano. Natural Hazards 7 (3): 257-277.

Smith, G., 1983. Correlation of the soils of the Commonwealth Caribbean, Puerto Rico, the Virgin Islands and Guyana. Soil and land use surveys, no. 1:7. Dept. of Soil Science, Faculty of Agriculture, Univ. of West Indies, Trinidad

Smith, RB, Schafer, P, Kirshbaum, D, Regina, E (2009) Orographic Enhancement of Precipitation inside Hurricane Dean. J. Hydrometeorol., 10, 820-831

Smith, RB, Schafer, P, Kirshbaum, D, Regina, E (2009) Orographic Precipitation in the Tropics: Experiments in Dominica. J Atmos Sci 66, 1698-1716

Soeters, R., Van Westen, C.J., 1996. Slope instability recognition, analysis and zonation. In: Turner, A.K., Schuster, R.L., (Eds.), Landslides, Investigation and Mitigation

SRU [Seismic Research Unit]. (2005). Volcanoes. University of the West Indies, Seismic Research Unit.

SRU [Seismic Research Unit]. (2007). Earthquakes. University of the West Indies, Seismic Research Unit.

Süzen, M.L., Doyuran, V., 2004. Data driven bivariate landslide susceptibility assessment using geographical information systems: a method and application to Asarsuyu catchment, Turkey. Engineering Geology, 71(3–4), 303-321.

Technical Committee 32 (Engineering Practice of Risk Assessment and Management) of the International Society of Soil Mechanics and Geotechnical Engineering (ISSMGE): Risk assessment – Glossary of terms. http://www.engmath.dal.ca/tc32/2004Glossary_Draft1.pdf

Thiery, Y., Malet, J.P., Sterlacchini, S., Puissant, A., Maquaire, O., 2007. Landslide susceptibility assessment by bivariate methods at large scales: Application to a complex mountainous environment. Geomorphology, 92(1–2), 38-59.

Tomblin, J. 1981. Earthquakes, volcanoes, and hurricanes: a review of natural hazard and vulnerability in the West Indies. Ambio 10(6), 340 – 345.

UN-ISDR, 2004. Terminology of disaster risk reduction. United Nations, International Strategy for Disaster Reduction, Geneva, Switzerland http://www.unisdr.org/eng/library/lib-terminology-eng%20home.htm

Van Asch, T.W.J., Malet, J.P., Van Beek, L.P.H. and Amitrato, D. (2007) Techniques, issues and advances in numerical modelling of landslide hazard. Bull. Soc. géol. Fr., 2007, 178 (2), 65-88

Van Westen, C. J.: 1993, Application of Geographic Information Systems to Landslide Hazard Zonation, Ph-D Dissertation Technical University Delft. ITC-Publication Number 15, ITC, Enschede, The Netherlands, 245 pp.

Van Westen, C.J., Soeters, R. and Sijmons, K. (2000) Digital geomorphological landslide hazard mapping of the Alpago area, Italy. In: International journal of applied earth observation and geoinformation : JAG, 2 (2000)1, pp. 51-60.

Van Westen, C.J., Castellanos Abella, E.A. and Sekhar, L.K. (2008) Spatial data for landslide susceptibility, hazards and vulnerability assessment : an overview. In: Engineering geology, 102 (2008)3-4, pp. 112-131

Walsh, R.P.D., 1982. A provisional survey of the effects of Hurricanes David and Frederic in 1979 on the terrestrial environment of Dominica, West Indies. Swansea Geog. 19:28 35.

Walsh, R.P.D., 1985. The influence of climate, lithology, and time drainage density and relief development in the volcanic terrain of the Windward Islands. In I. Douglas and T. Spencer (eds.), Environmental change and tropical geomorphology, p. 93-122. London: Allen and Unwin.

Wieczorek GF, Glade T (2005) ,Climatic factors influencing occurrence of debris flows. In: Debris flow Hazards and Related Phenomena (Jakob M, Hungr O, eds). Springer Berlin Heidelberg, 325–362

Watson, J.P. and Jones, T.A (1958). Soil map of Saint Vincent and the Grenadines, 1:20,000. The Regional Research Centre of the British Caribbean, at the Imperial College of Tropical Agriculture, Trinidad, Soil and Landuse Survey , No. 3.l

World Bank, GFDRR (2014). Rapid Damage and Loss Assessment (DaLA). December 24-25, 2013 Floods. A report by the Government of Saint Vincent and the Grenadines. http://documents.worldbank.org/curated/en/2014/01/18892616/rapid-damage-loss-assessment-dala-december-24-25-2013-floods-report-government-saint-vincent-grenadines

Zezere JL, Trigo RM, Trigo IF (2005) Shallow and deep landslides induced by rainfall in the Lisbon region (Portugal): assessment of relationships with the North Atlantic Oscillation. Nat Hazards Earth Syst Sci 5(3):331–344